# Kinematic, Precipitation, and Microphysics Structures of Typhoon Nari (2001)

*Ming-Jen Yang*

*Dept. of Atmospheric Sciences, Inst. of Hydrological & Oceanic Sciences*

*National Central University, Taiwan*

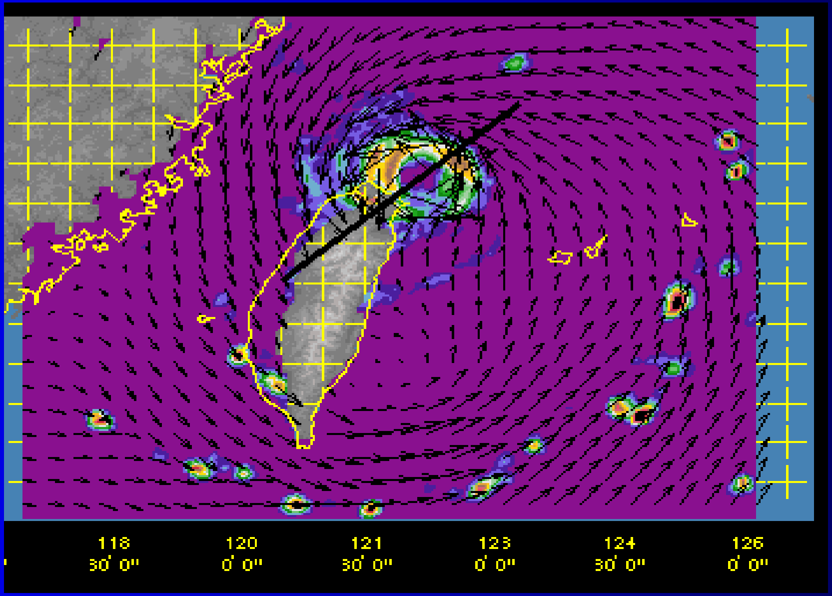


Seminar at CCU, 2009/03/19

# TRMM Observations

# 2001/09/15 0026 UTC

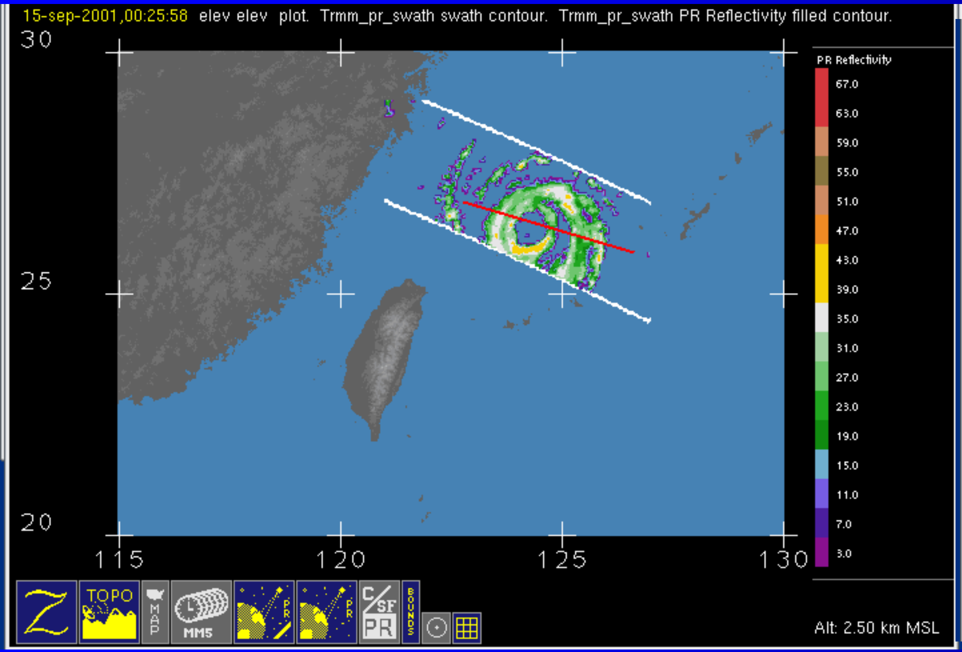


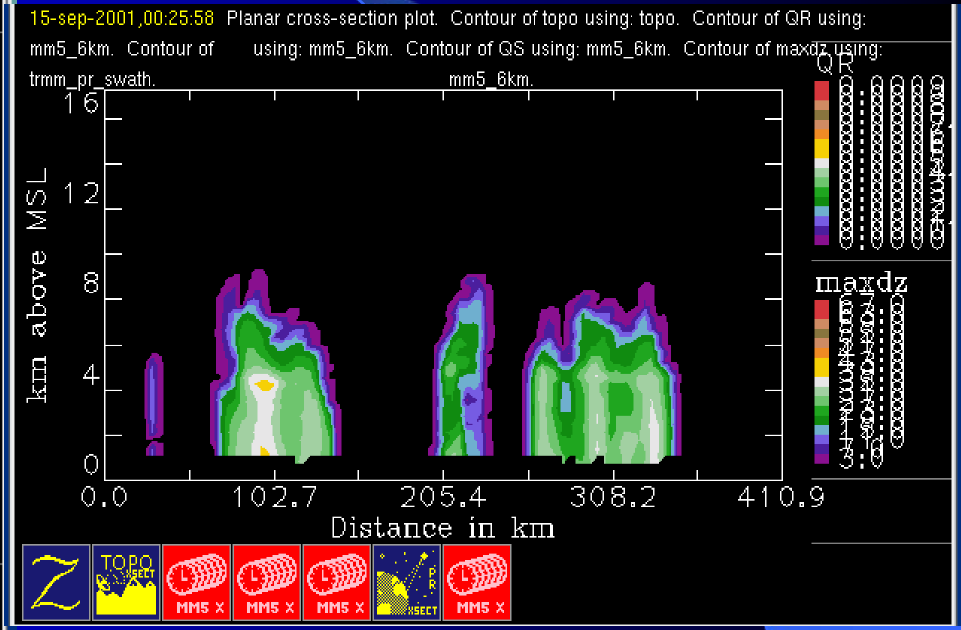


Courtesy of Prof. Bob Houze (UW)

# 2001/09/15 0026 UTC

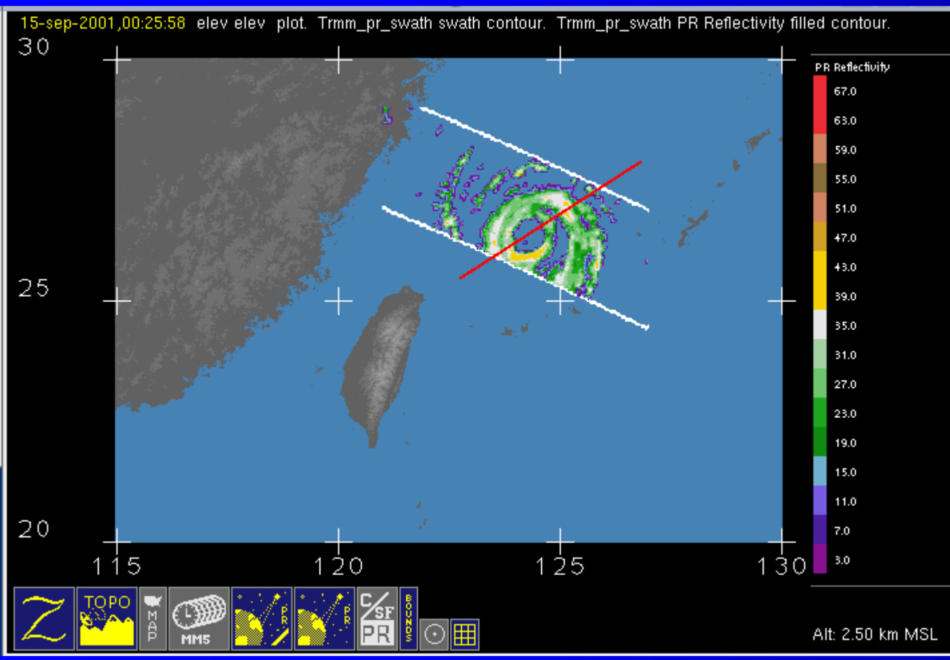


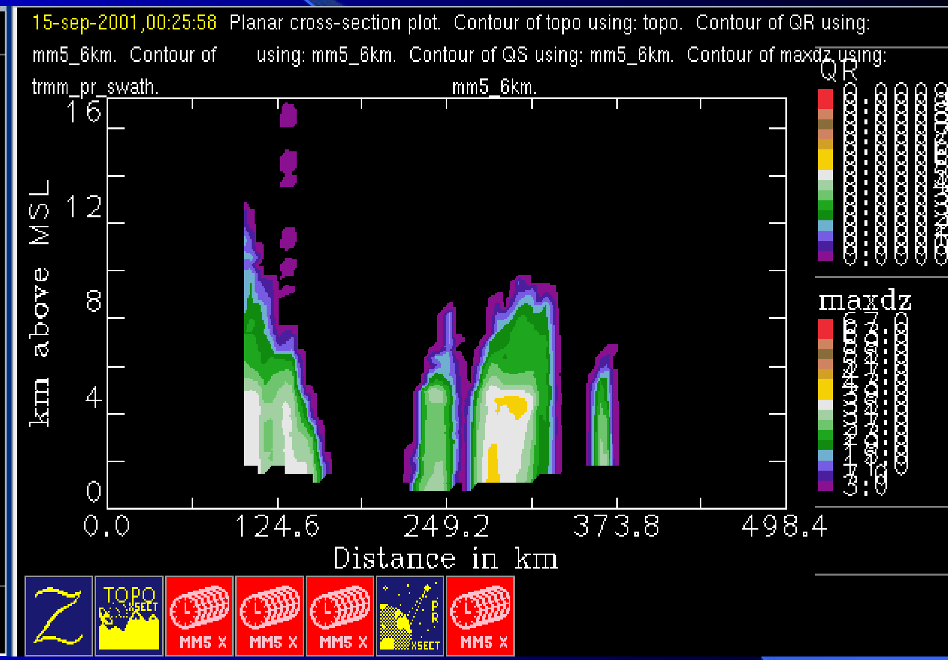


Courtesy of Prof. Bob Houze (UW)

# 2001/09/16 1740 UTC

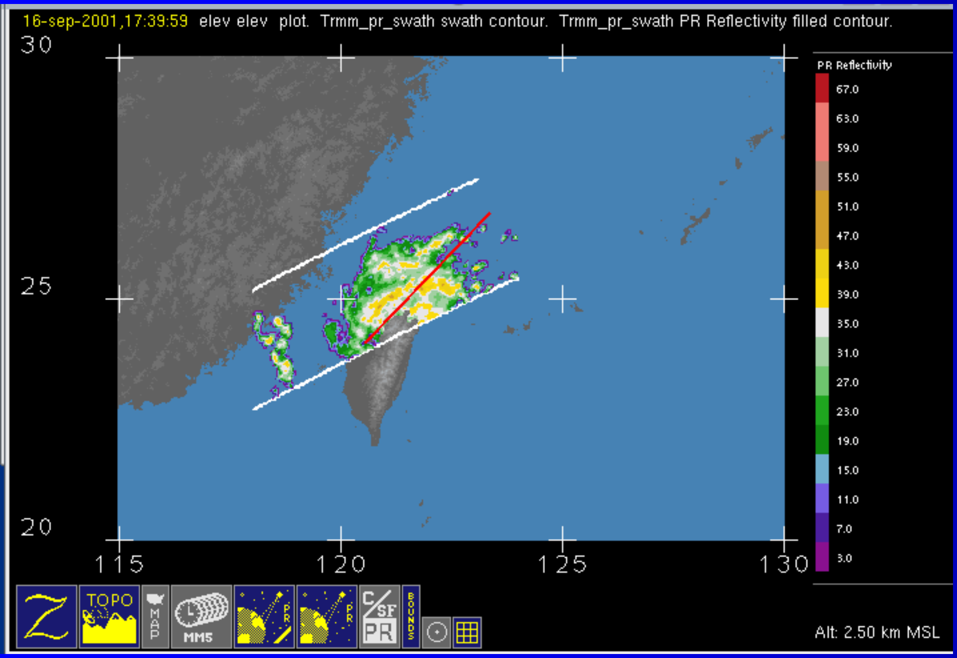


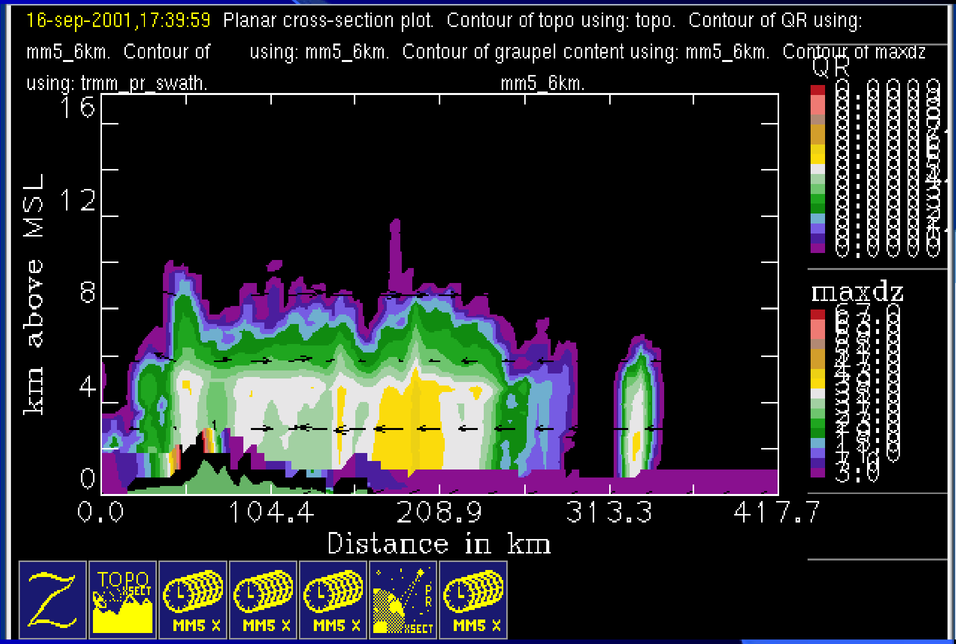


Courtesy of Prof. Bob Houze (UW)

# 2001/09/16 1740 UTC

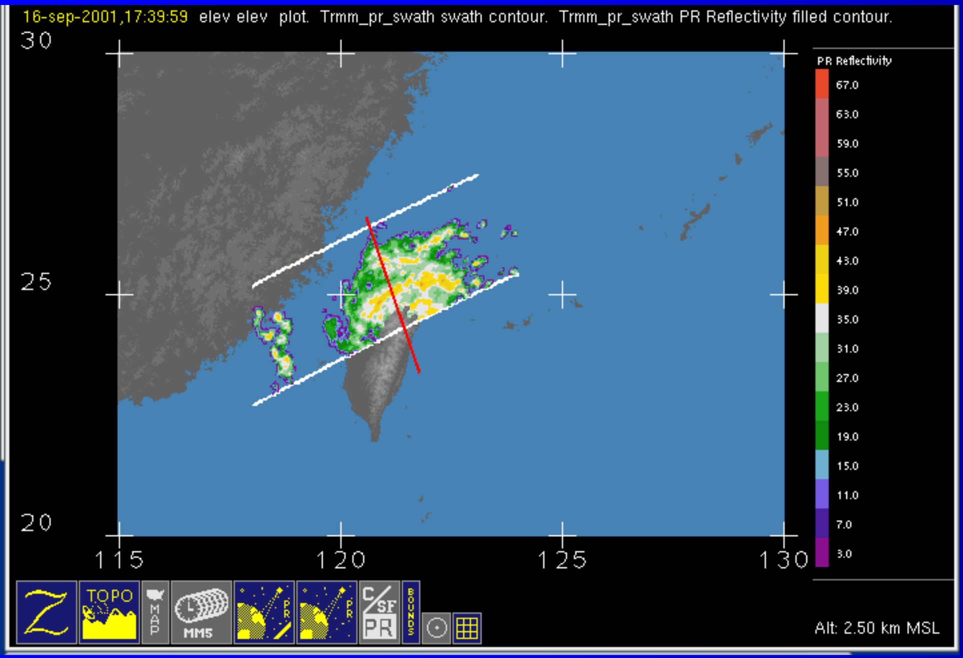


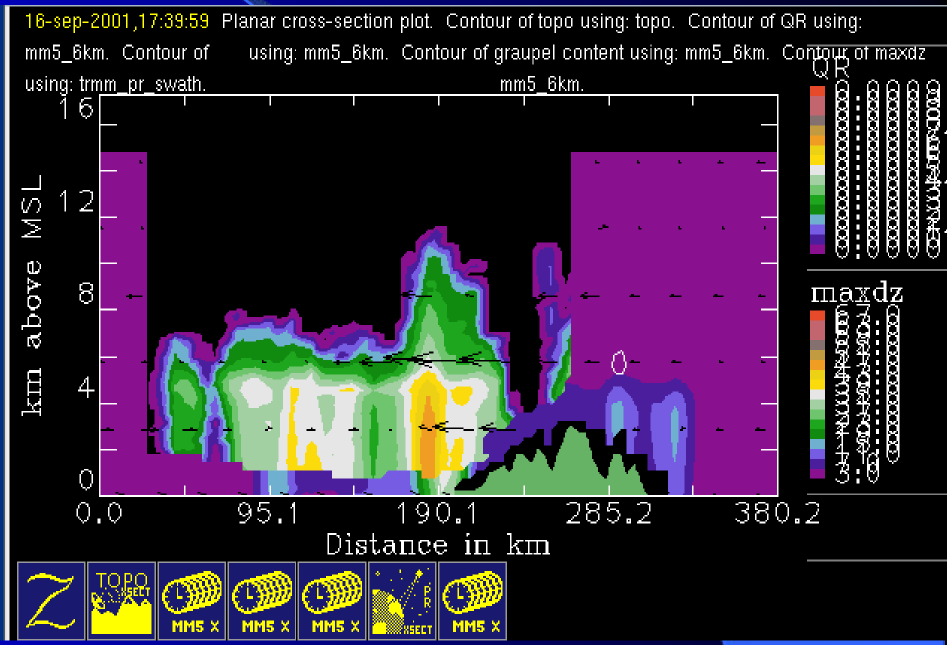


Courtesy of Prof. Bob Houze (UW)

# 2001/09/17 0012 UTC

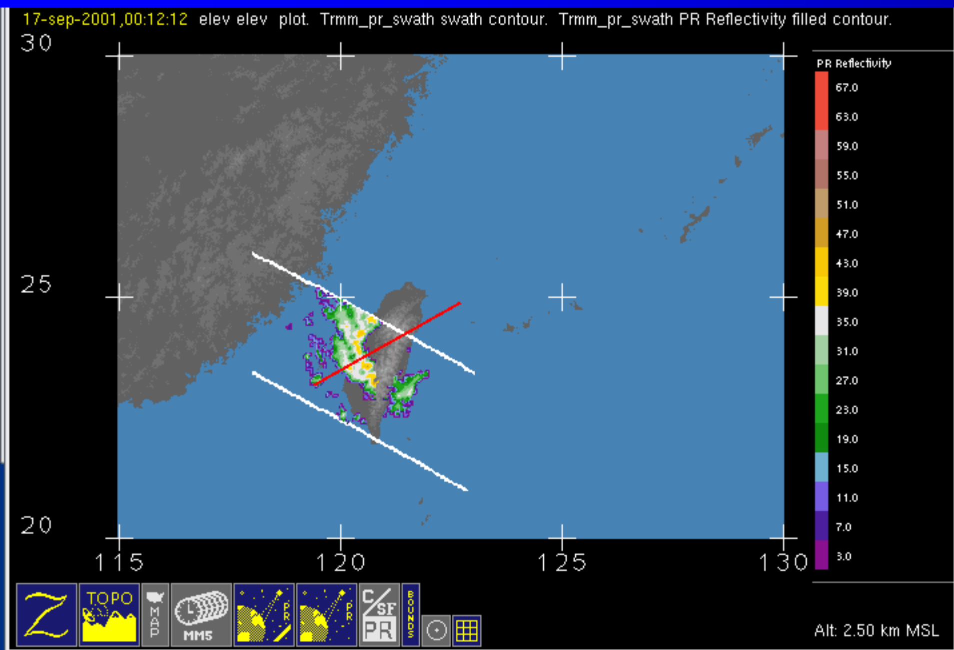


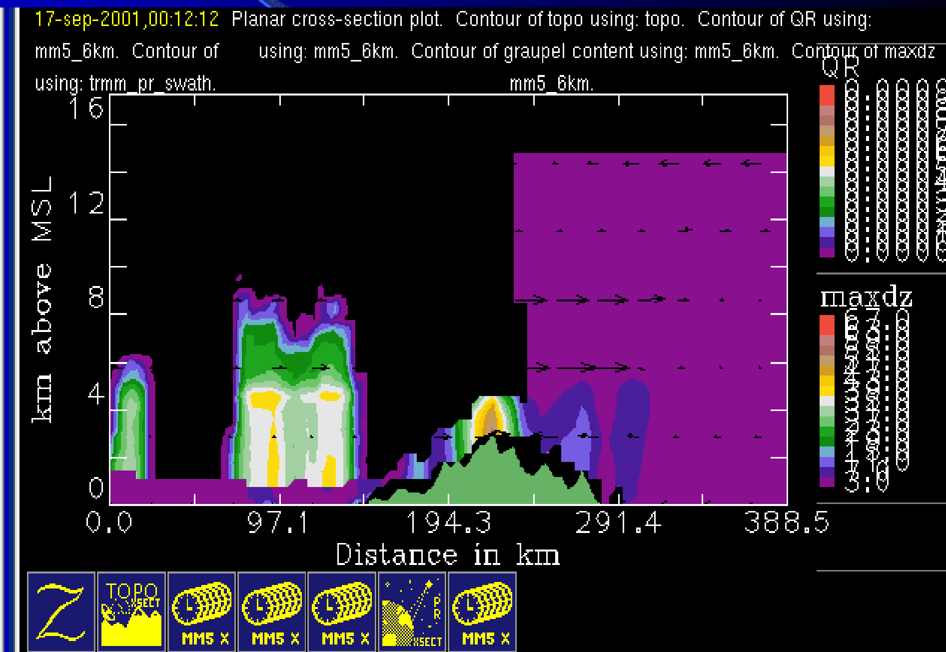


Courtesy of Prof. Bob Houze (UW)

# 2001/09/19 2303 UTC

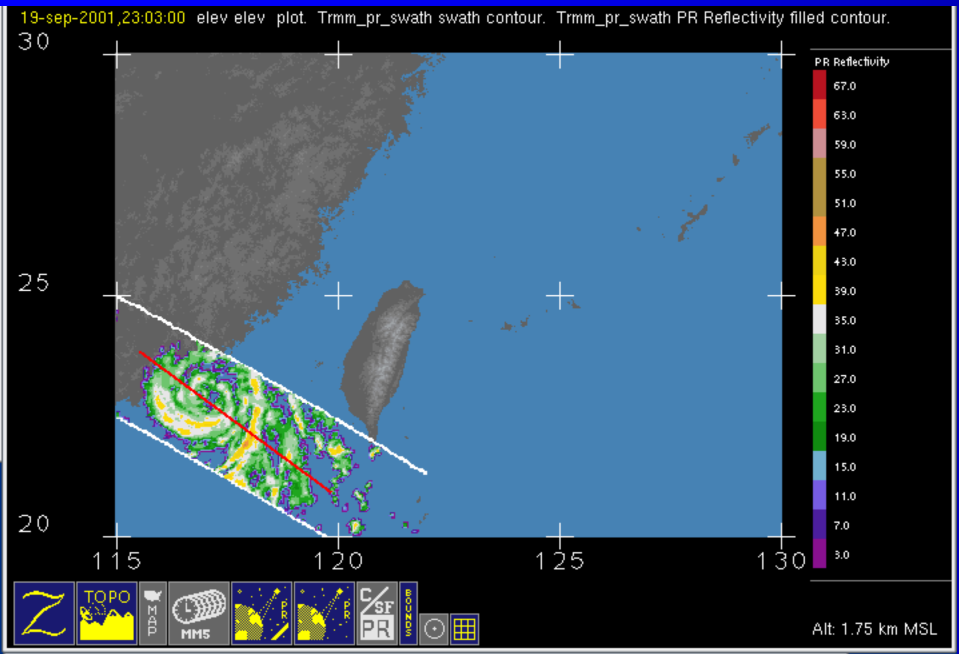


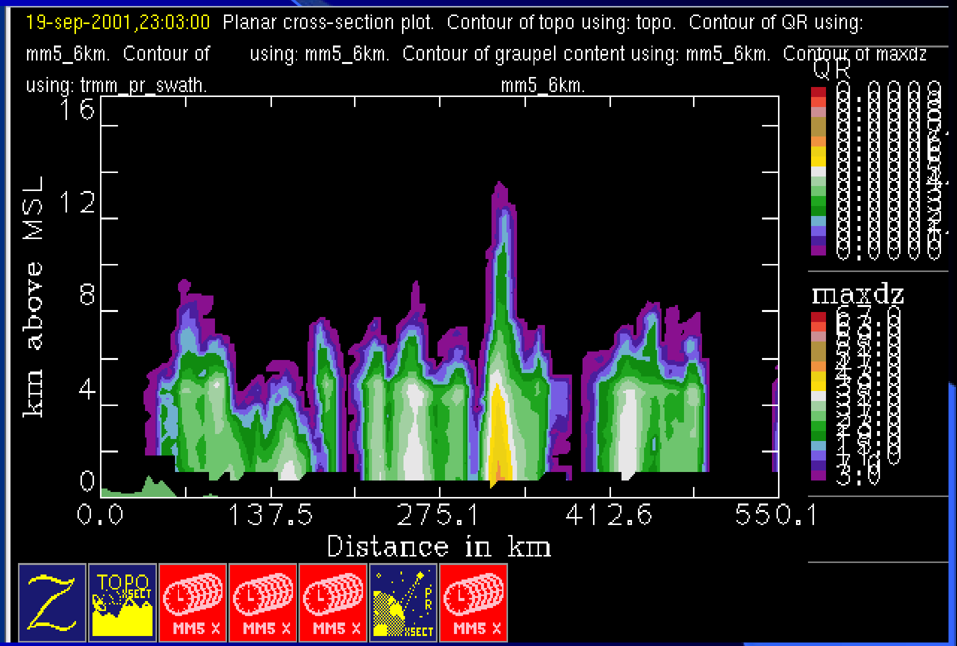


Courtesy of Prof. Bob Houze (UW)

# 2001/09/19 2303 UTC

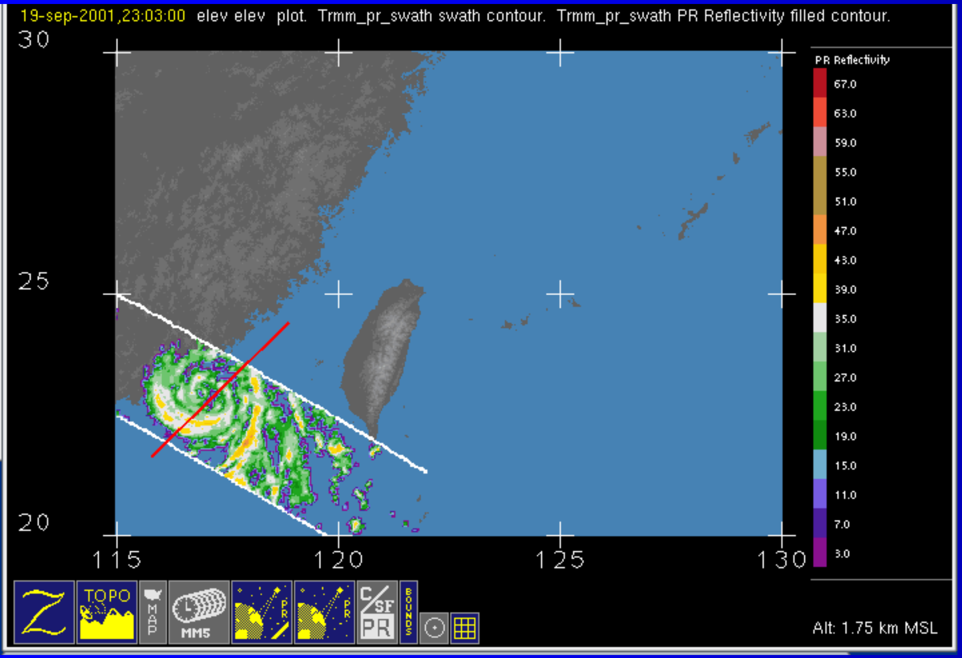


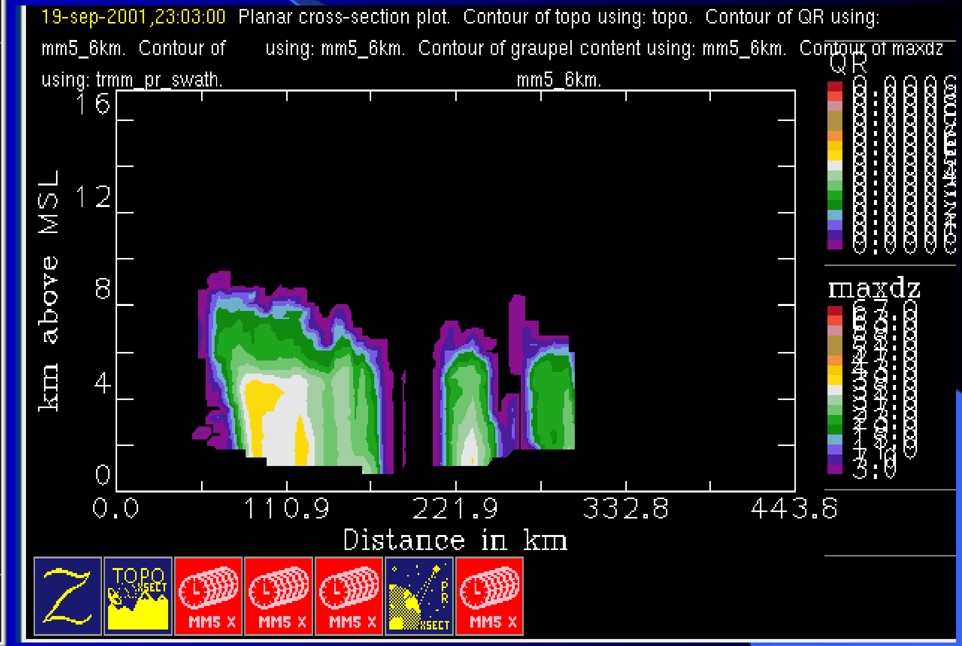


Courtesy of Prof. Bob Houze (UW)

# MM5 Simulation

Yang, M.-J., D.-L. Zhang, and H.-L. Huang, 2008: A modeling study of Typhoon Nari (2001) at landfall. Part I: Topographic effects. *J. Atmos. Sci.*, 65, 3095–3115.

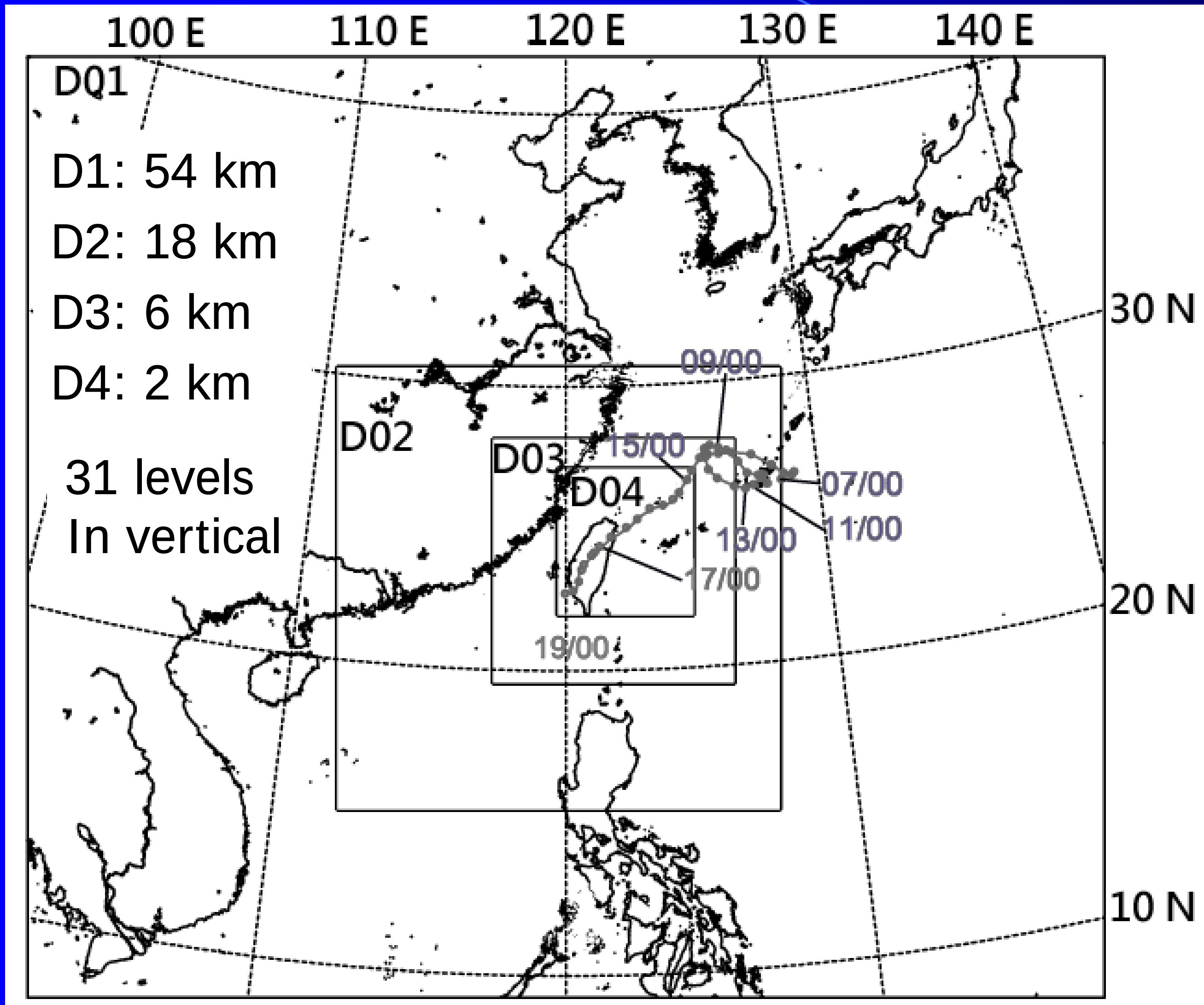


**Accumulated Rainfall**

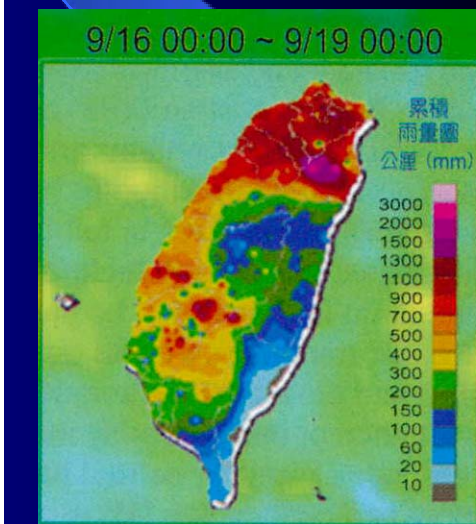


Max ~ 1500 mm

# Track Comparison

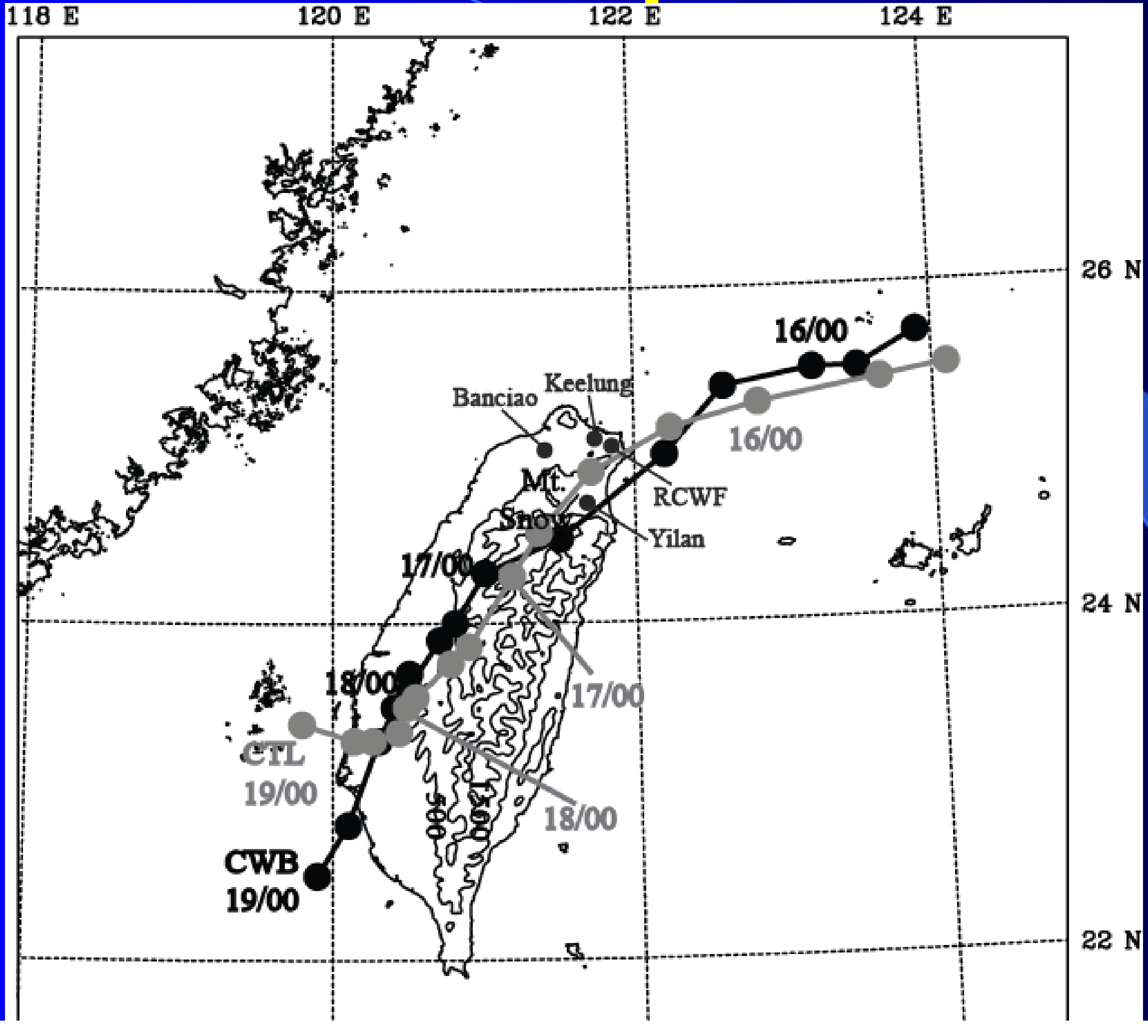


| Simulation time (hr) | 12 | 24 | 36 | 48 | 60 | 72 | 84 |
|---|---|---|---|---|---|---|---|
| Track error (km) | 43.3 | 61.2 | 26.8 | 13.4 | 12 | 8.5 | 104.8 |

# Time Series of SLP and Vmax

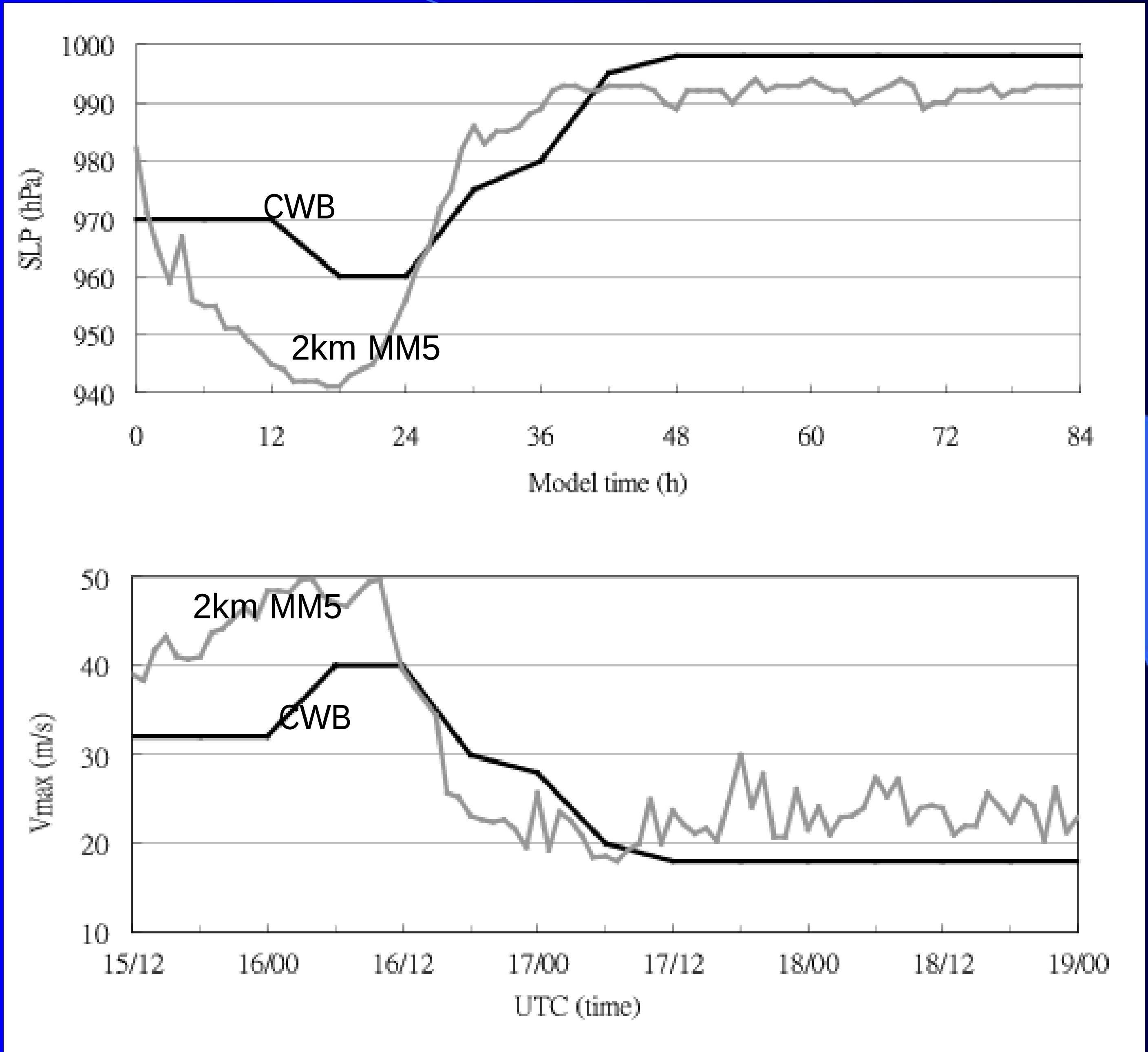

# 3-day rainfall (09/16~09/18)

OBS

6km MM5

2km MM5

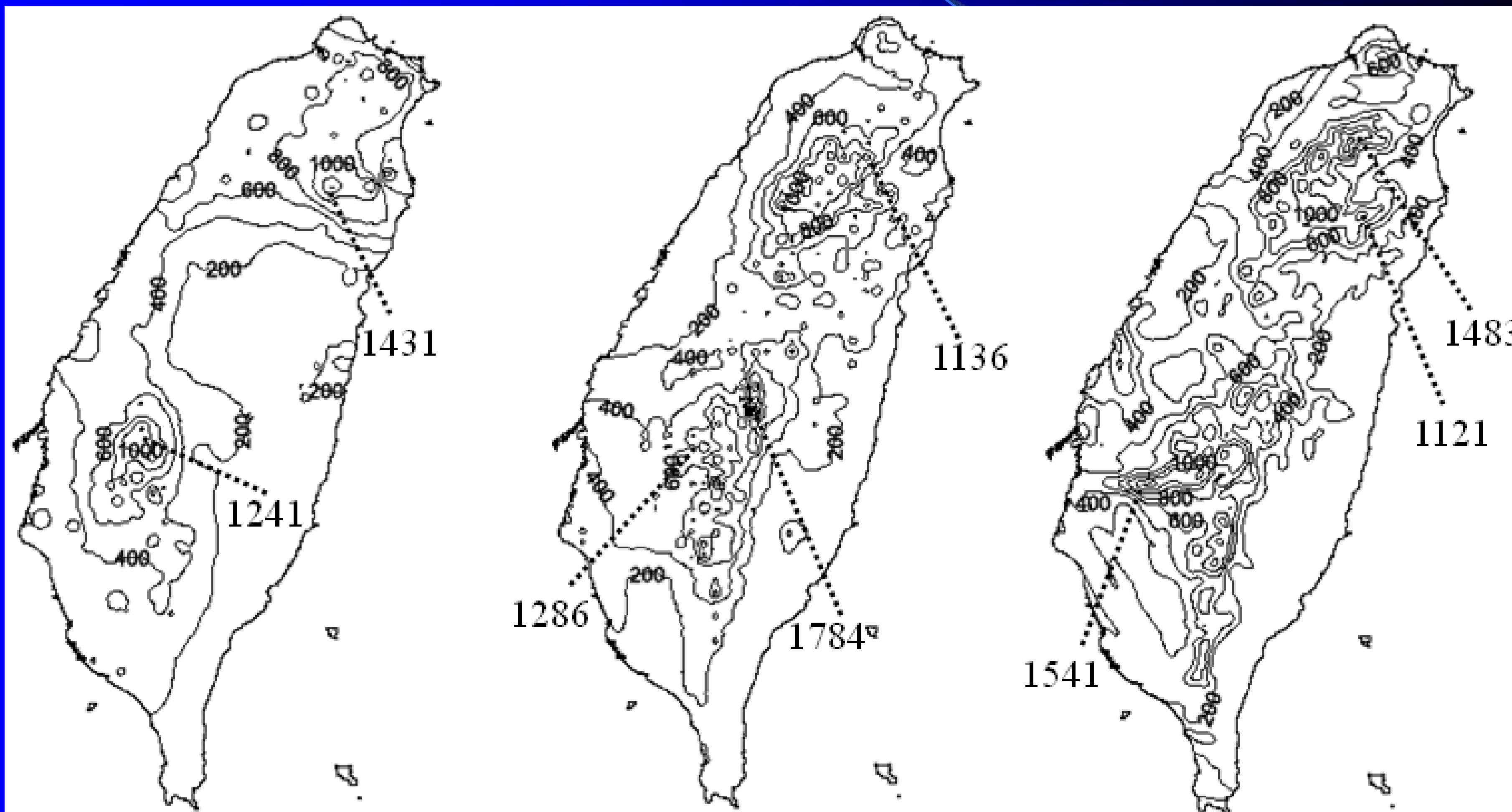

# Average Rainfall on Taiwan

| Item | N | 09/16 | 09/17 | 09/18 | 3-Day Total |
|---|---|---|---|---|---|
| OBS (in mm) | 325 | 132 | 206 | 97 | 435 |
| 6km MM5 | 1073 | 159 | 104 | 75 | 348 |
| 2km MM5 | 9602 | 175 | 133 | 84 | 383 |

# Percentage wrt Rain Gauge OBS

| MM5/OBS | 09/16 | 09/17 | 09/18 | 3-Day Total |
|---|---|---|---|---|
| 6km MM5 | 121 % | 51 % | 78 % | 80 % |
| 2km MM5 | 133 % | 65 % | 87 % | 88 % |

# Radar Composite Before Landfall

**OBS**

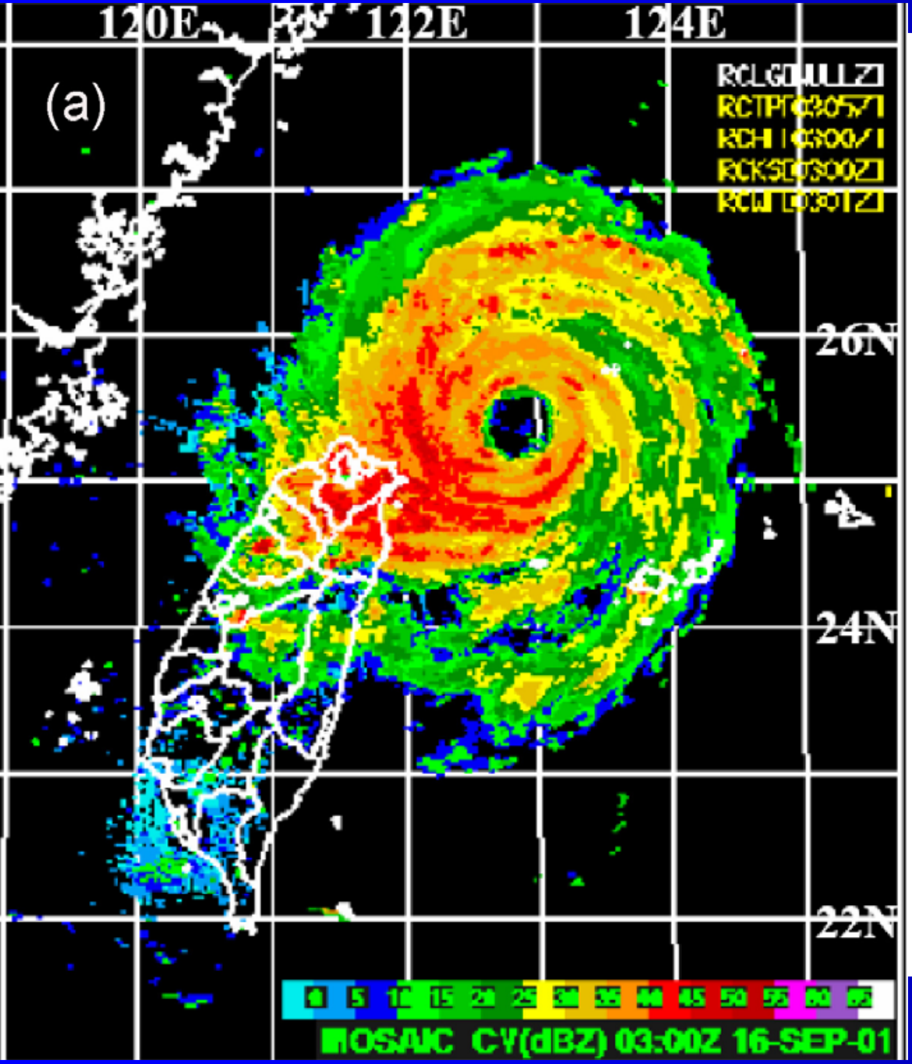


**2-km MM5**

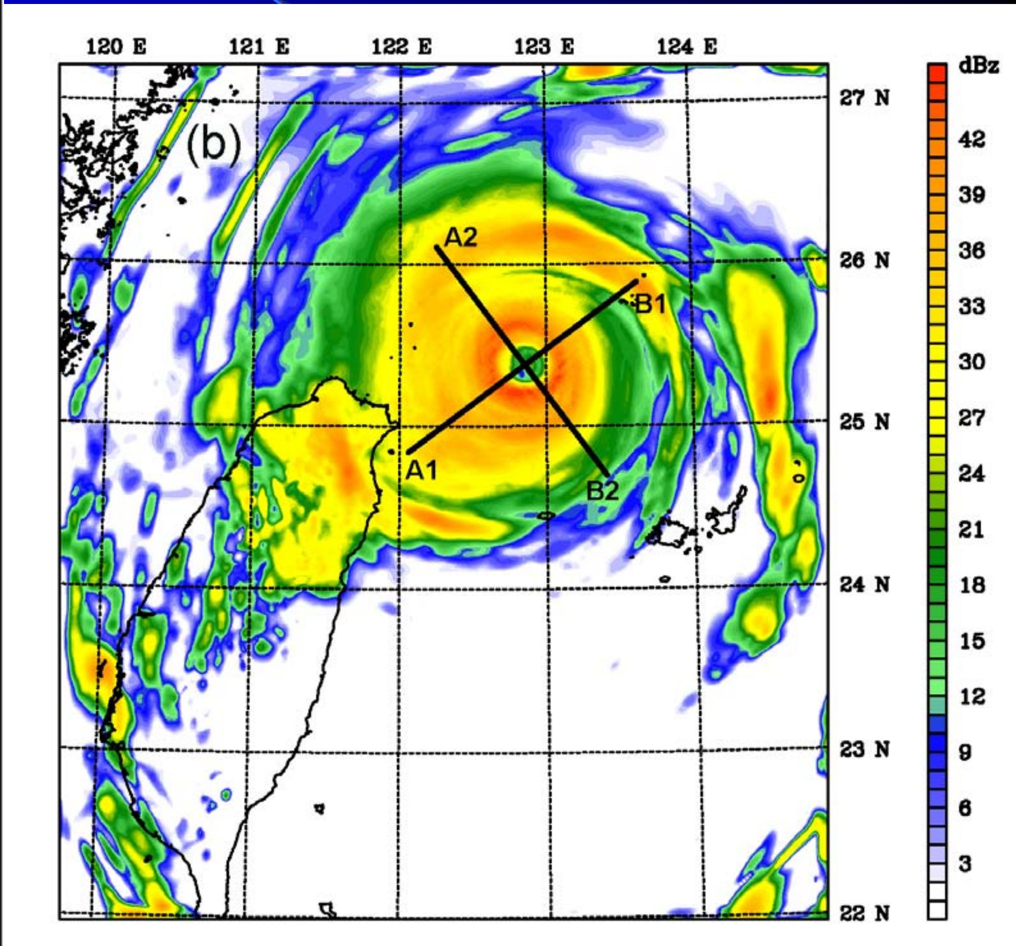


**MM5 Radar CV @ 9/16 0130Z (1-h time averaged)**

# Radar Composite After Landfall

**OBS**

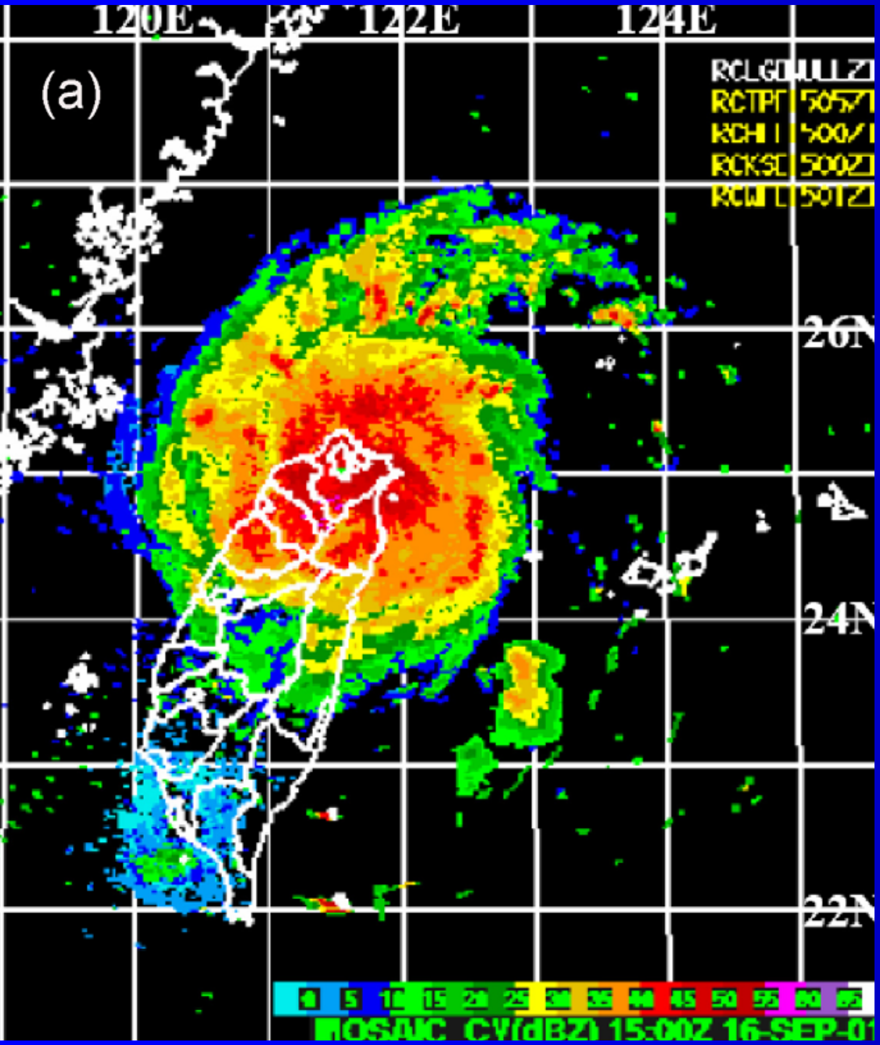


**2-km MM5**

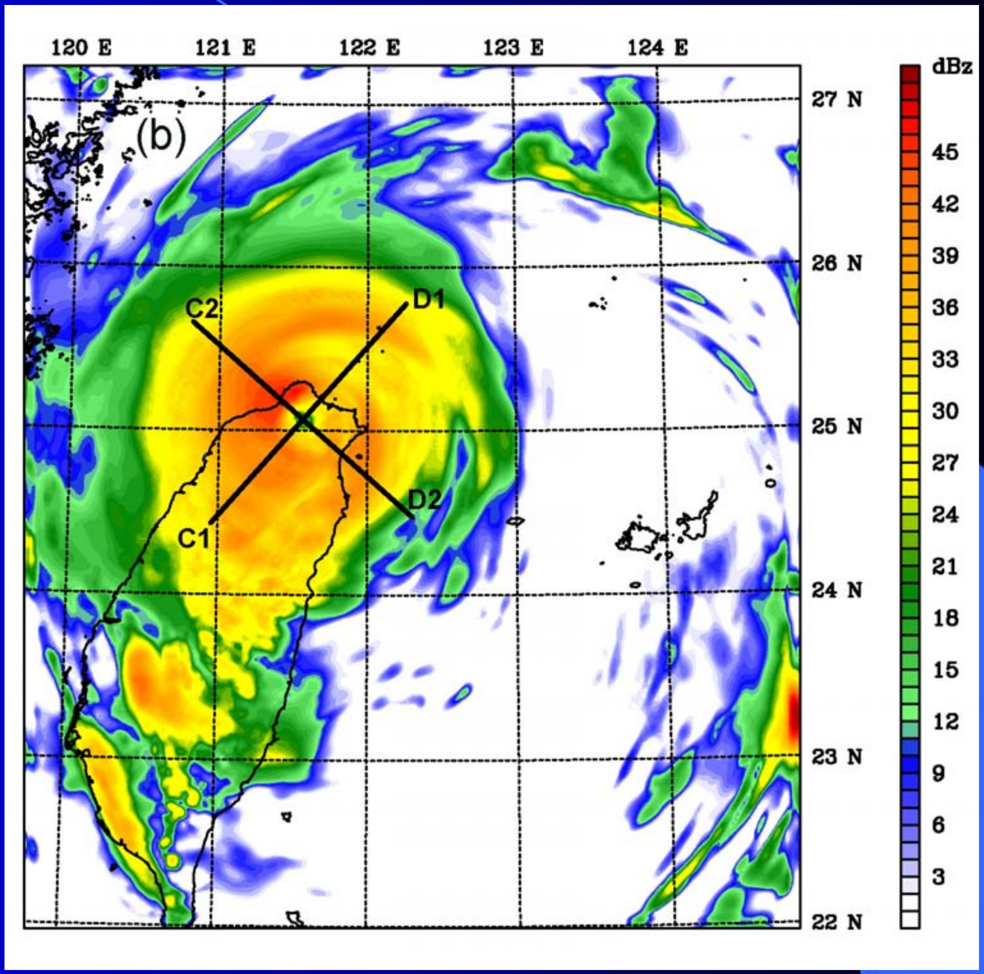


**MM5 Radar CV @ 9/16 1200Z (1-h time averaged)**

# Conceptual Model of the Inner-Core Structure in a Mature Hurricane

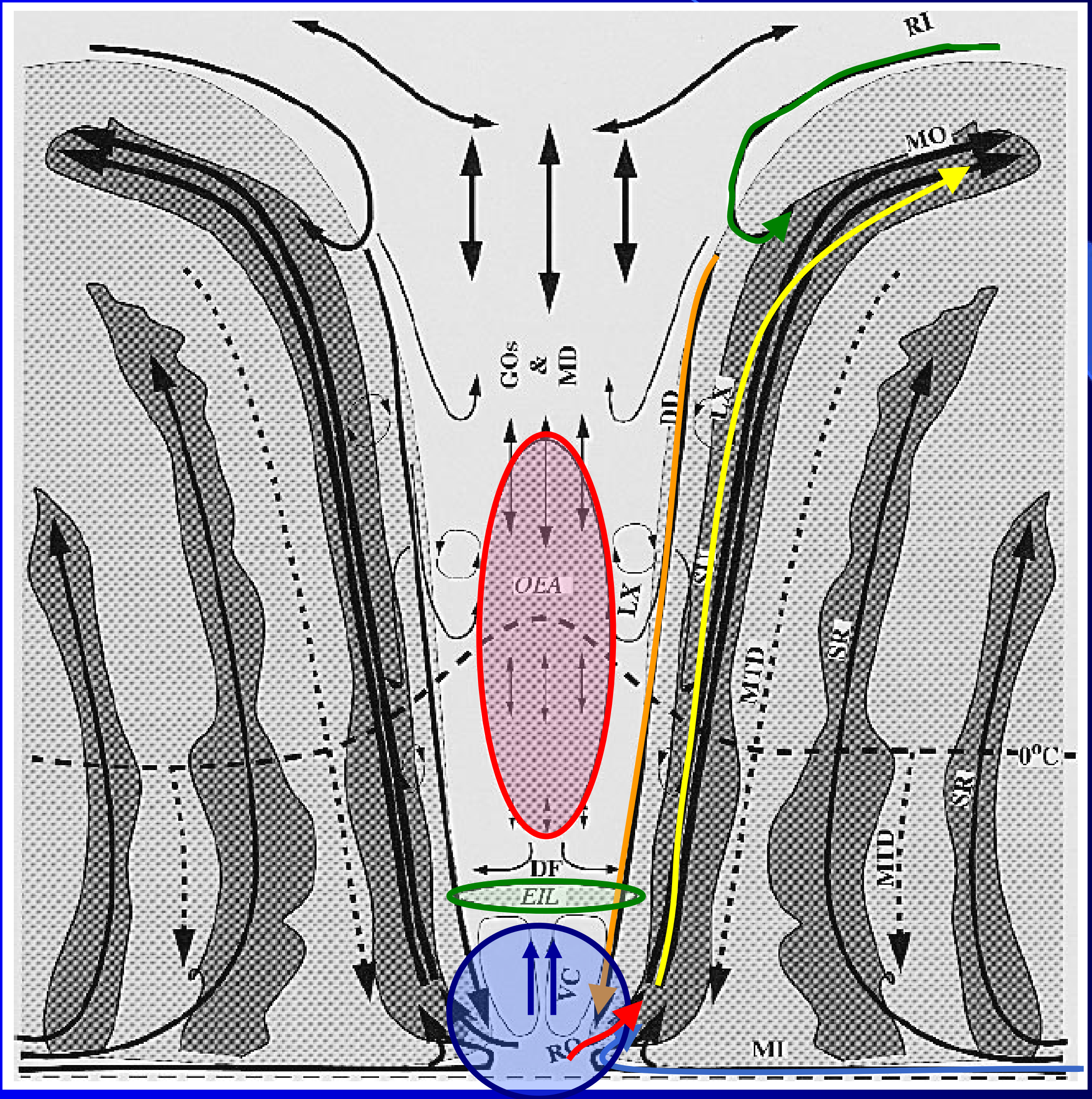


Liu et al. (1999) Part II

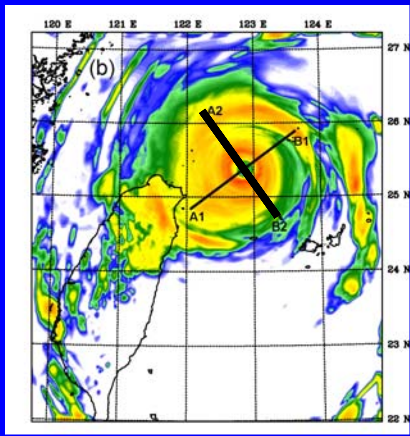


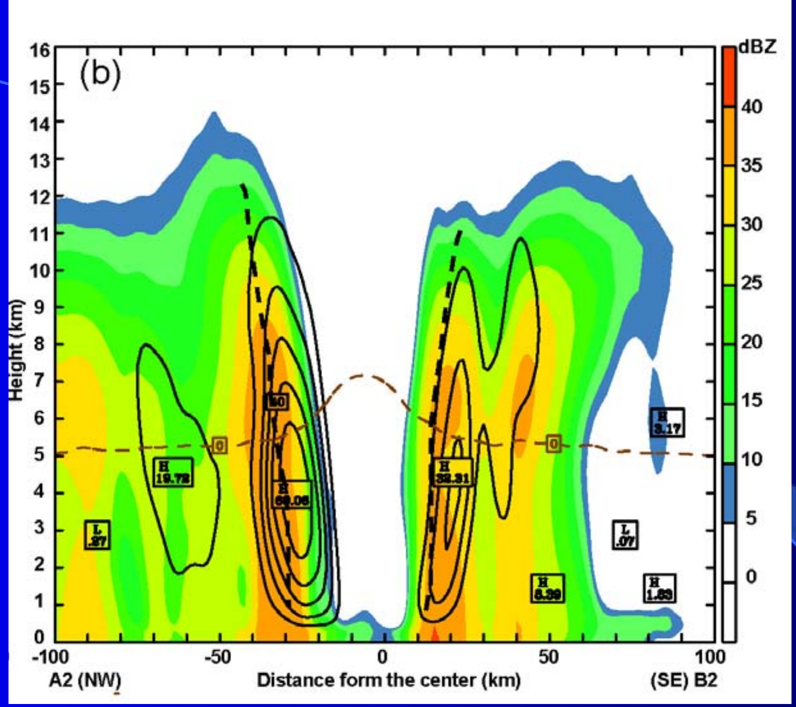


# Before Landfall

Radar Echo (color)
Condensational Heating (contour)

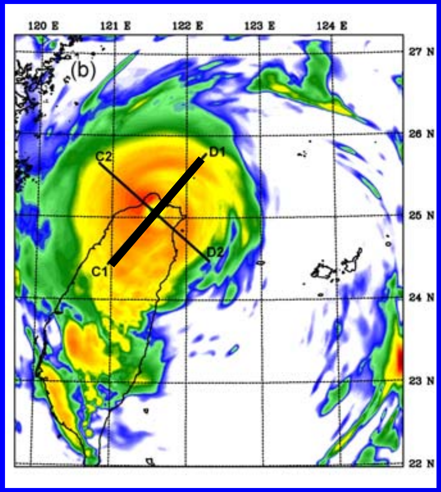


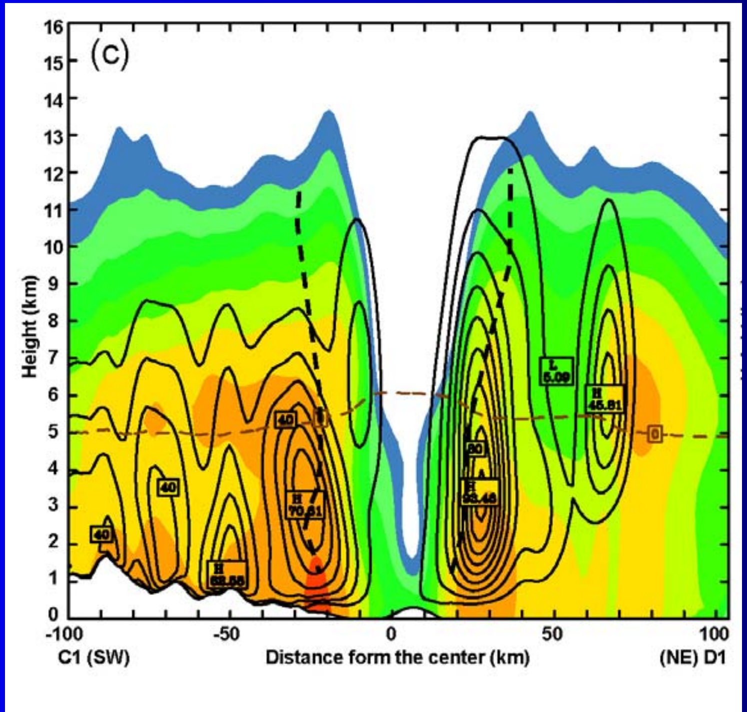


# After Landfall

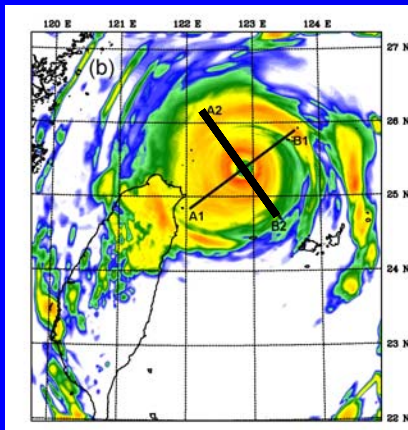


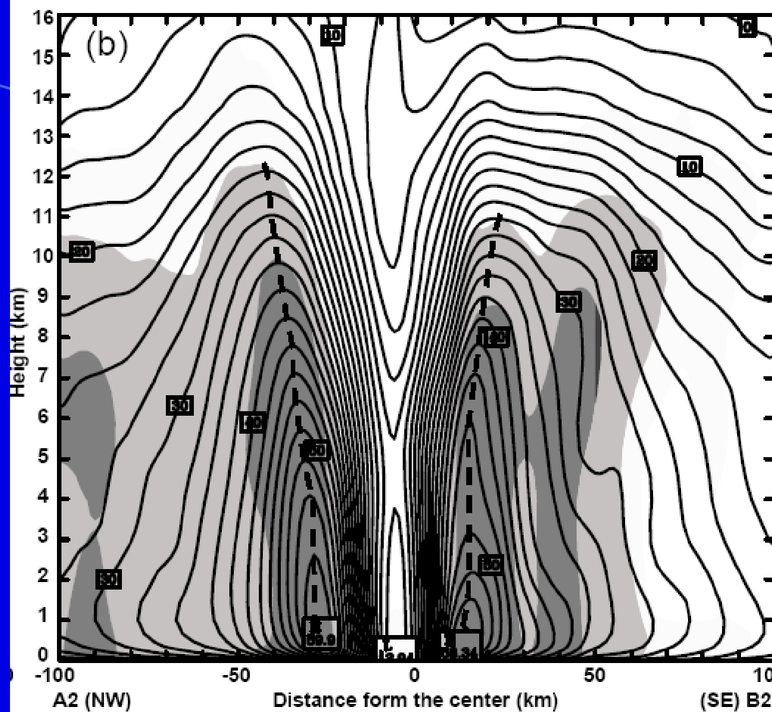


# Before Landfall

Radar Echo (shading)
Tangential Velocity (contour)

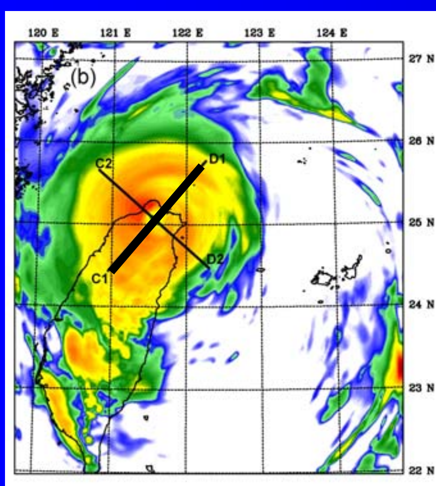


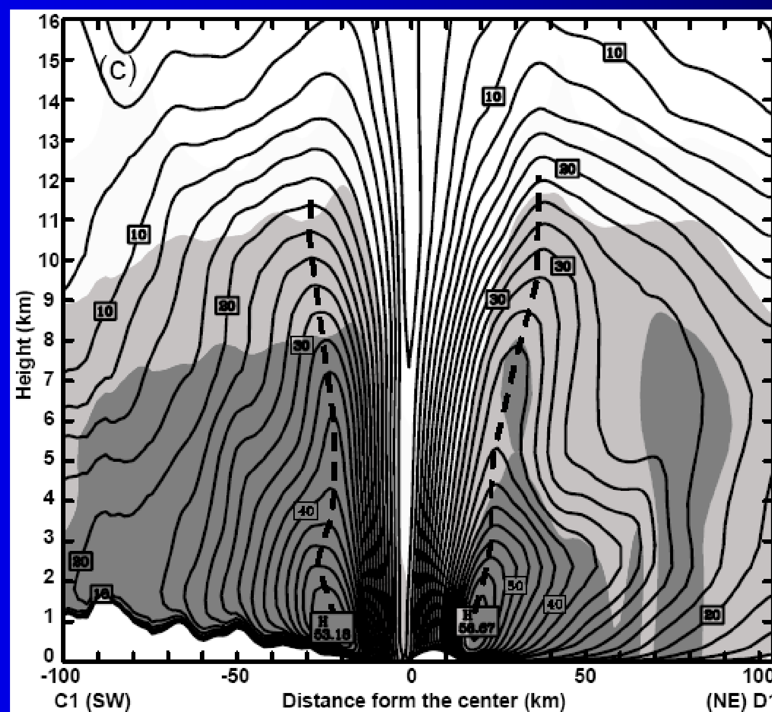


# After Landfall

## Before Landfall

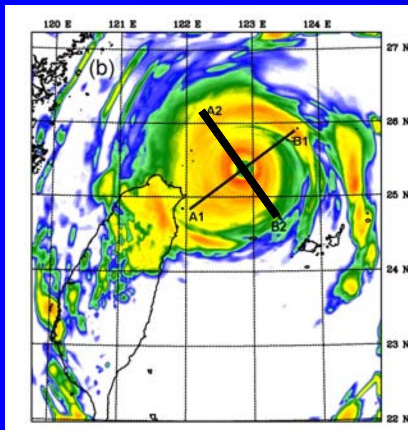


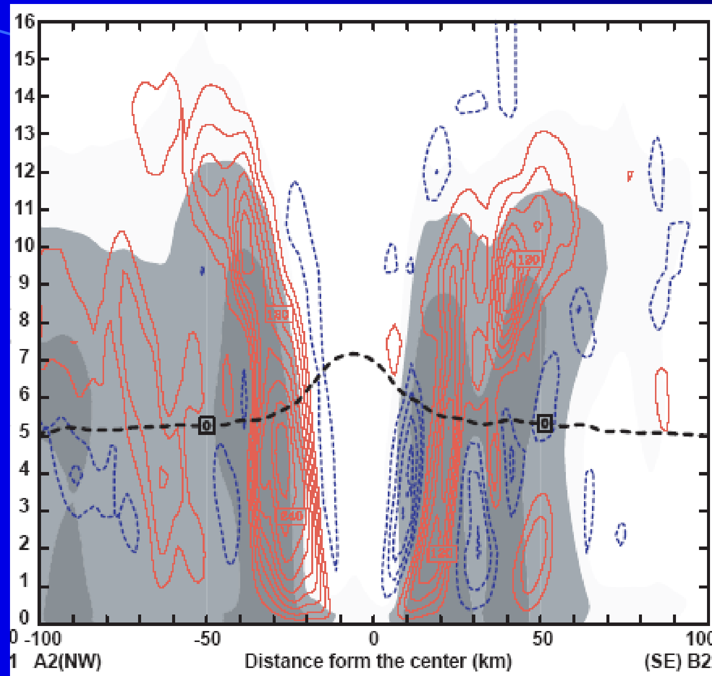


Radar Echo (shading)
Updraft (solid red)
Downdraft (dashed blue)

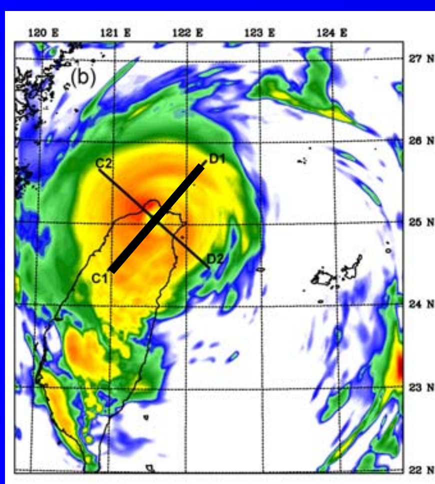


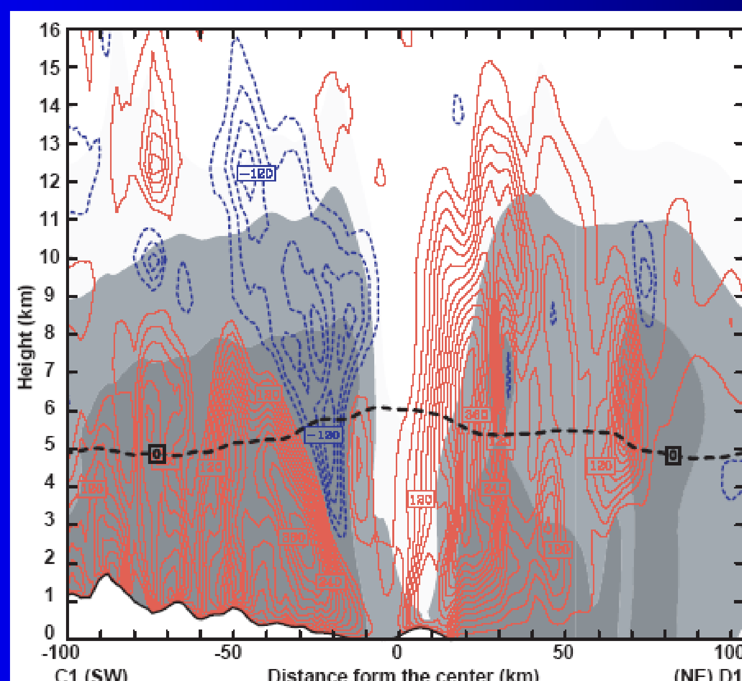


## After Landfall

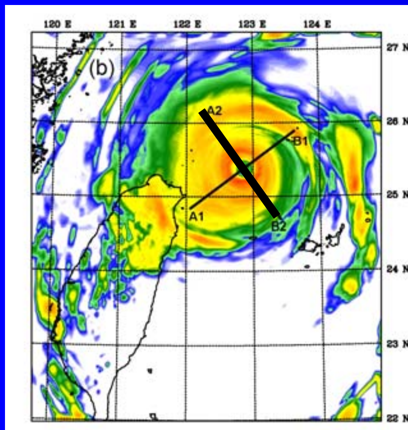


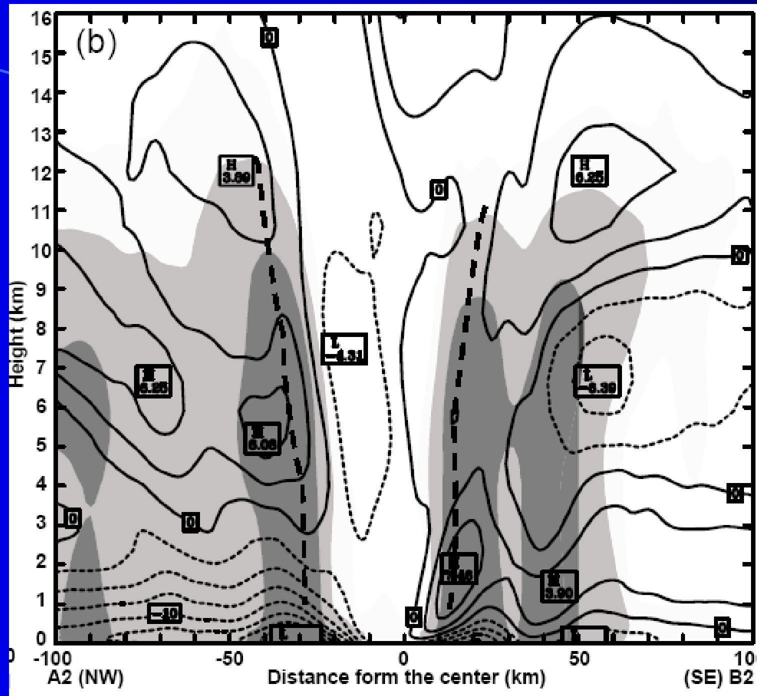


**Before Landfall**

Radar Echo (shading)
Radial Velocity
(contour)

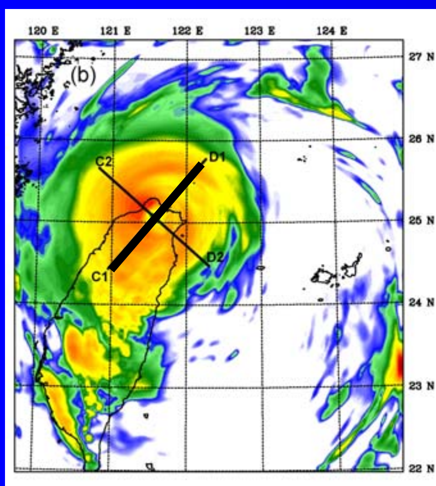


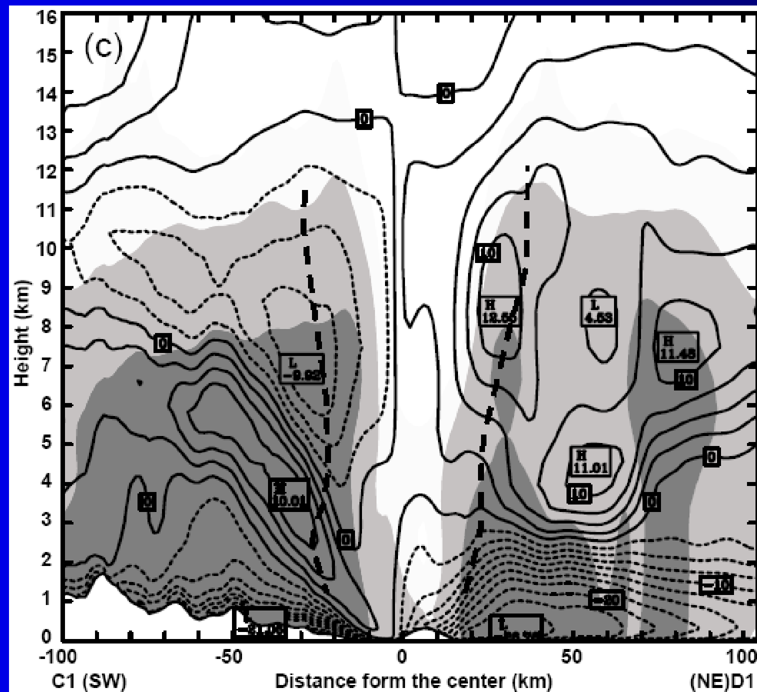


**After Landfall**

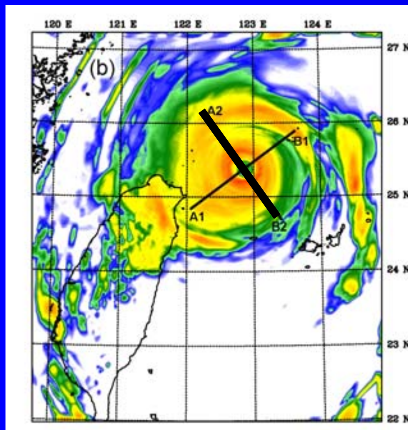


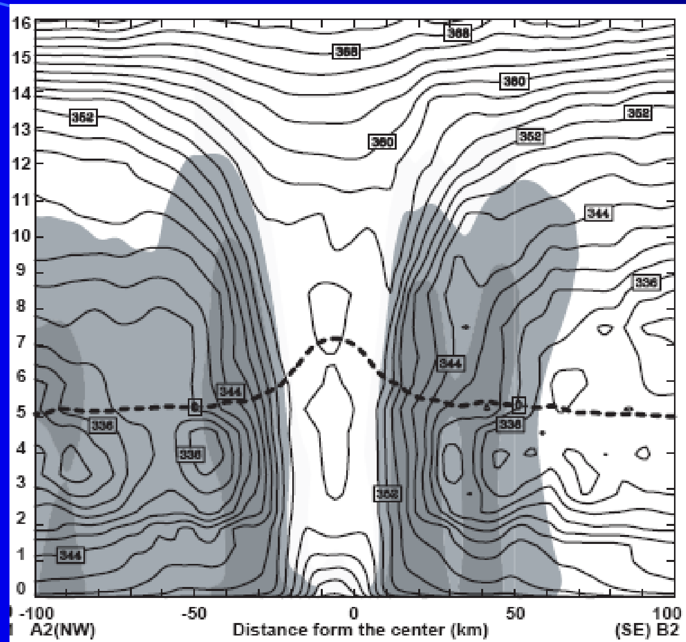


# Before Landfall

Radar Echo (shading)
Theta-E (Contour)

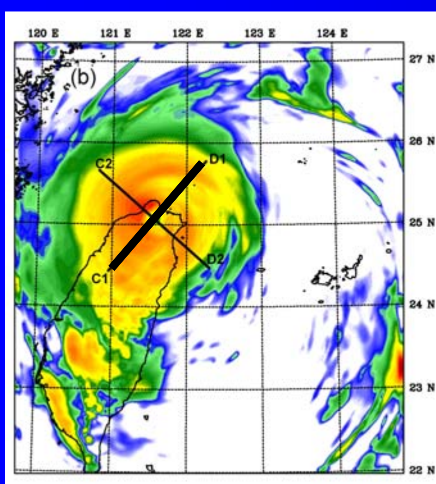


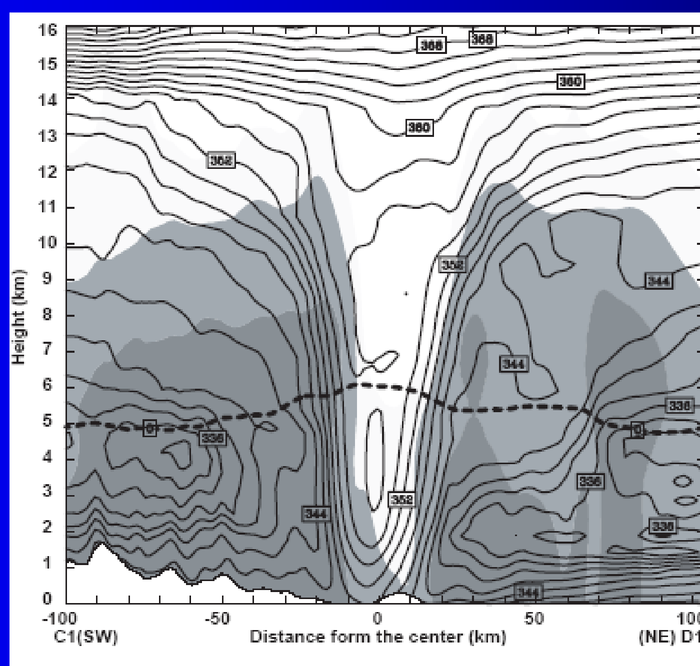


# After Landfall

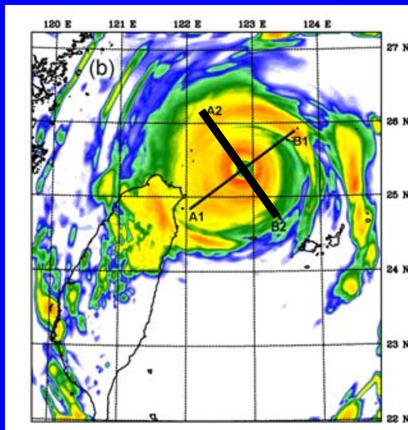


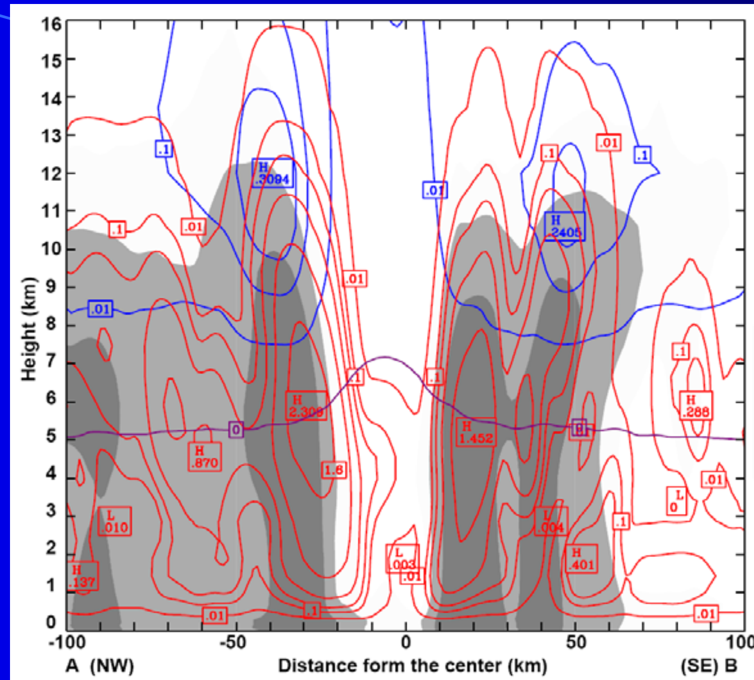


## Before Landfall

Radar Echo (shading)
Cloud Ice (blue line)
Cloud Water (red line)

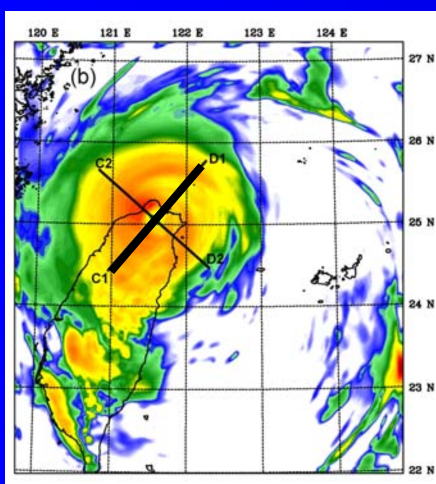


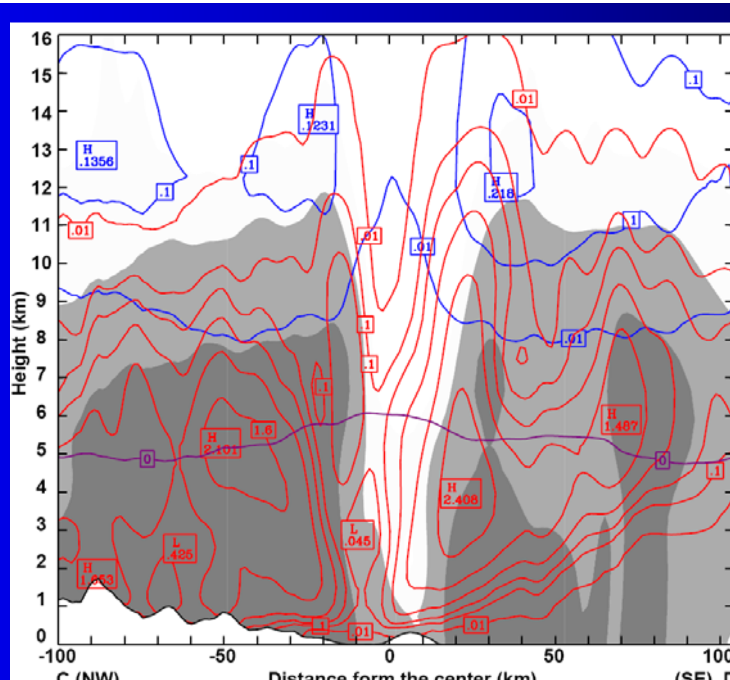


## After Landfall

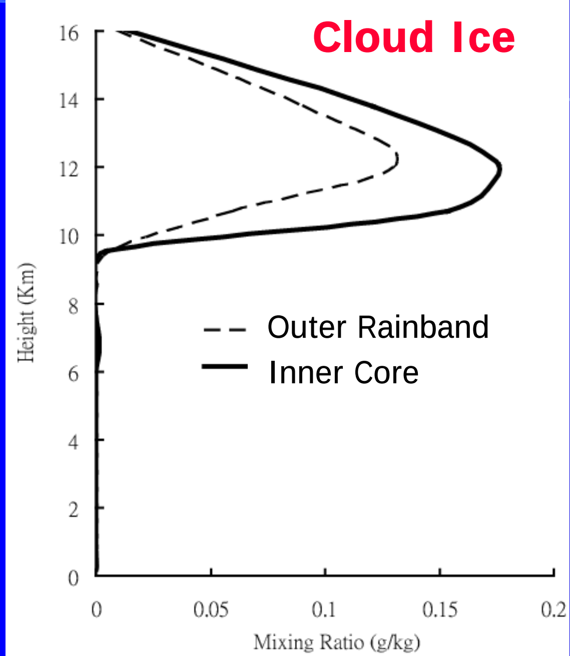


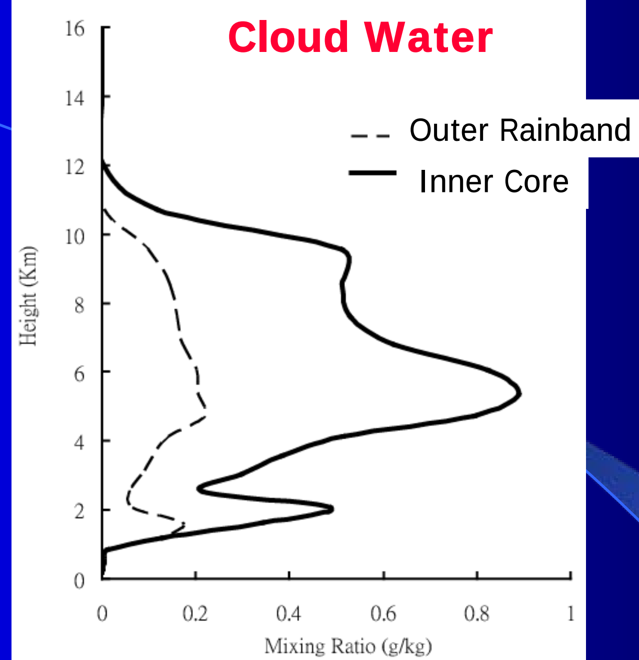


**Before Landfall**

Cloud Water

Cloud Ice

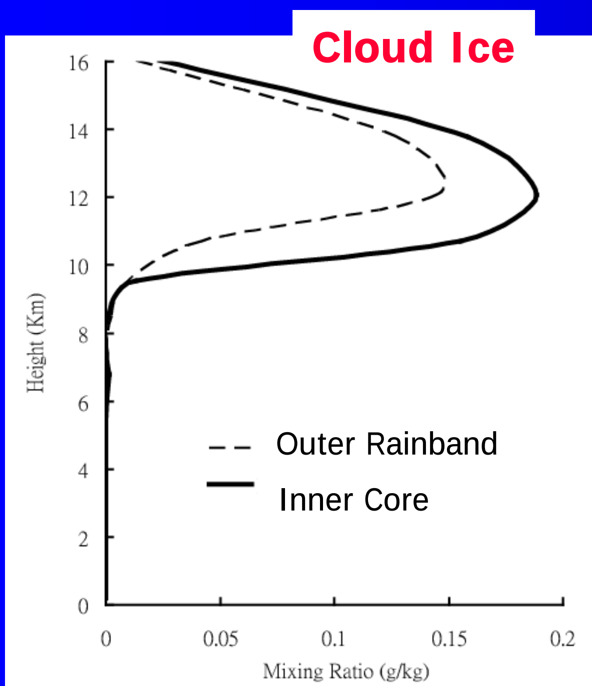


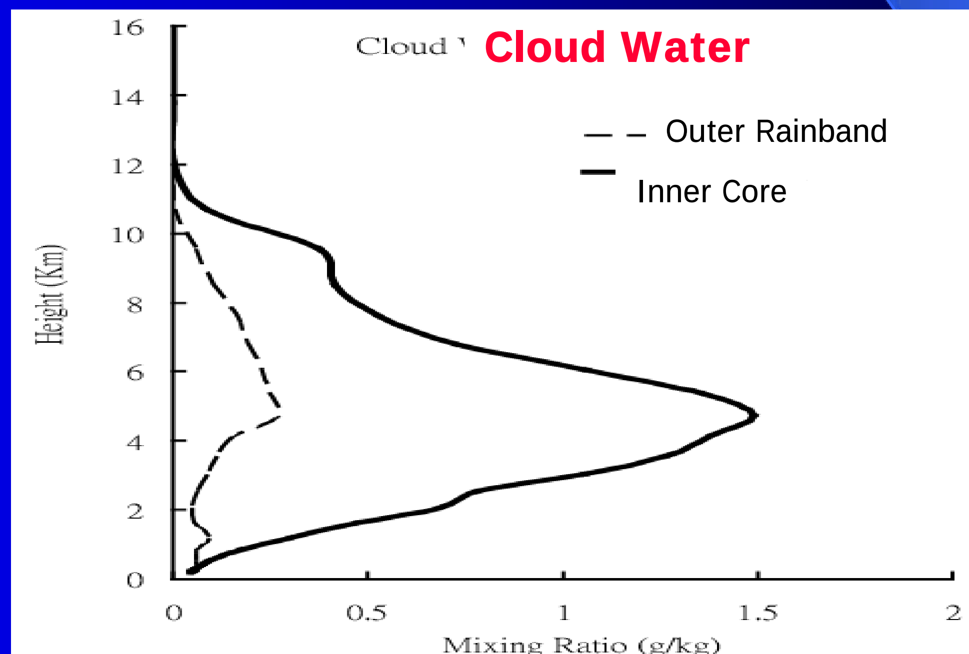


**After Landfall**

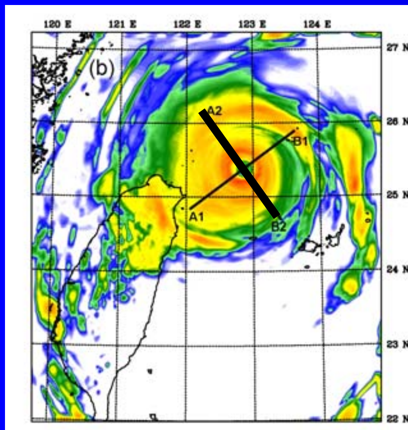


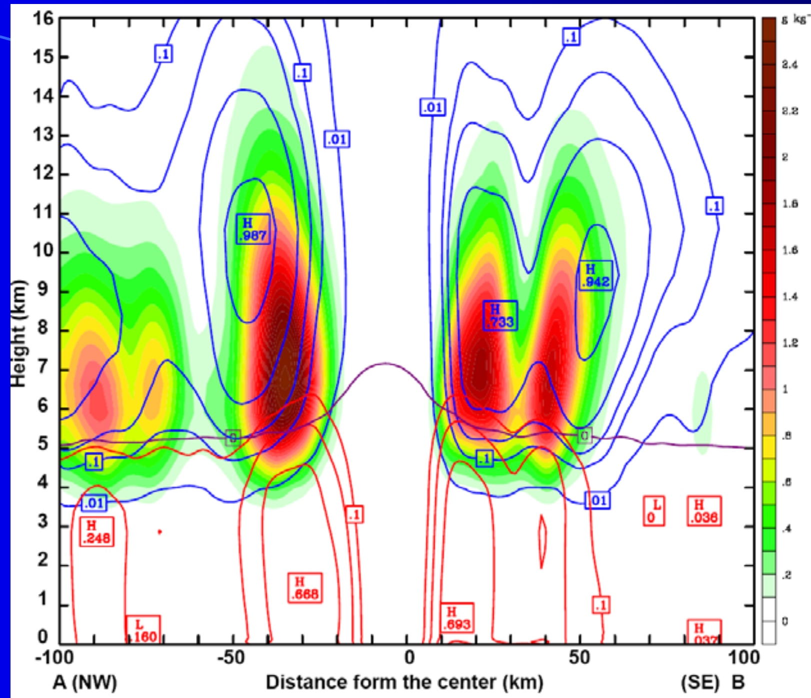


# Before Landfall

Snow (blue line)
Rain (red line)
Graupel (colored)

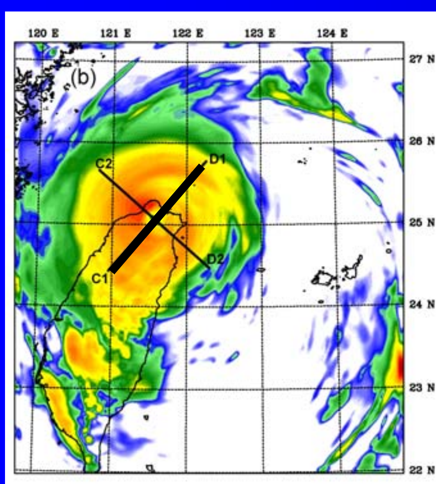


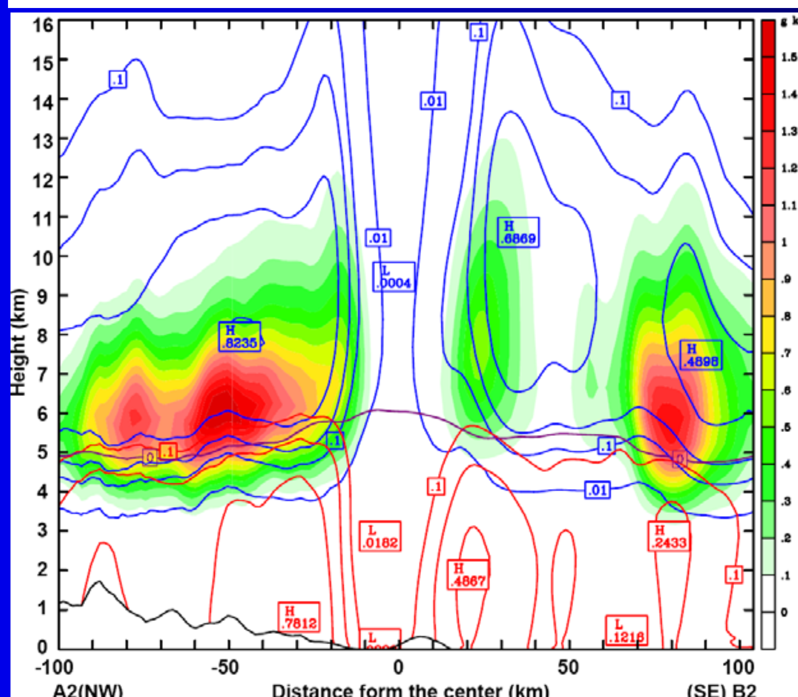


# After Landfall

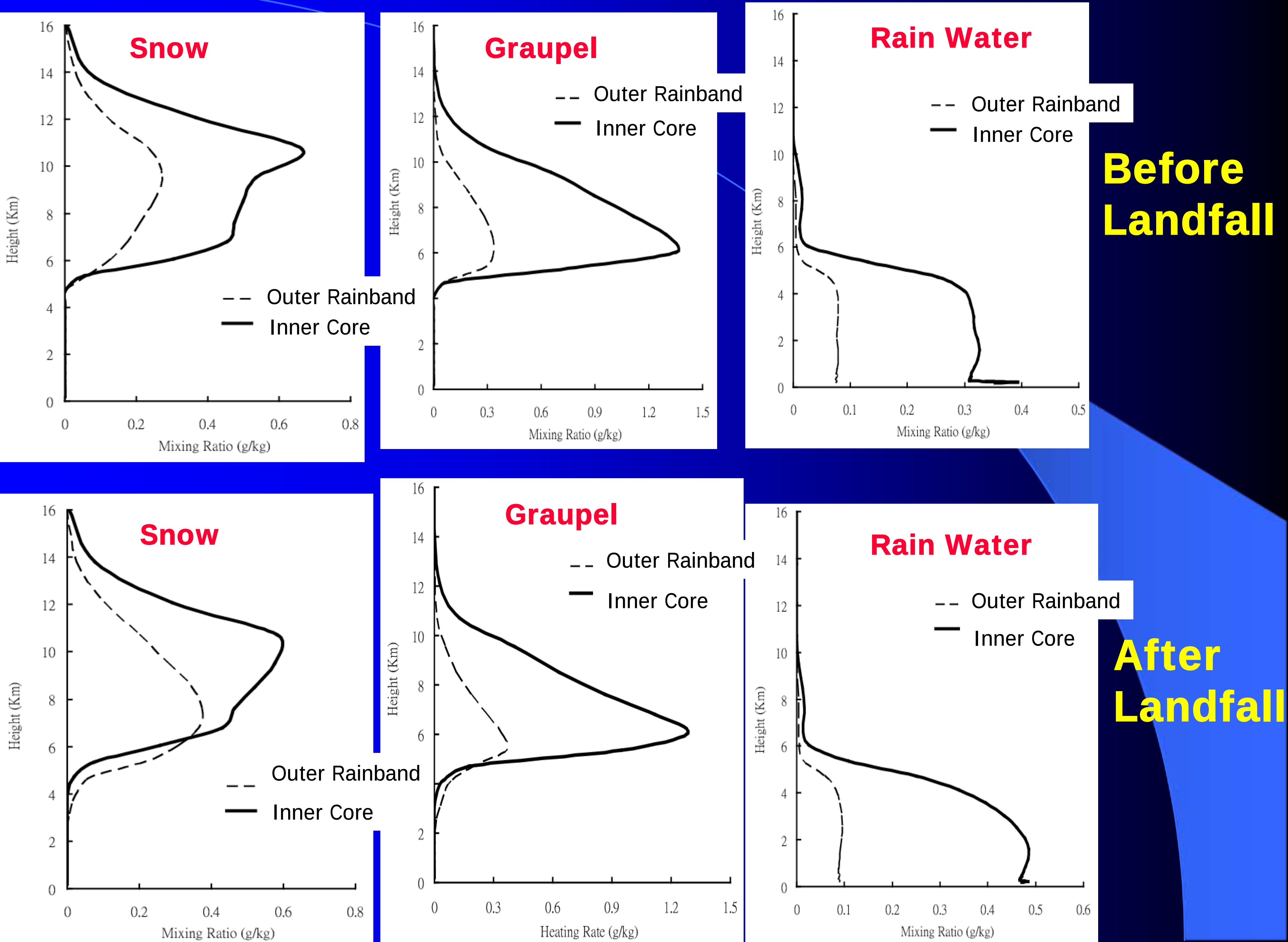
Snow
Outer Rainband
Inner Core
Height (Km)
Mixing Ratio (g/kg)
Graupel
Outer Rainband
Inner Core
Height (Km)
Mixing Ratio (g/kg)
Rain Water
Outer Rainband
Inner Core
Height (Km)
Mixing Ratio (g/kg)
Before Landfall
Snow
Outer Rainband
Inner Core
Height (Km)
Mixing Ratio (g/kg)
Graupel
Outer Rainband
Inner Core
Height (Km)
Heating Rate (g/kg)
Rain Water
Outer Rainband
Inner Core
Height (Km)
Mixing Ratio (g/kg)
After Landfall

## Before Landfall

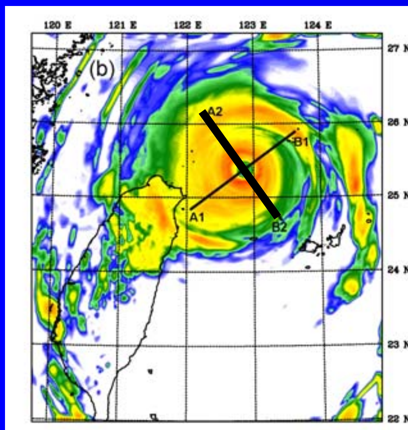


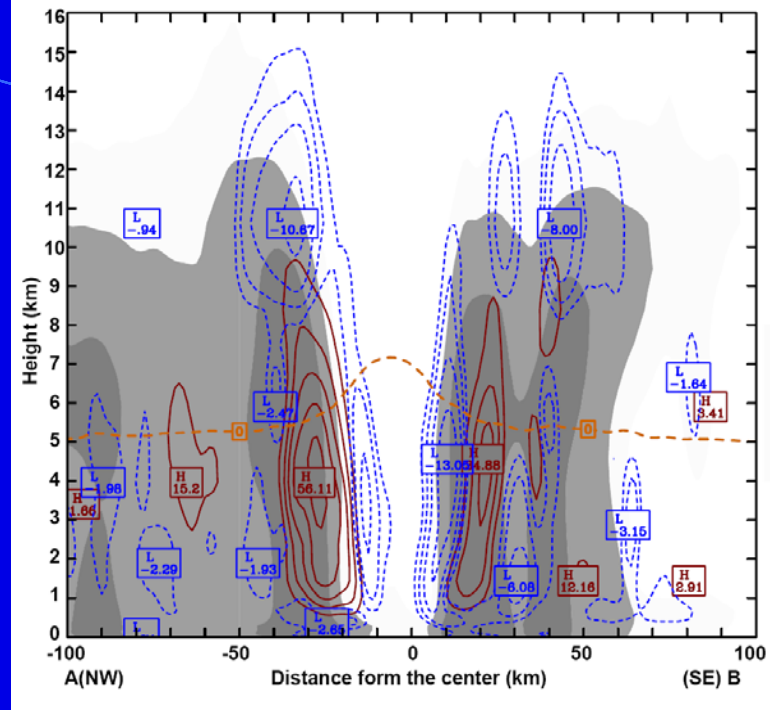


Condensation Heating (solid line)
Evaporation Cooling (dashed line)

## After Landfall

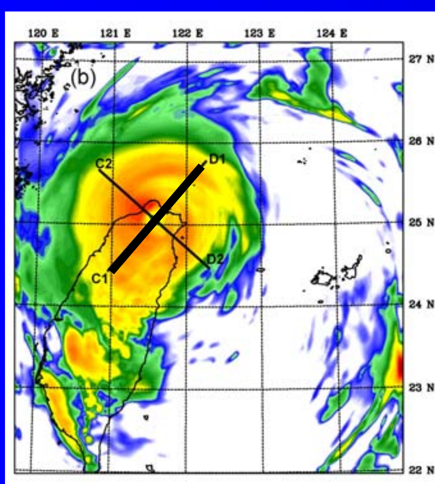


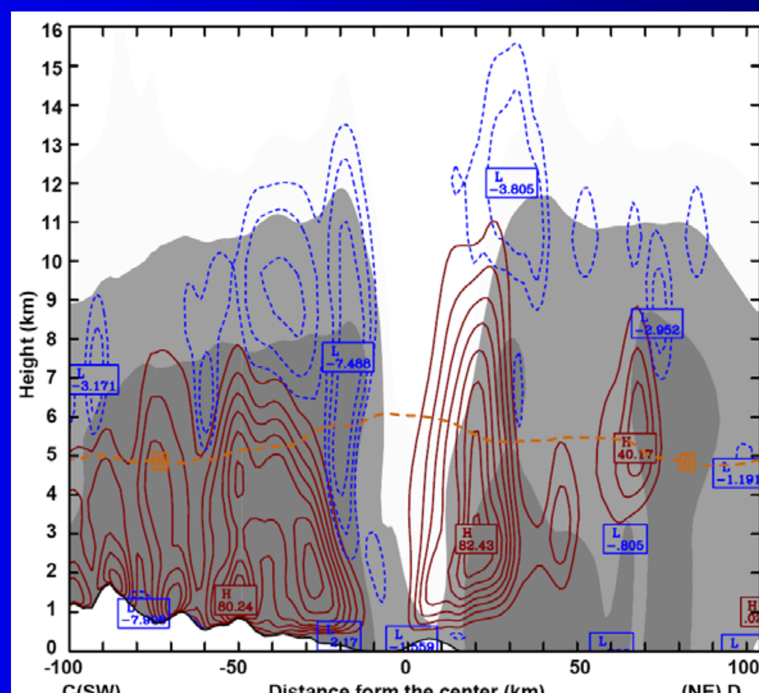

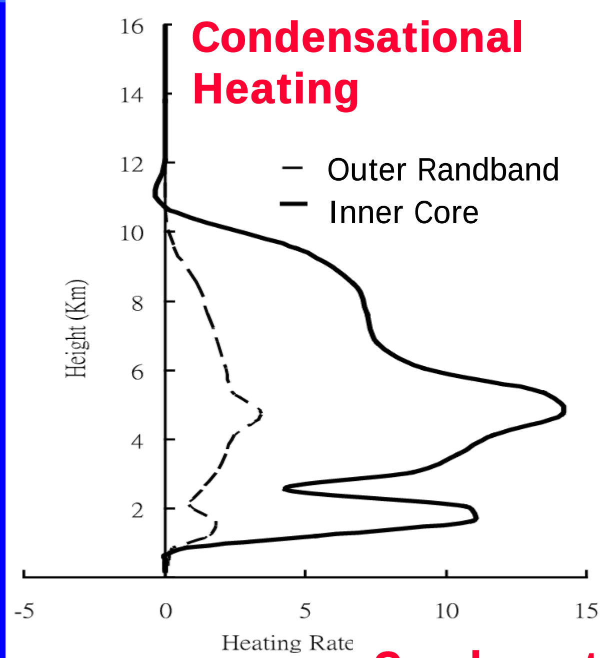


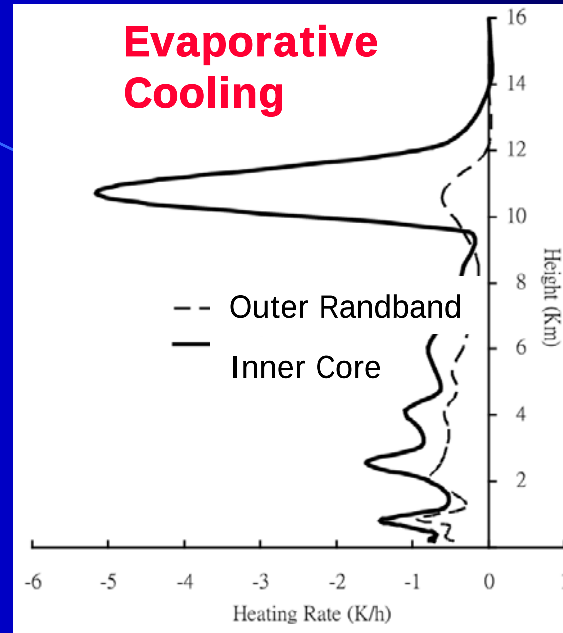


**Before Landfall**

Condensation Heating

Evaporative Cooling

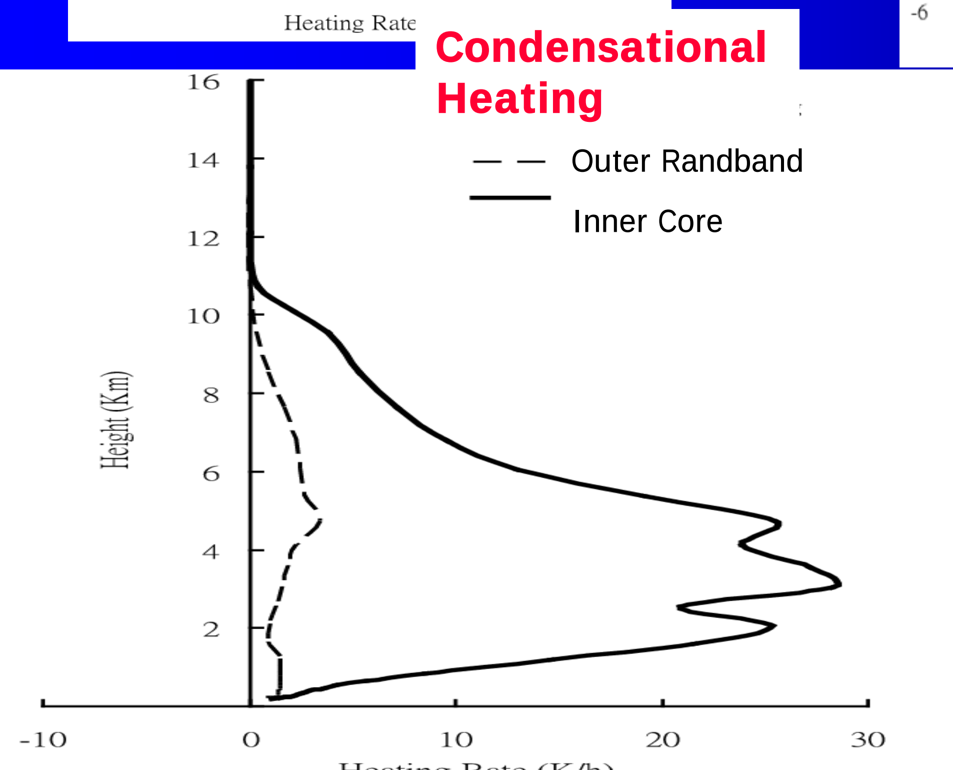


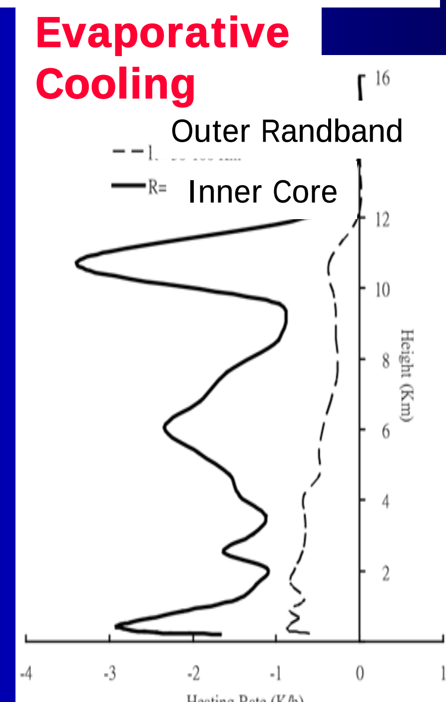


**After Landfall**

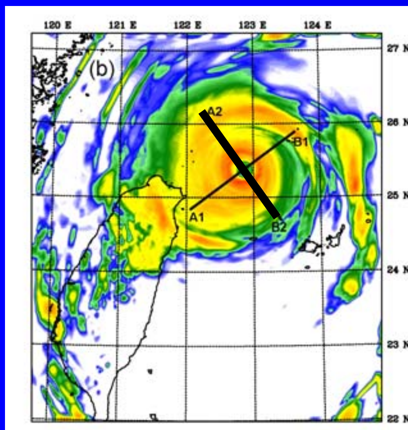


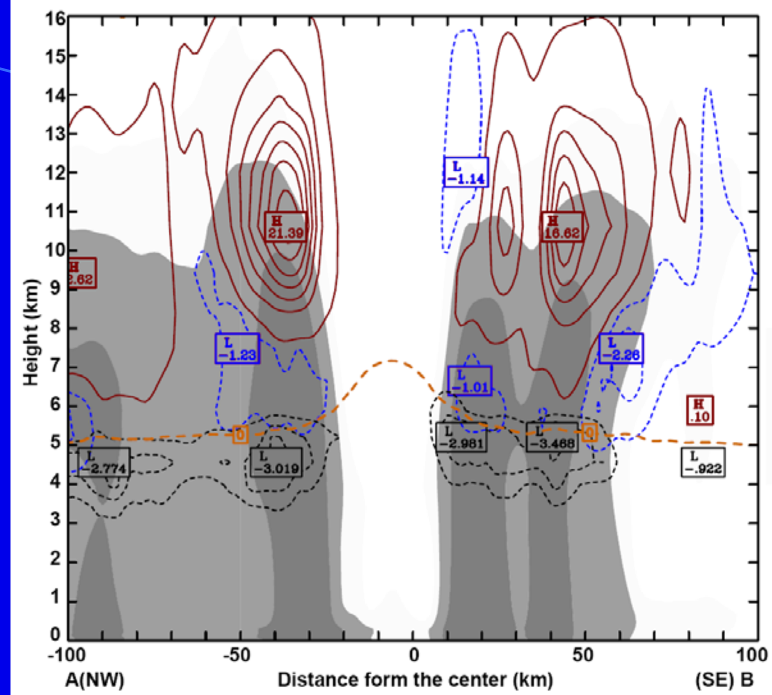


# Before Landfall

Deposition Heating (solid black)

Sublimative Cooling (dashed blue)

Melting Cooling (dashed black)

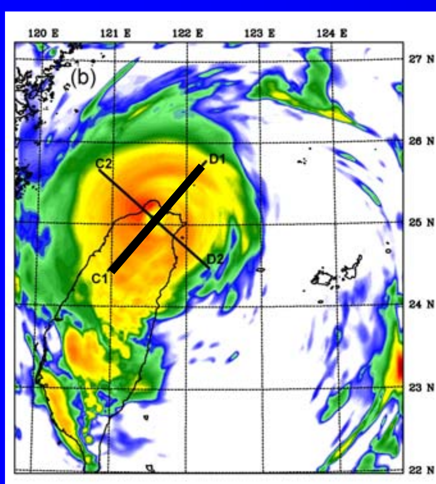


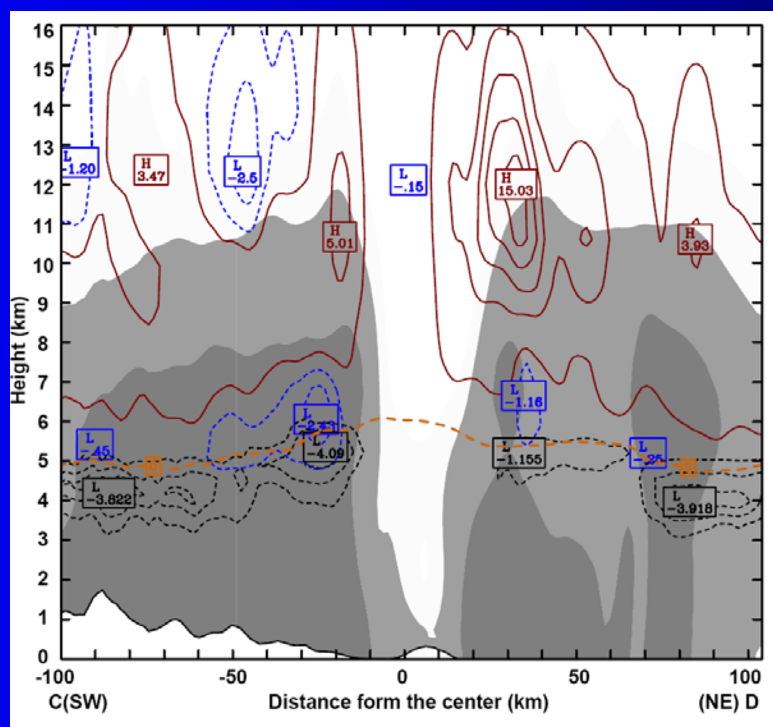


# After Landfall

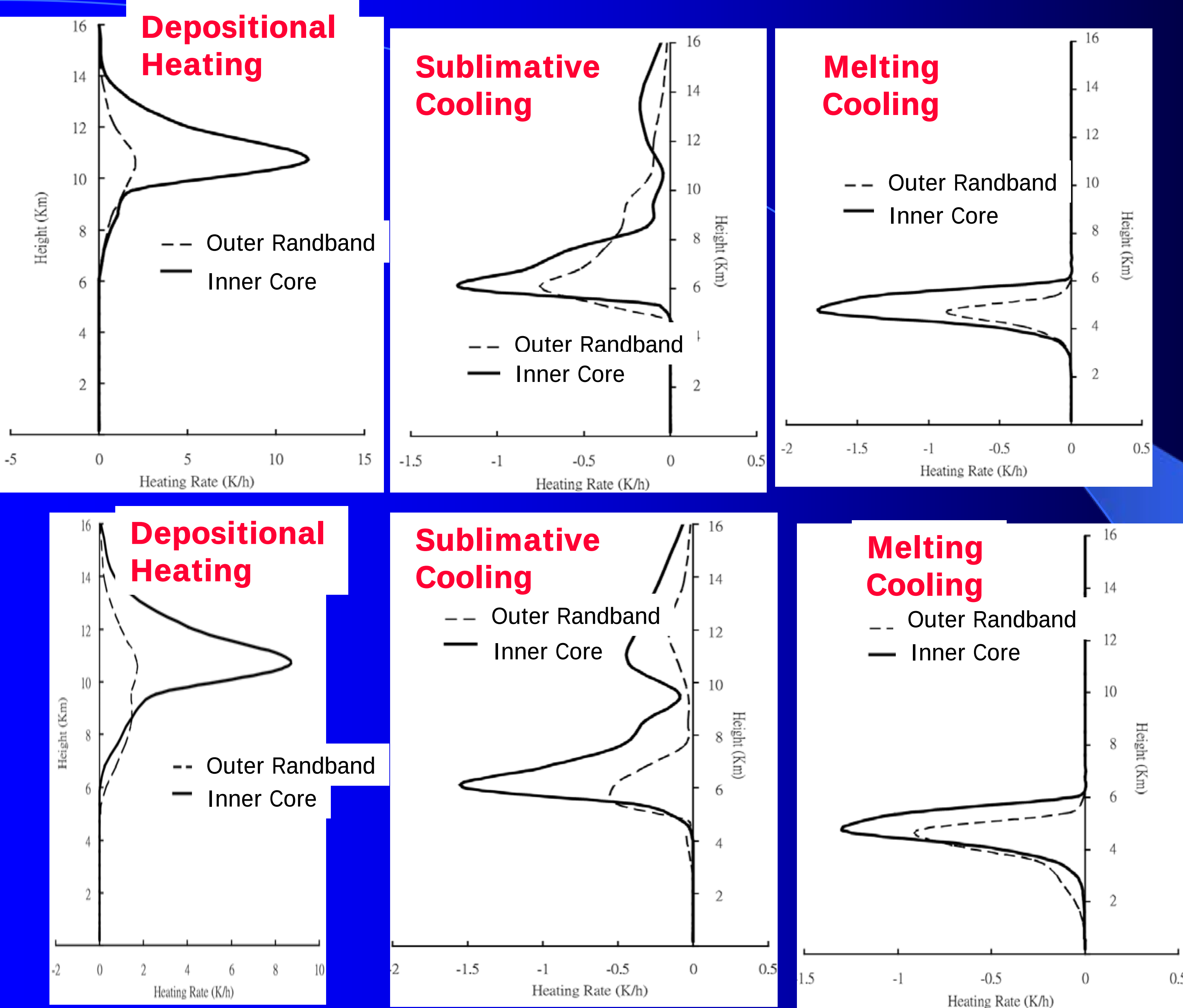


Before Landfall

After Landfall

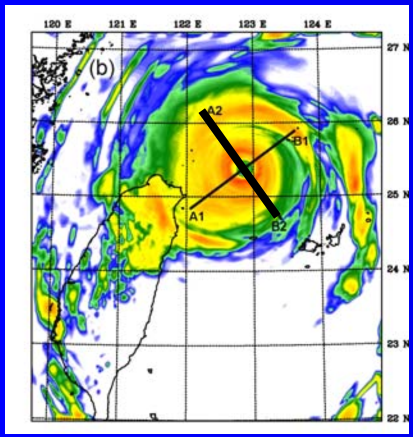


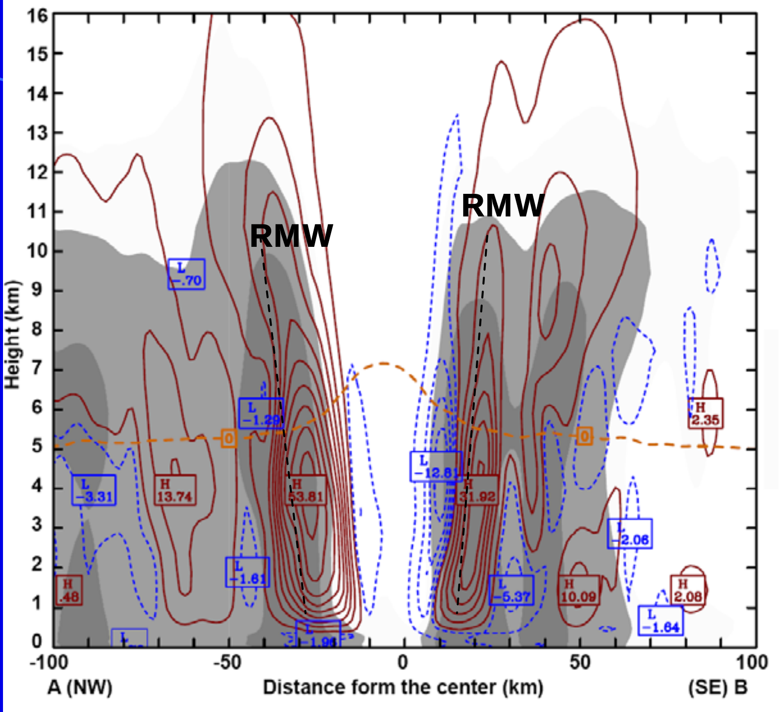


# Before Landfall

Total Latent Heating
(solid black)
Total Latent Cooling
(dashed blue)

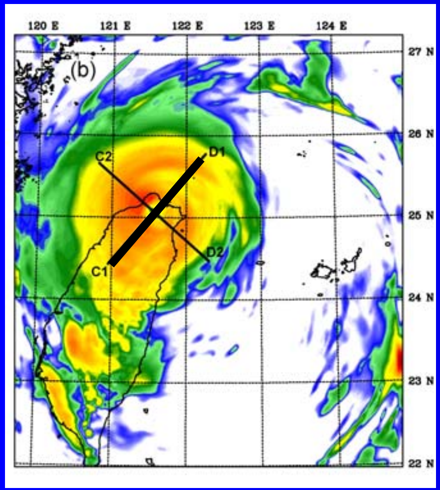


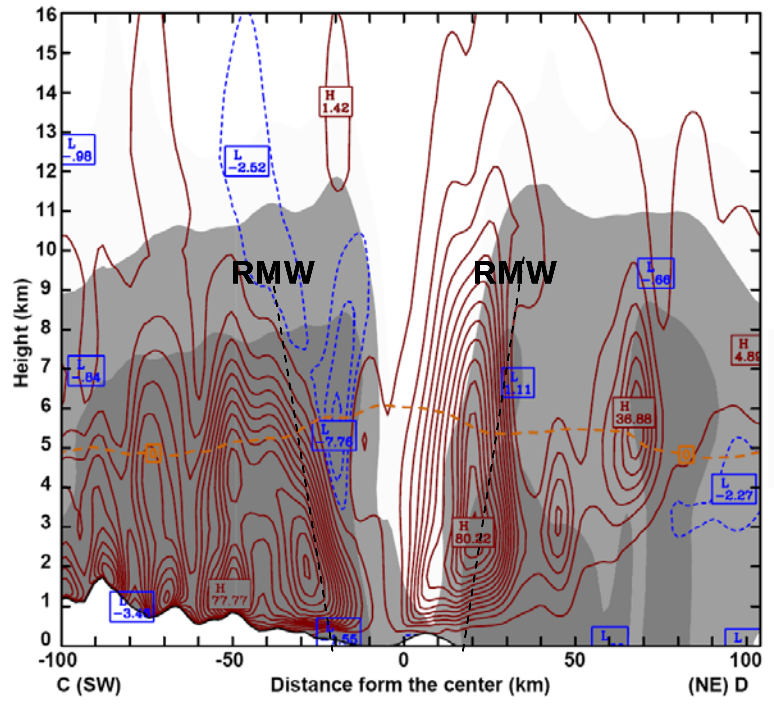


# After Landfall

# Before Landfall

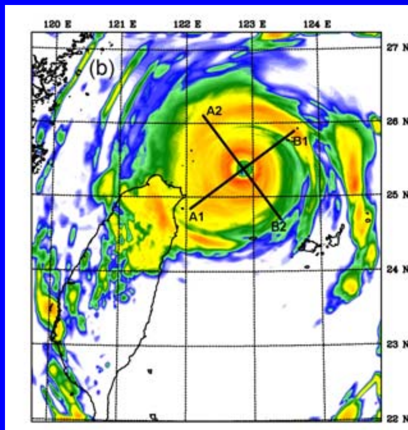


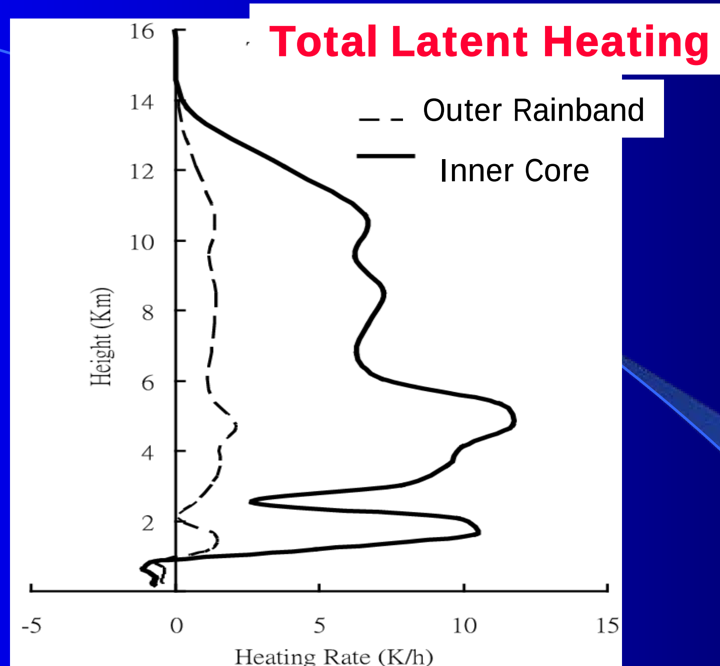


Total Latent Heating
& Cooling

# After Landfall

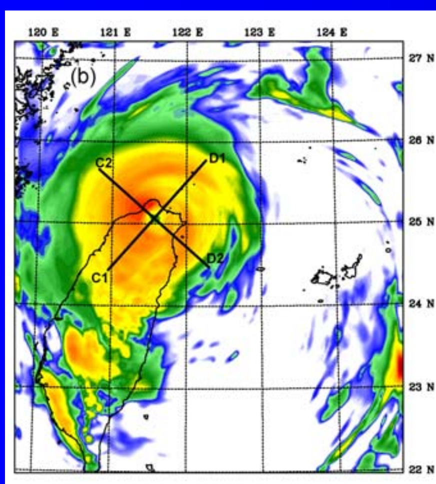


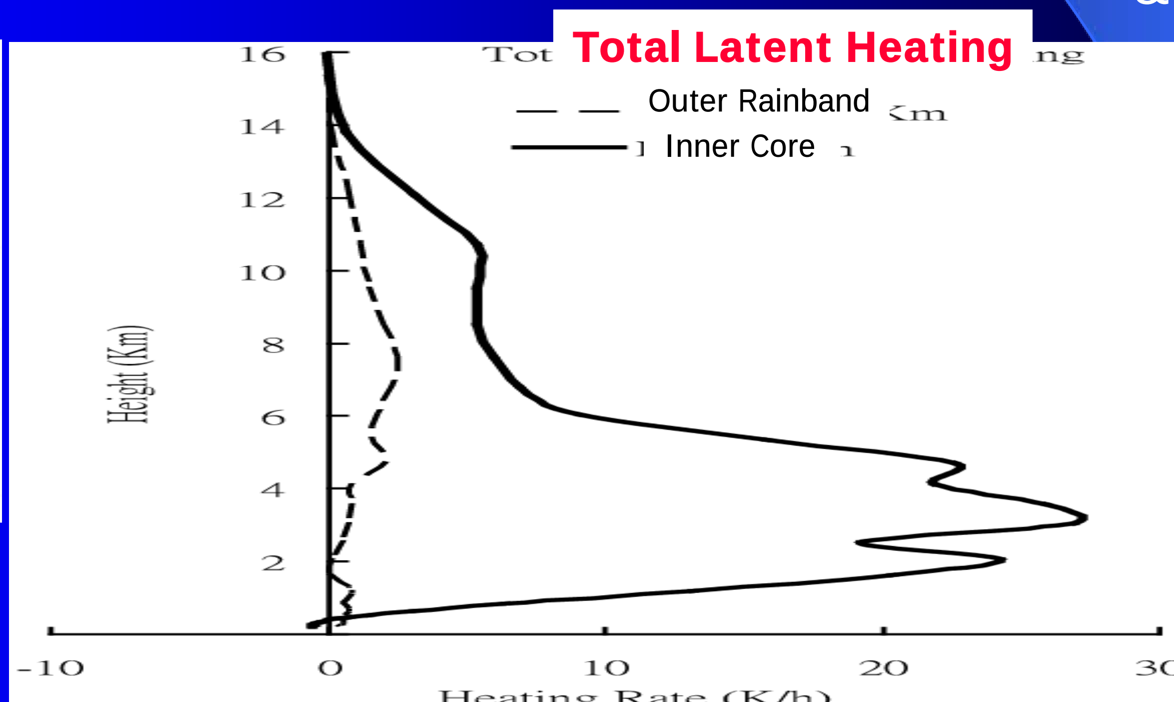

## Midlatitude MCS/Cv

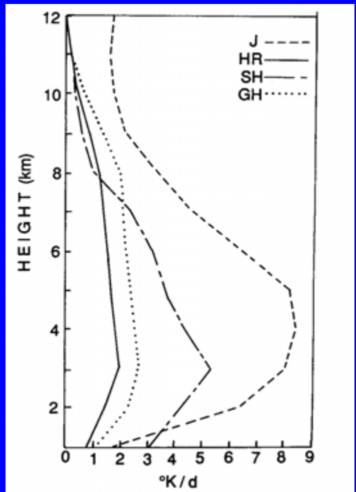


Houze (1989; QJRMS)

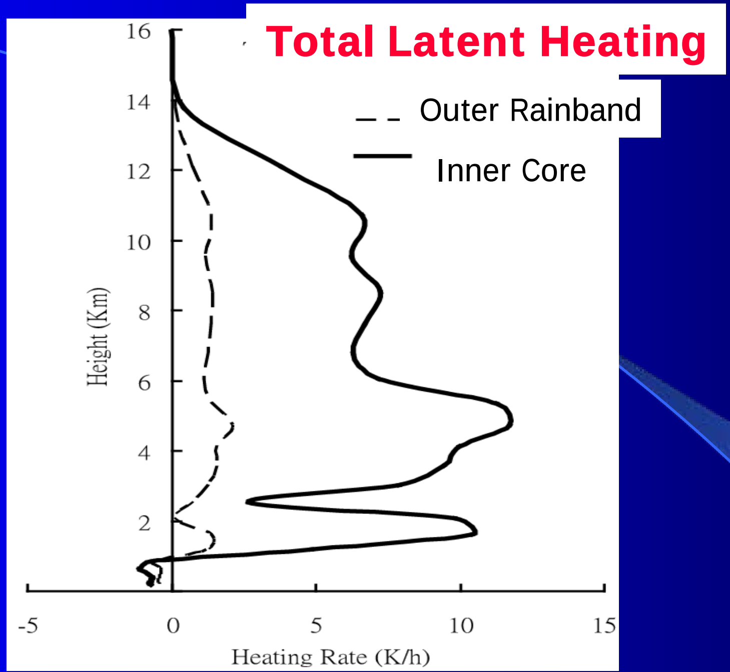


# Before Landfall

Total Latent Heating
& Cooling

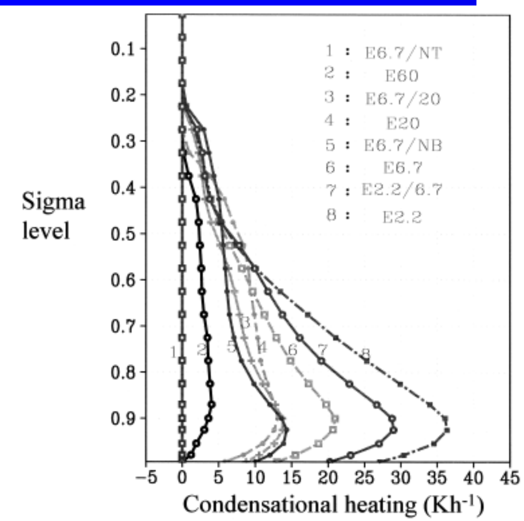


FIG. 12. Same as Fig. 11 but for condensational heating (K h$^{-1}$).

Wu et al. (2002; WAF)

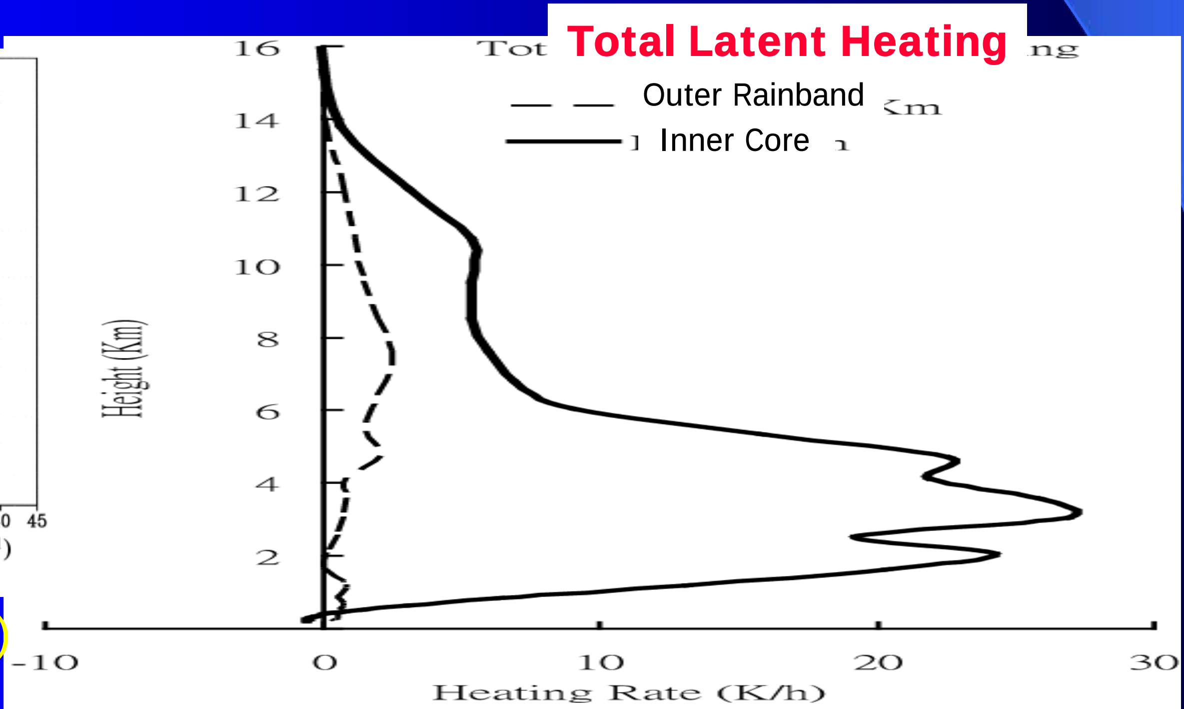


# After Landfall

# Trajectory Analyses

# Air-Parcel Forward Trajectories (t= 6-24 h) Starting @ R=30 km; sigma=0.95

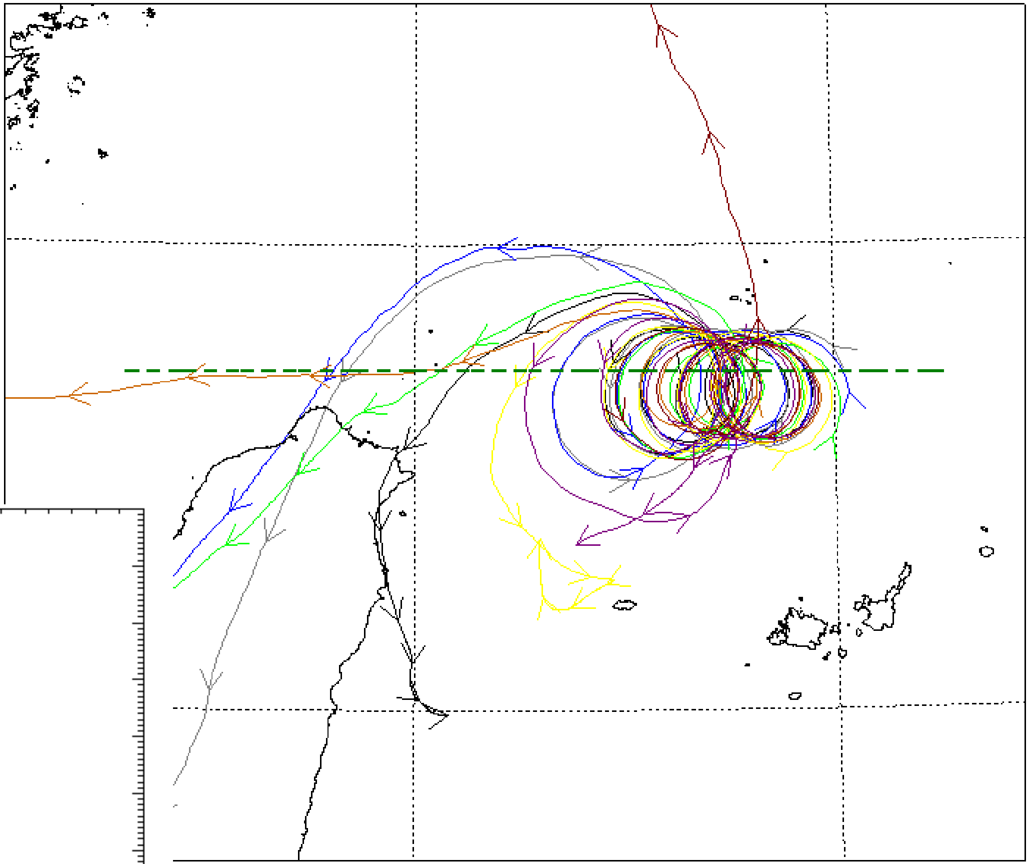

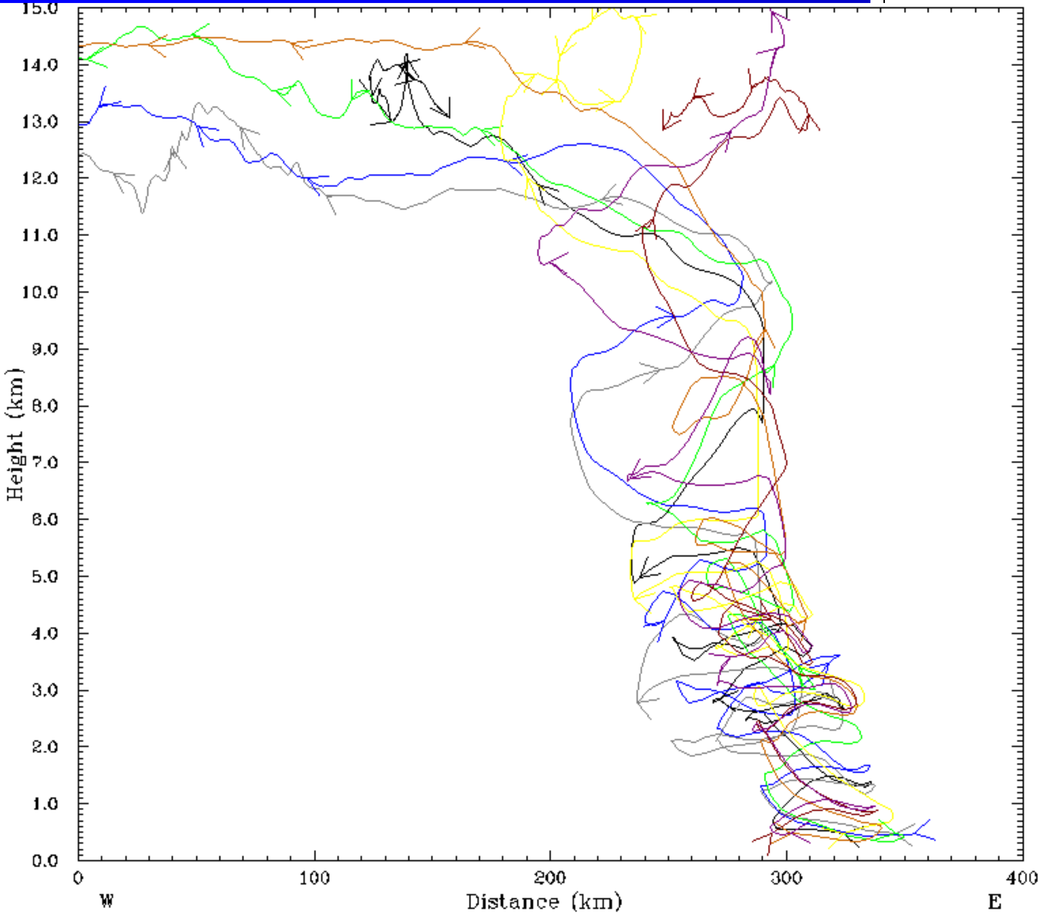

# Air-Parcel Forward Trajectories (t= 24-42 h) Starting @ R=30 km; sigma=0.95

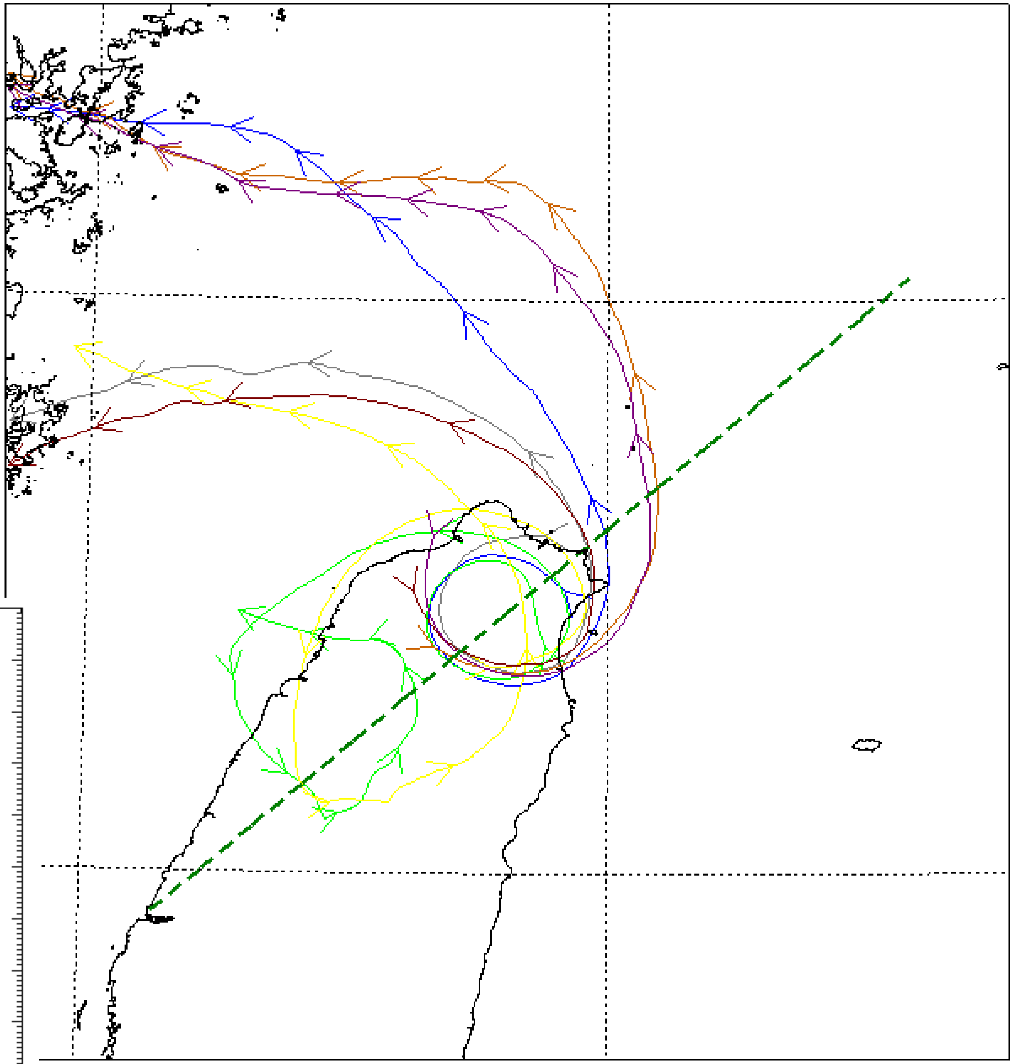

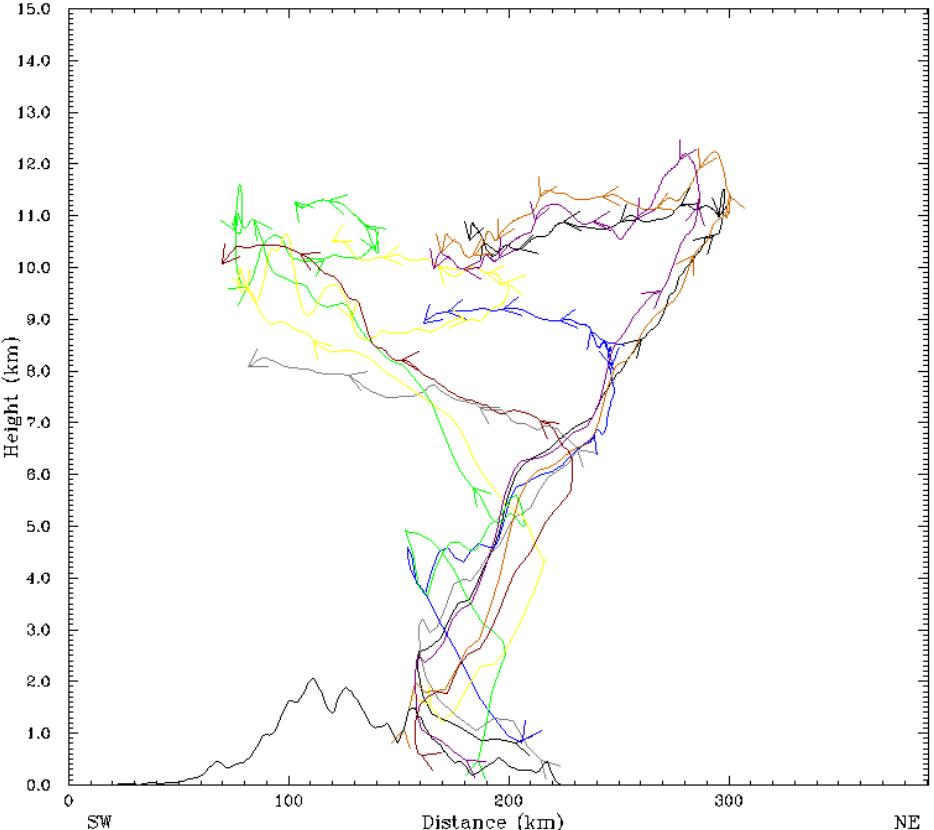

# 24-06h backward hydrometeor trajectories starting @ R=30km; sigma=0.995

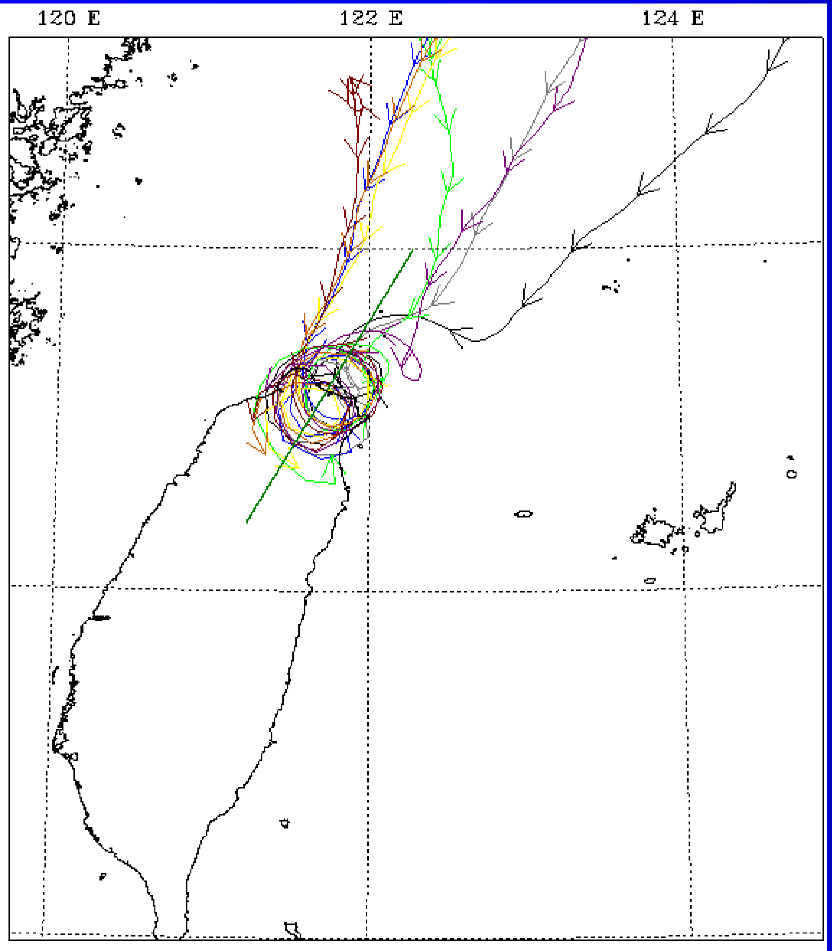


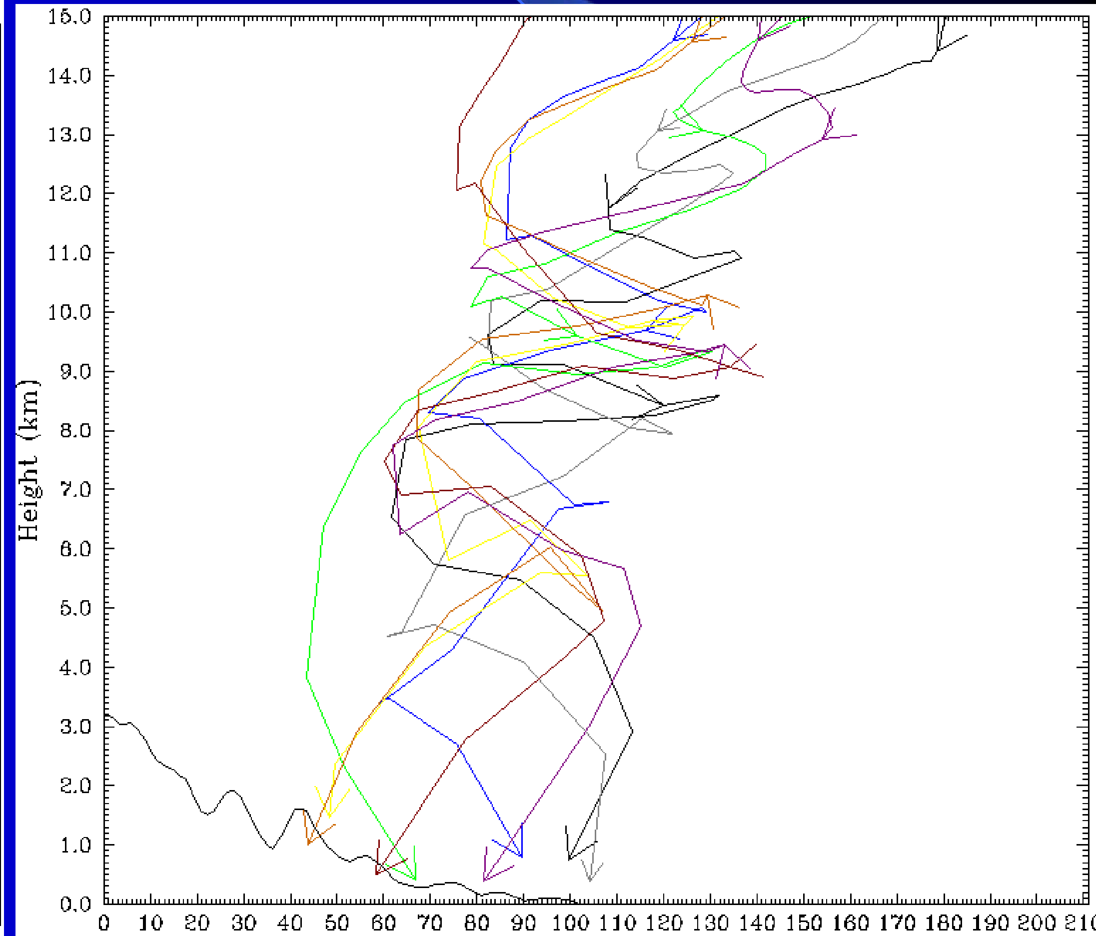

# 24-h Accumulated Rainfall on 09/17

OBS

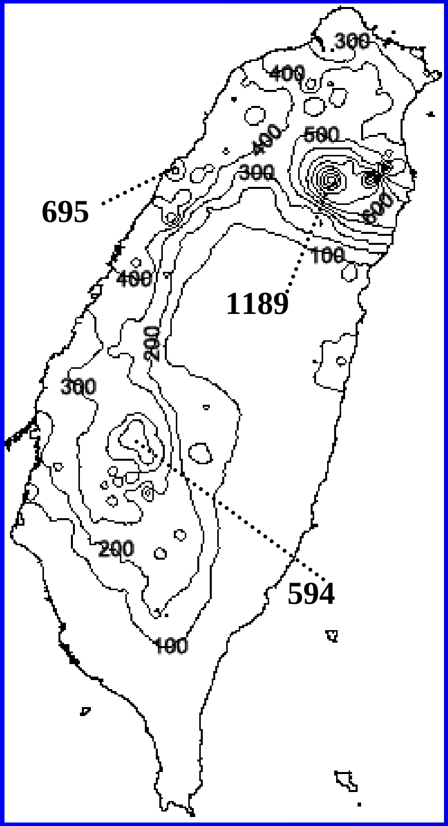


6km MM5

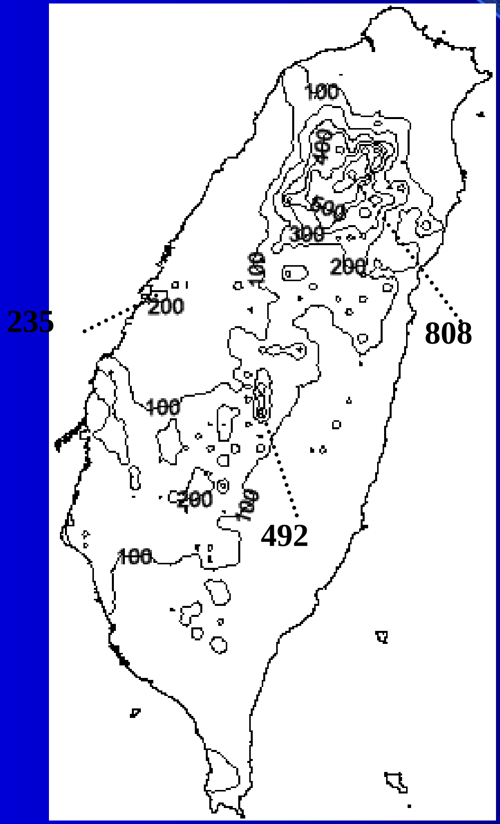


2km MM5

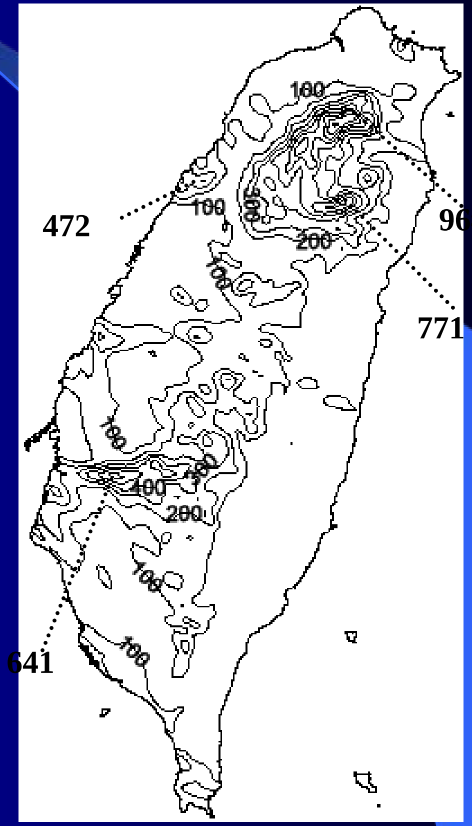

# 42-24h backward hydrometeor trajectories starting @ R=30km; sigma=0.995

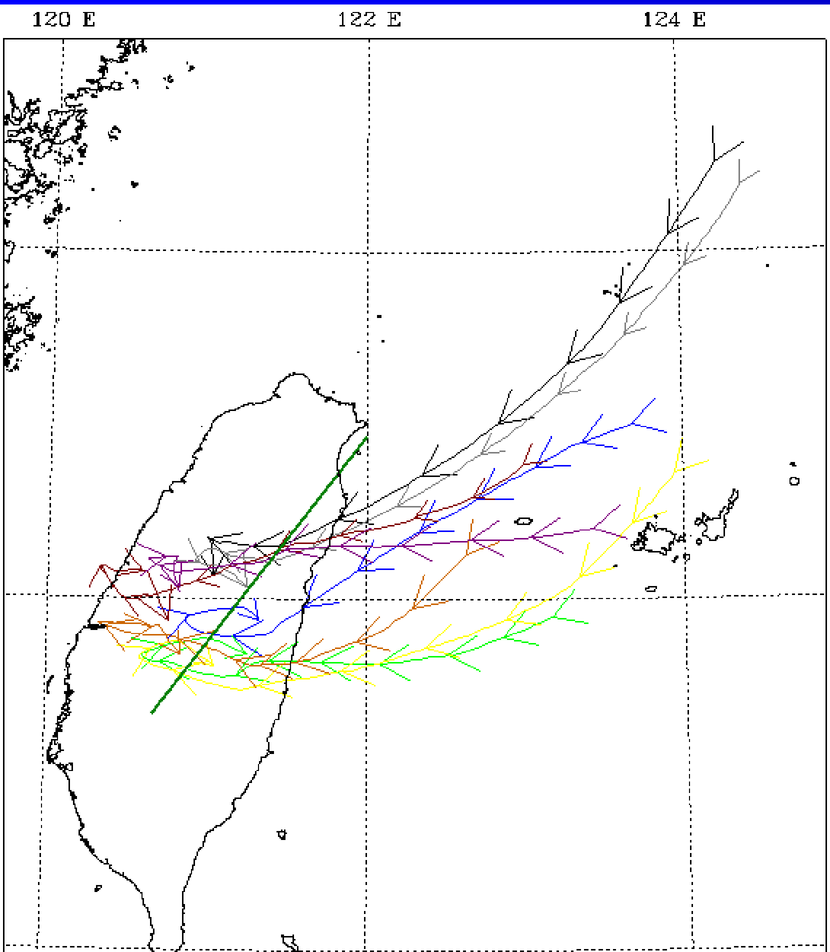


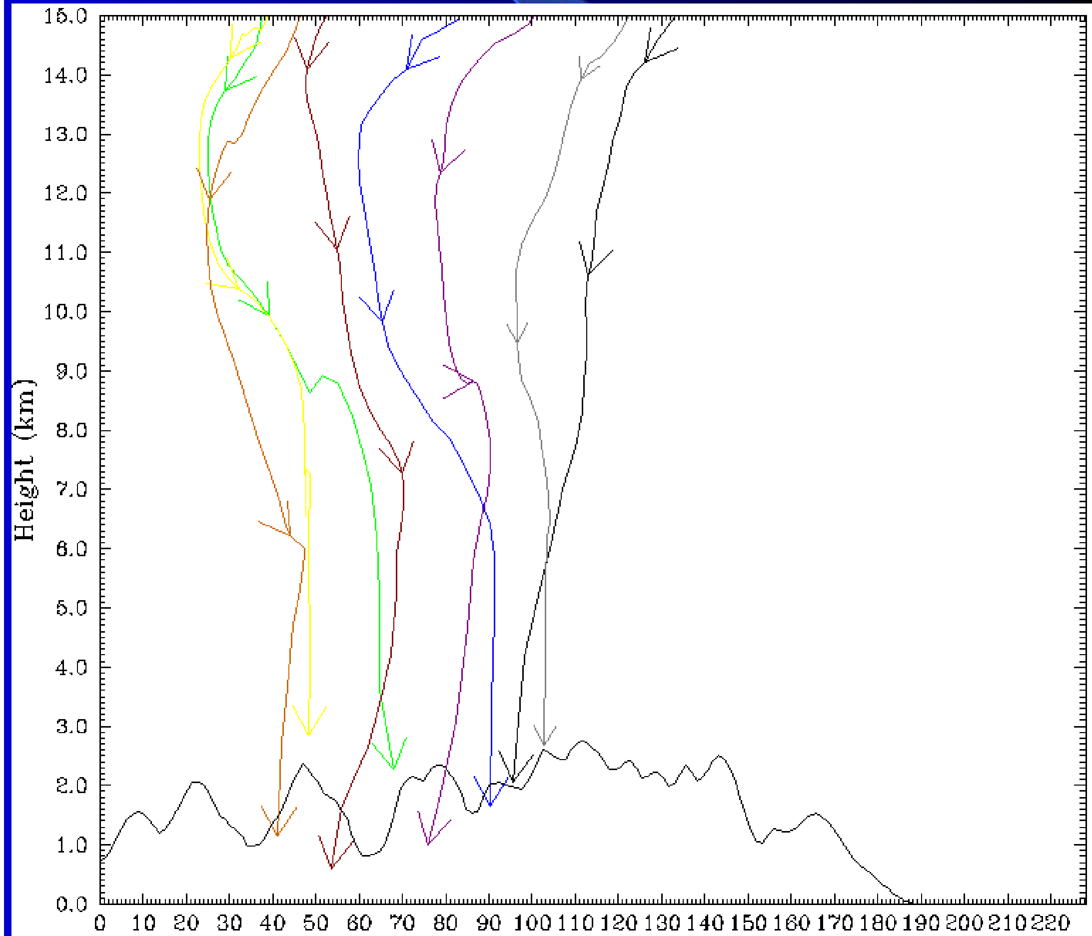

# Axisymmetric Structure (Before vs. After Landfall)

# Azimuthal-avg. structure (r=200 km) while Nari is over ocean

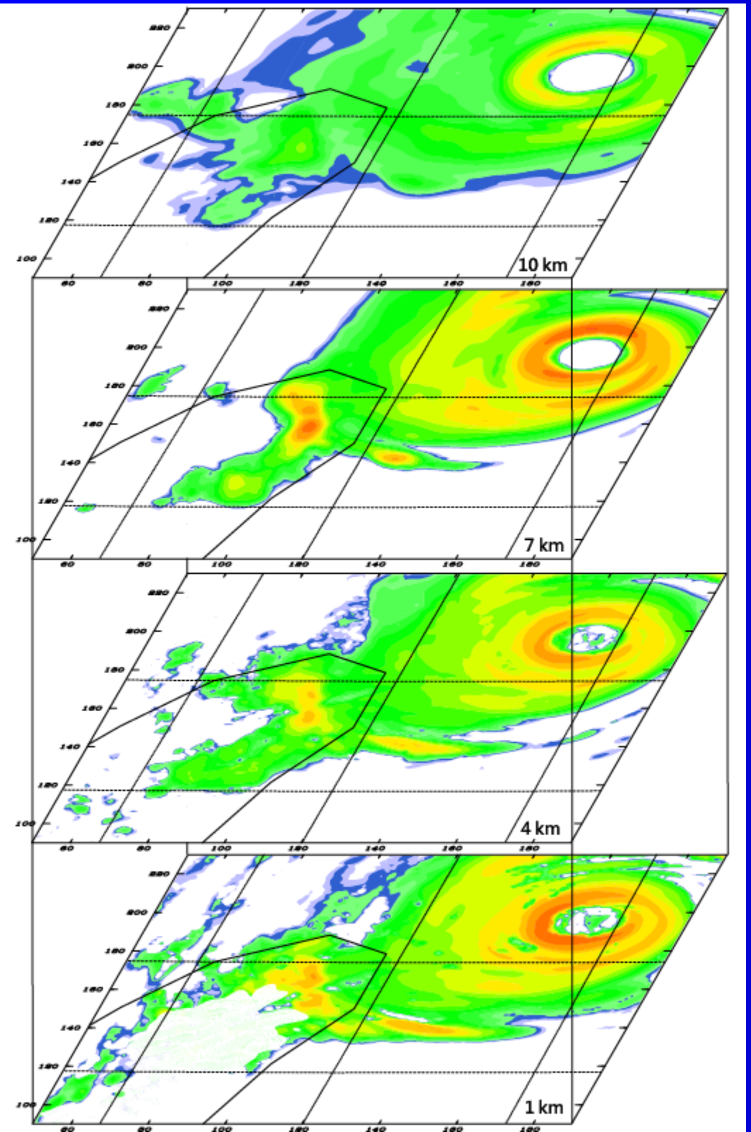


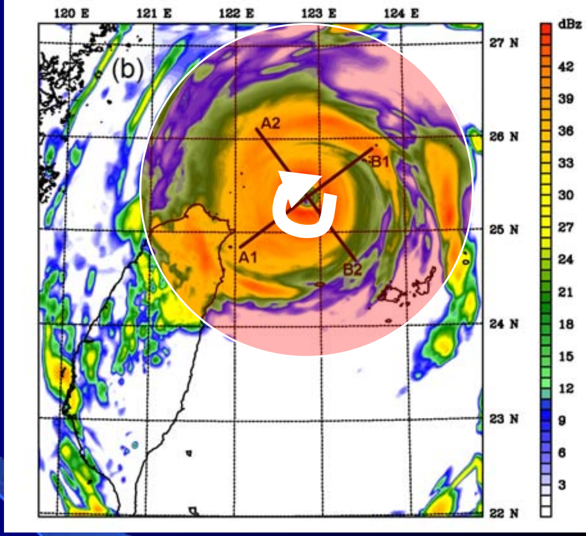


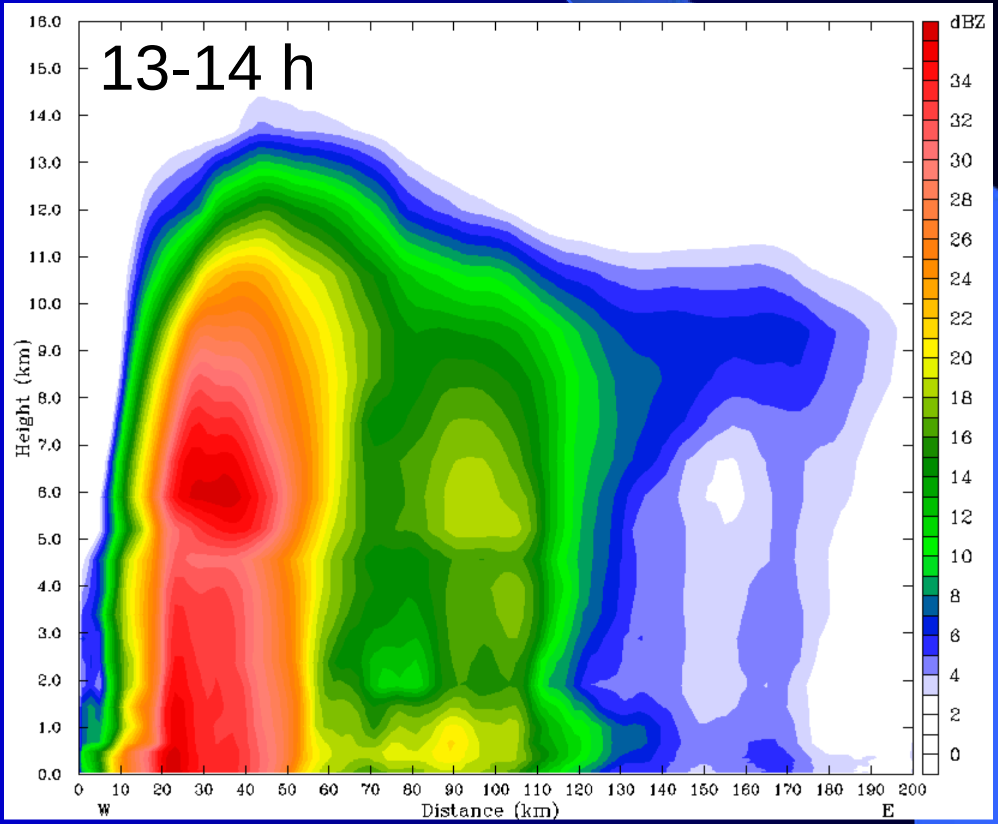

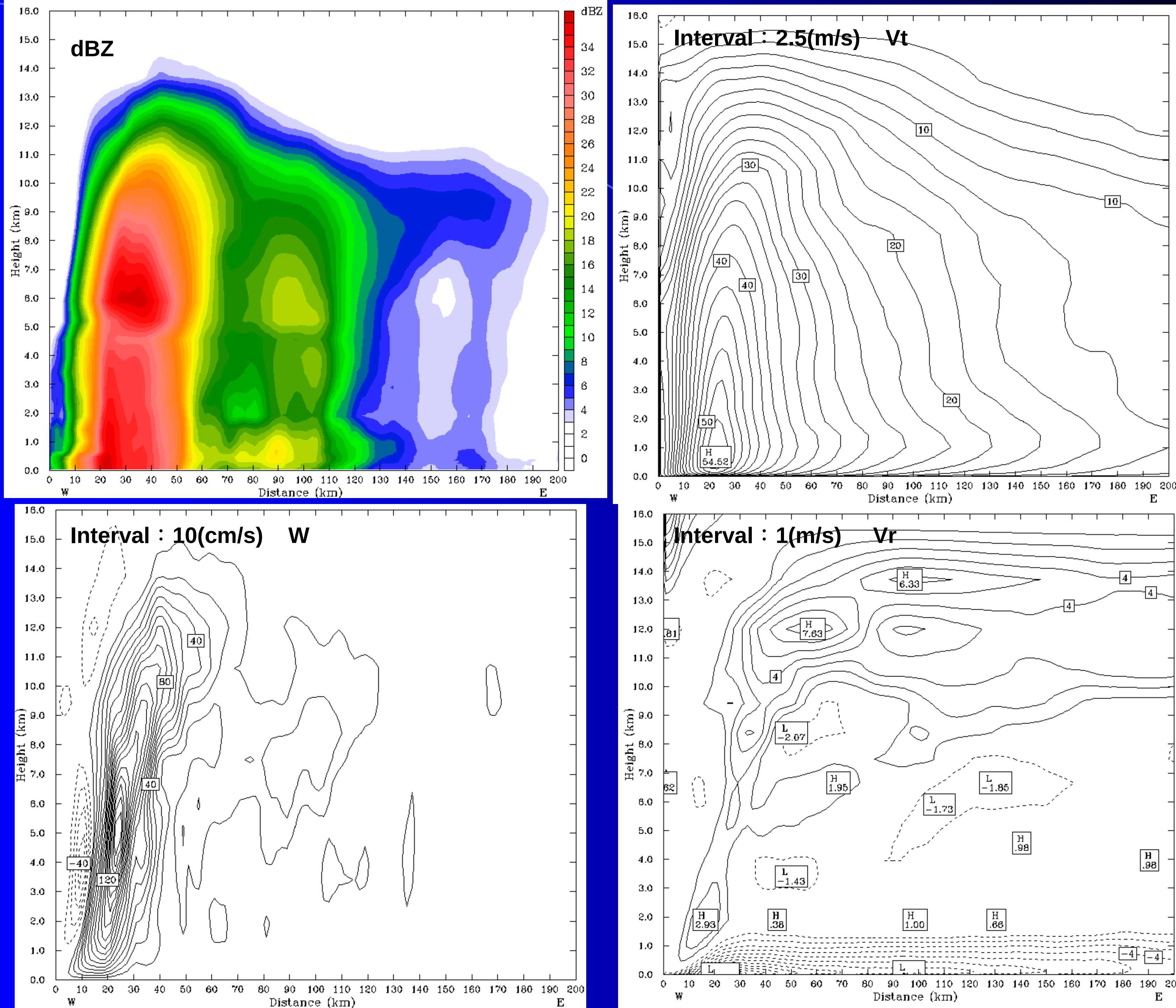

dBZ
Height (km)
Distance (km)
W
E
Interval：2.5(m/s) Vt
Height (km)
Distance (km)
W
E
Interval：10(cm/s) W
Height (km)
Distance (km)
W
E
Interval：1(m/s) Vr
Height (km)
Distance (km)
W
E

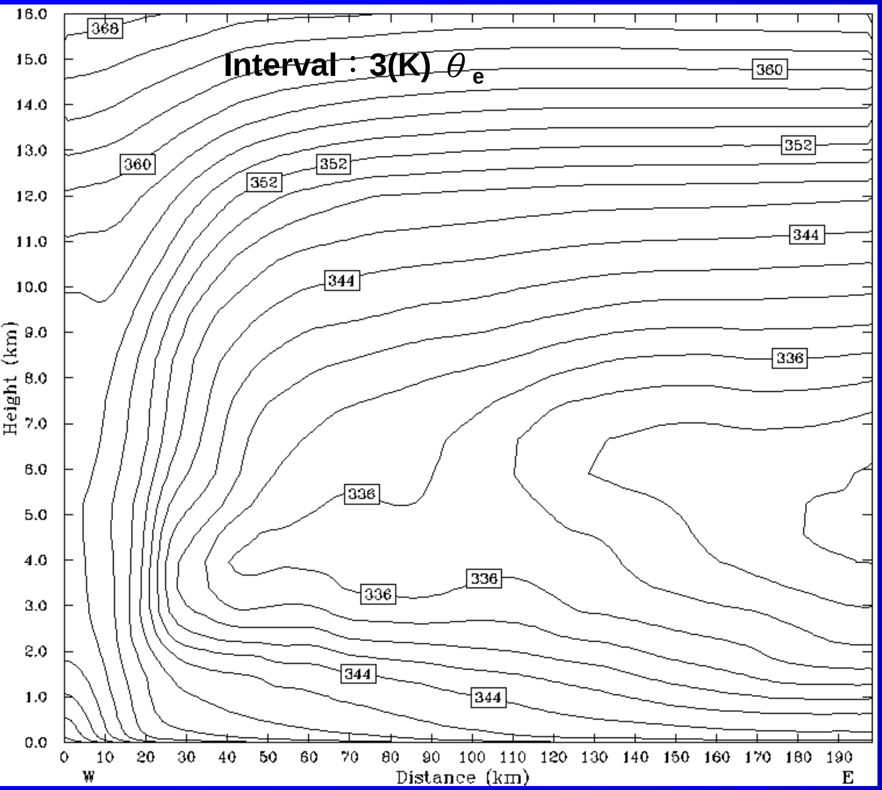

Interval：3(K) $\theta_e$
Height (km)
Distance (km)
W
E
368
360
352
344
336


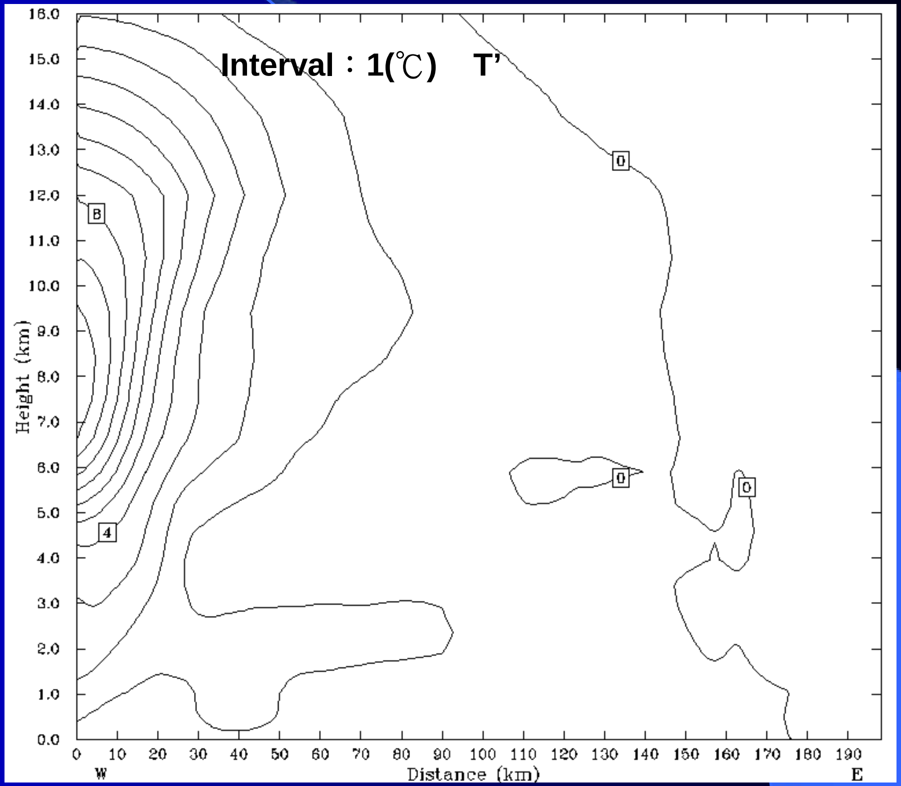

Interval：1(℃) T'
Height (km)
Distance (km)
W
E
8
4
0

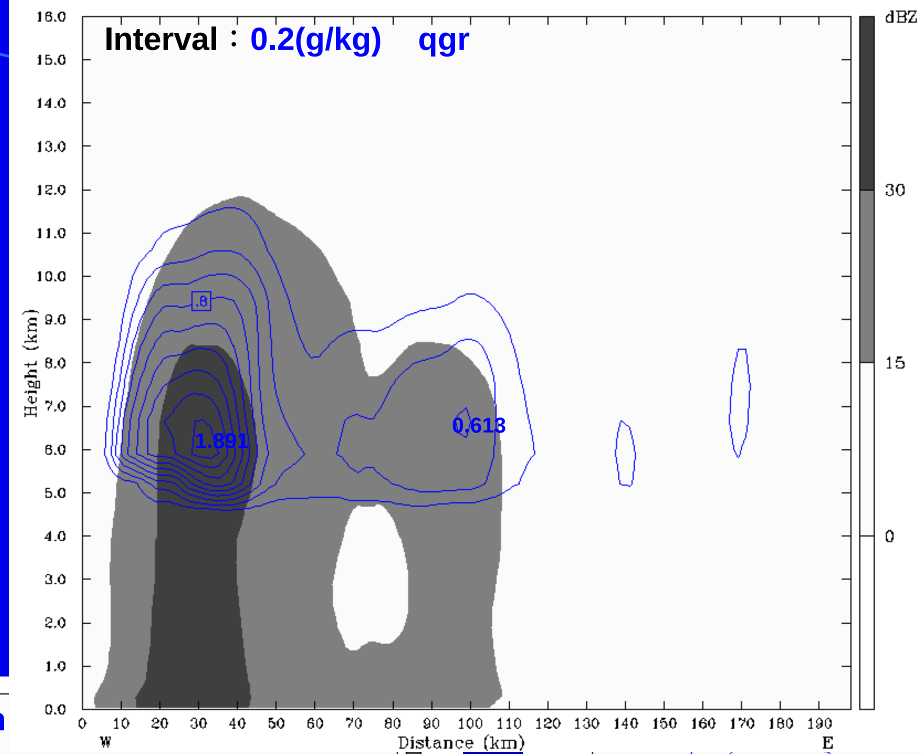
Interval：0.2(g/kg) qgr
dBZ
30
15
0
Height (km)
Distance (km)
W
E
.8
1.891
0.613

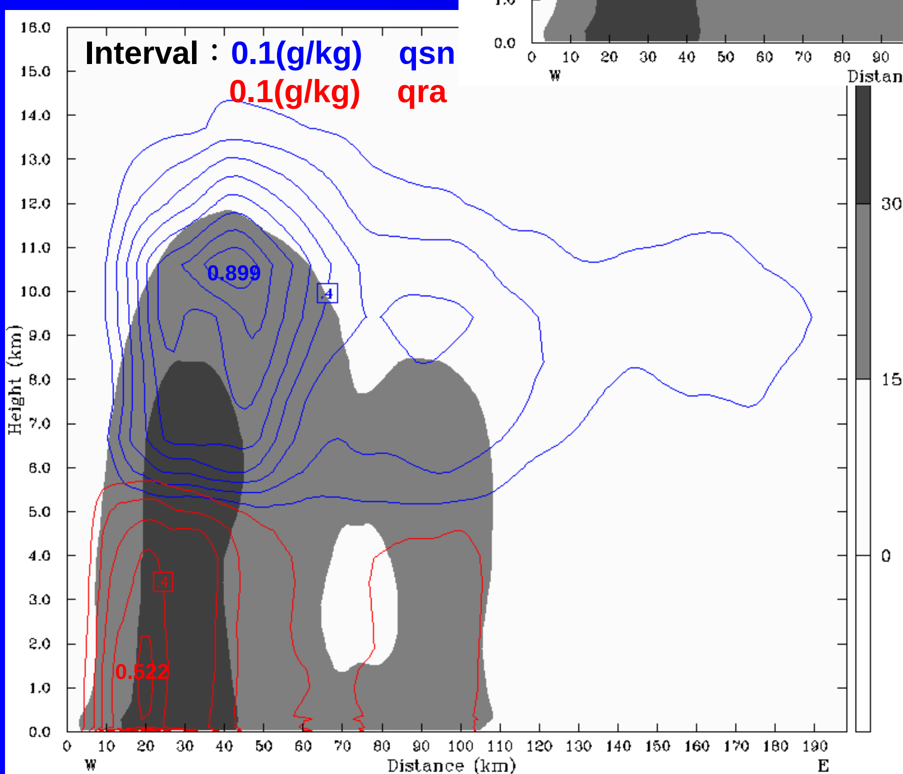
Interval：0.1(g/kg) qsn
0.1(g/kg) qra
30
15
0
Height (km)
Distance (km)
W
E
0.899
.4
.4
0.522

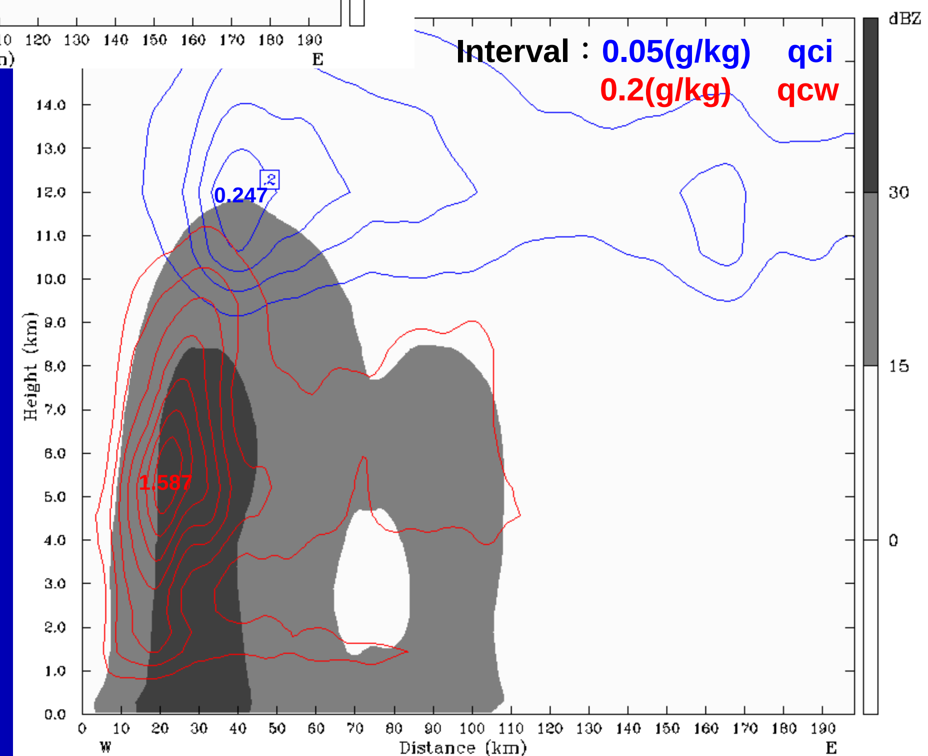
Interval：0.05(g/kg) qci
0.2(g/kg) qcw
dBZ
30
15
0
Height (km)
Distance (km)
W
E
.2
0.247
1.587

# Semicircle-avg. structure (r=180 km) Nari@landfall

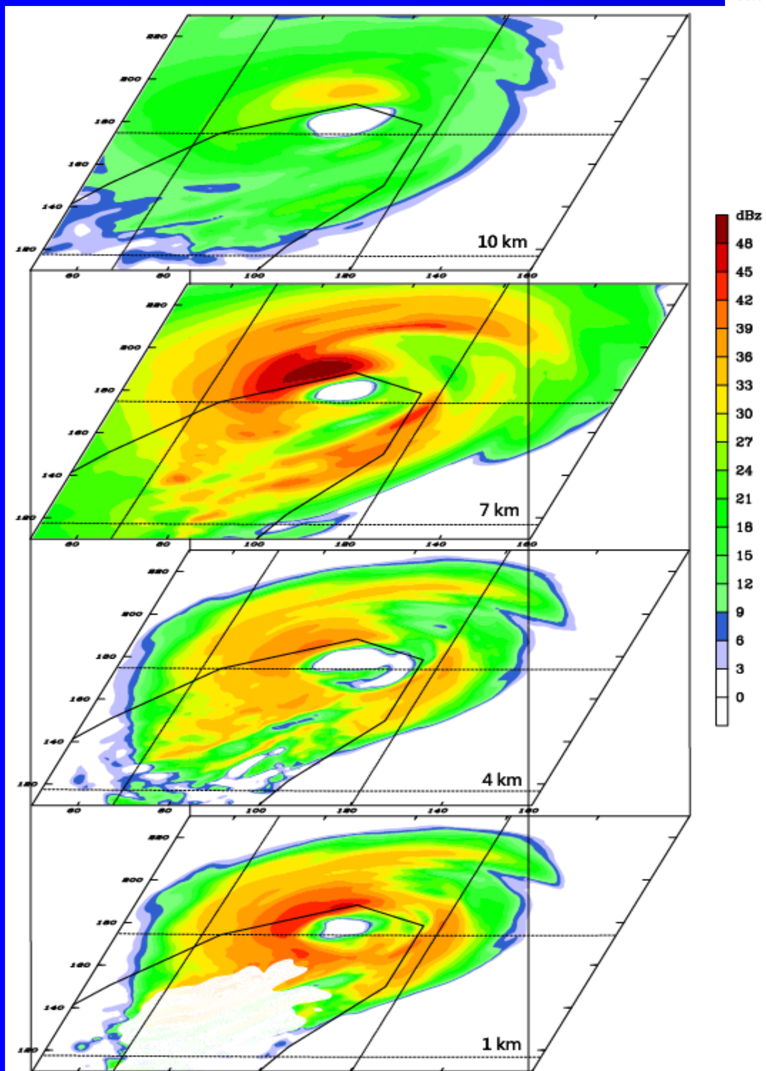


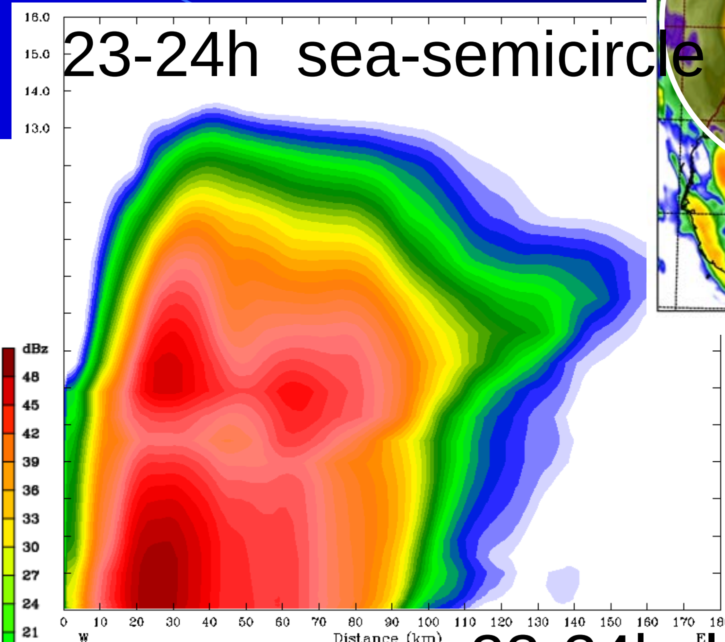


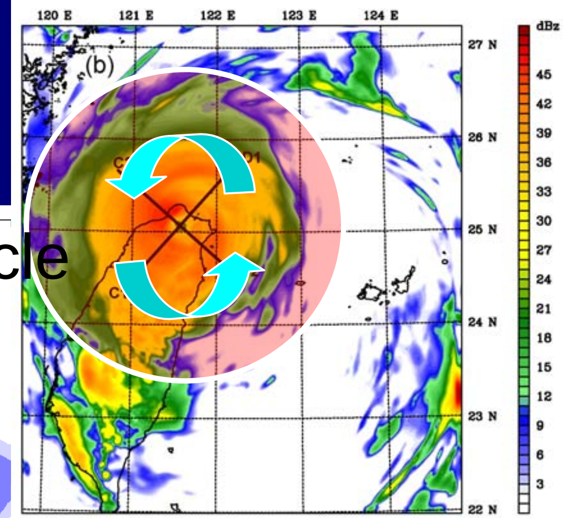


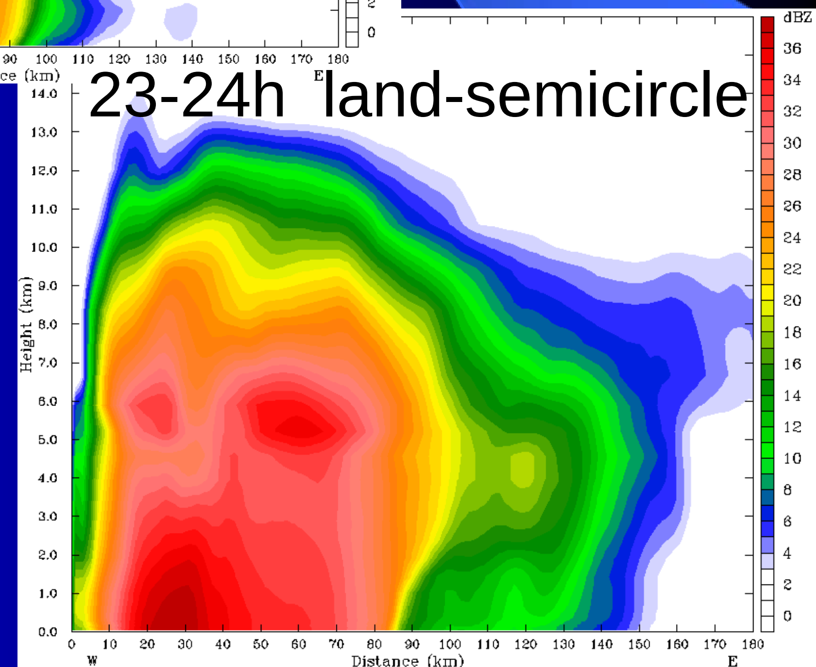

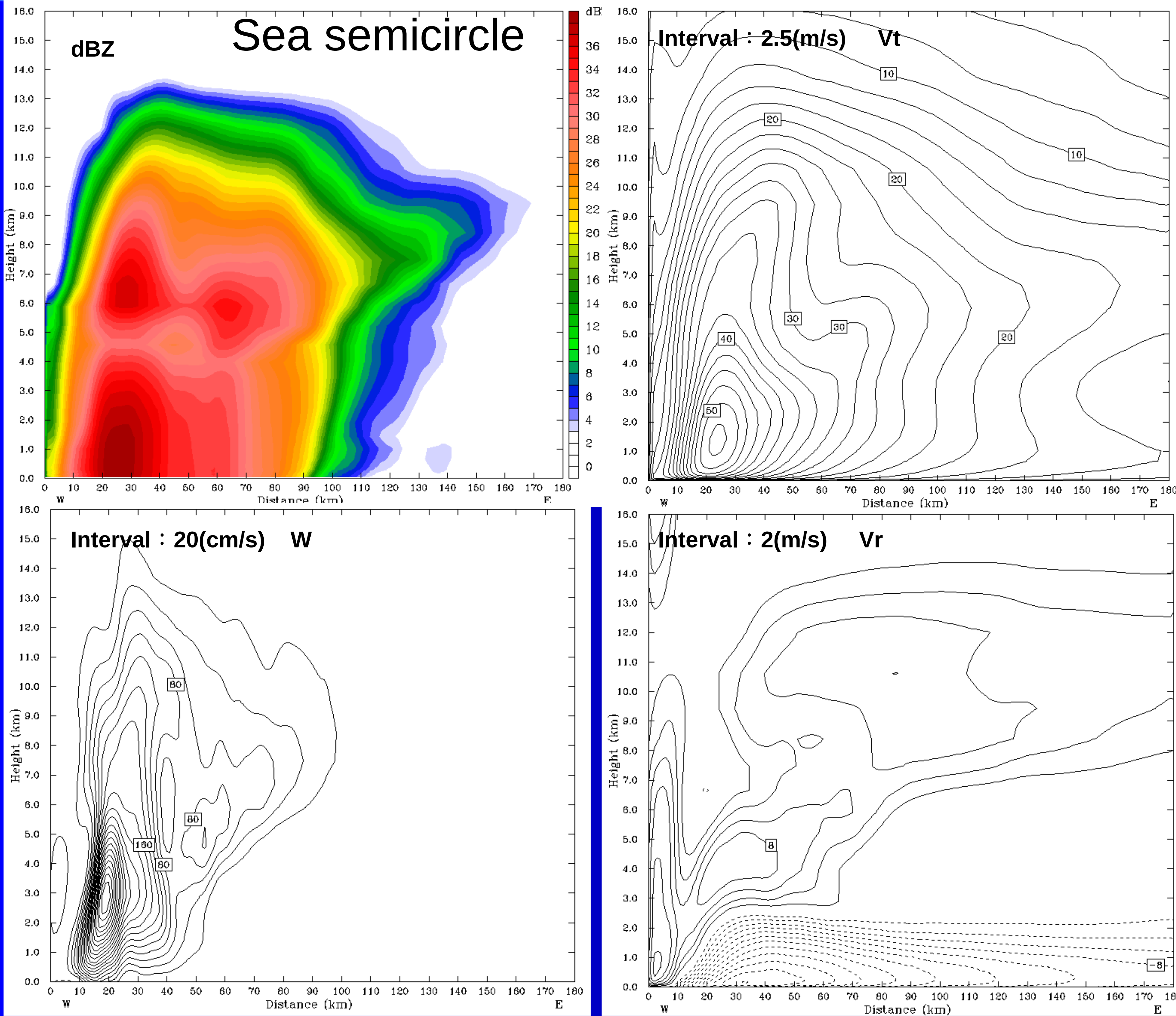
Sea semicircle
dBZ
dB
Interval：2.5(m/s) Vt
Interval：20(cm/s) W
Interval：2(m/s) Vr
Height (km)
Distance (km)
W
E

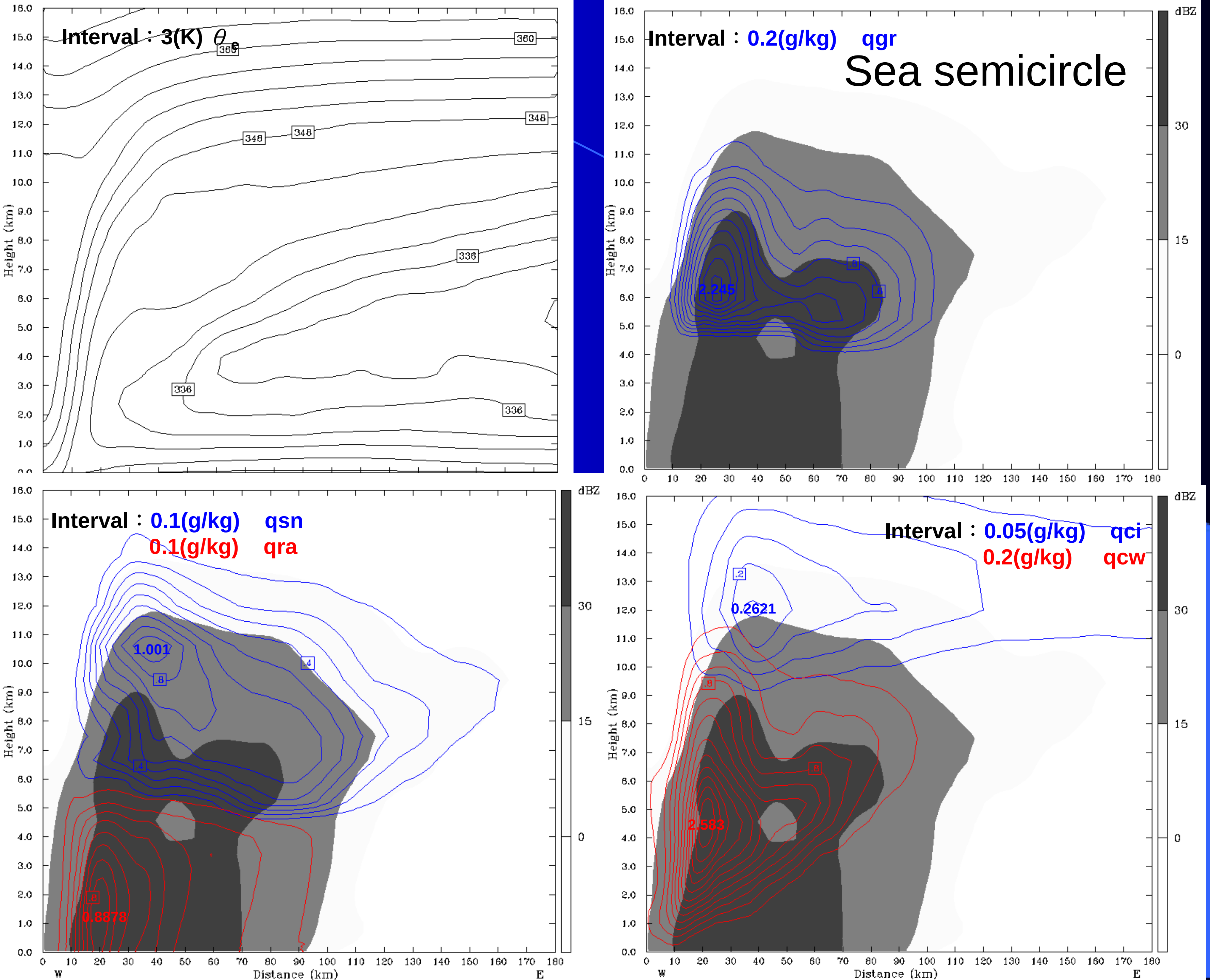

Sea semicircle
Interval：3(K) $\theta_e$
360
348
336
Interval：0.2(g/kg) qgr
2.245
Interval：0.1(g/kg) qsn
0.1(g/kg) qra
1.001
0.8878
Interval：0.05(g/kg) qci
0.2(g/kg) qcw
0.2621
2.583
Height (km)
Distance (km)
dBZ
W
E

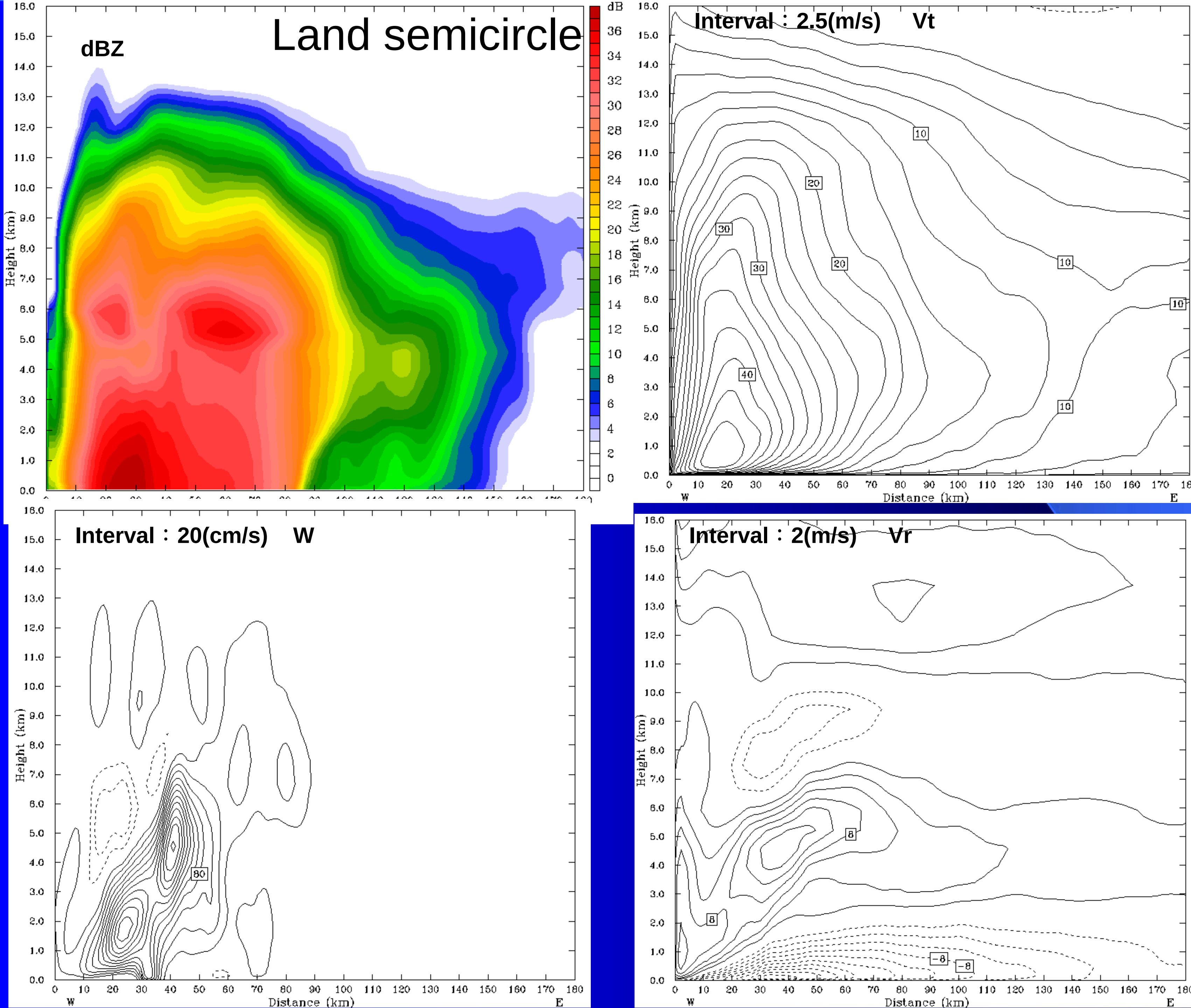
Land semicircle
dBZ
dB
Height (km)
Interval：2.5(m/s) Vt
Height (km)
Distance (km)
W
E
Interval：20(cm/s) W
Height (km)
Distance (km)
W
E
Interval：2(m/s) Vr
Height (km)
Distance (km)
W
E

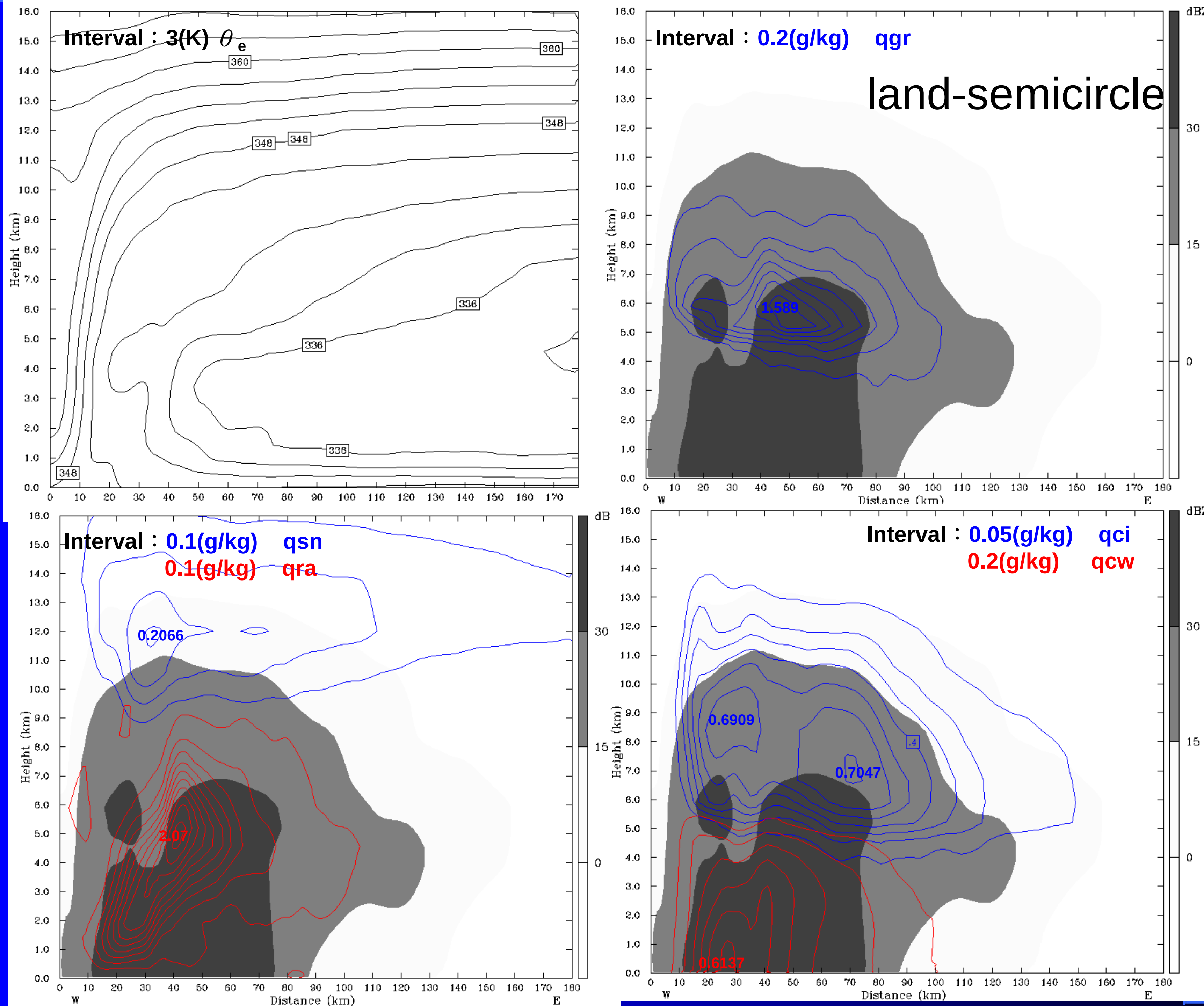

Interval : 3(K) $\theta_e$
360
348
336
Height (km)
Interval : 0.2(g/kg) qgr
land-semicircle
1.589
dBZ
Distance (km)
W
E
Interval : 0.1(g/kg) qsn
0.1(g/kg) qra
0.2066
2.07
Interval : 0.05(g/kg) qci
0.2(g/kg) qcw
0.6909
0.7047
0.6137

# Azimuthally averaged
(r=180 km)

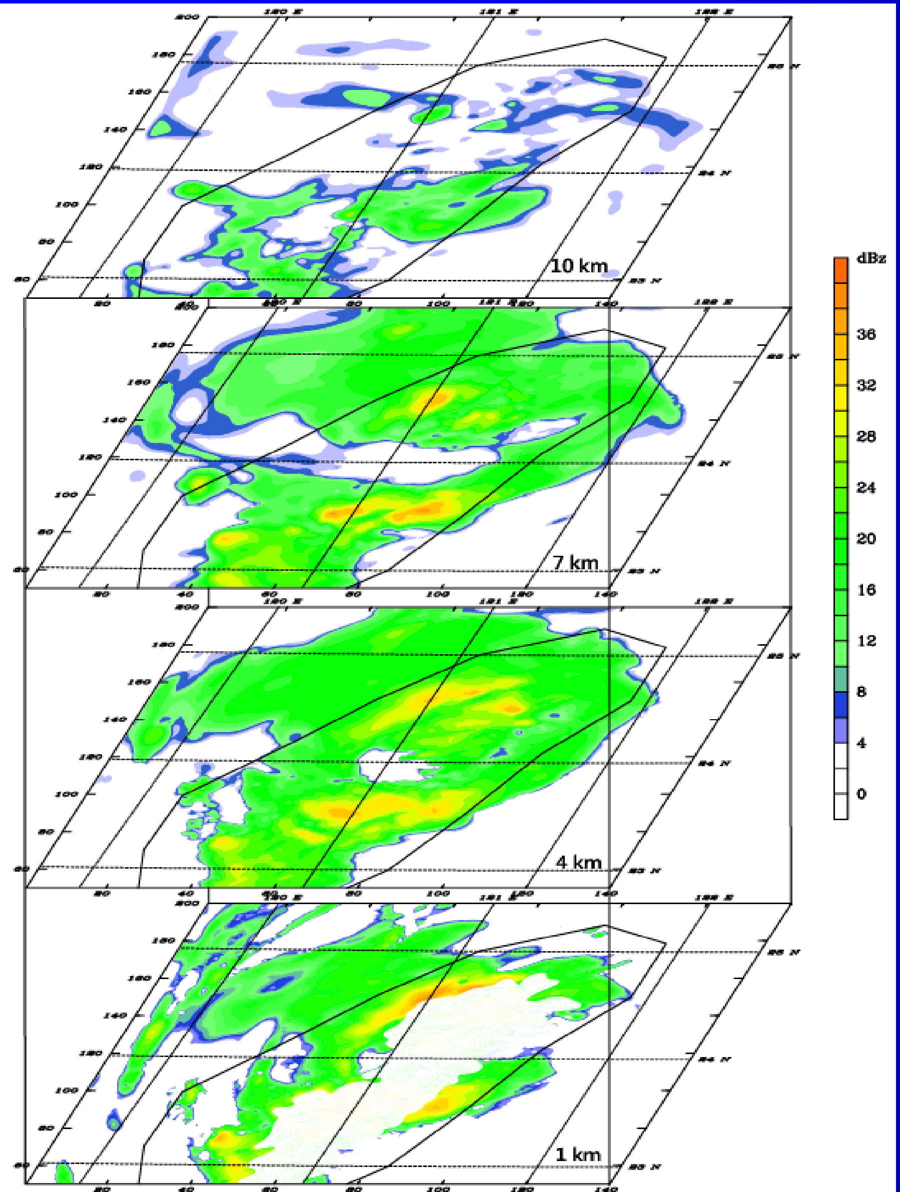


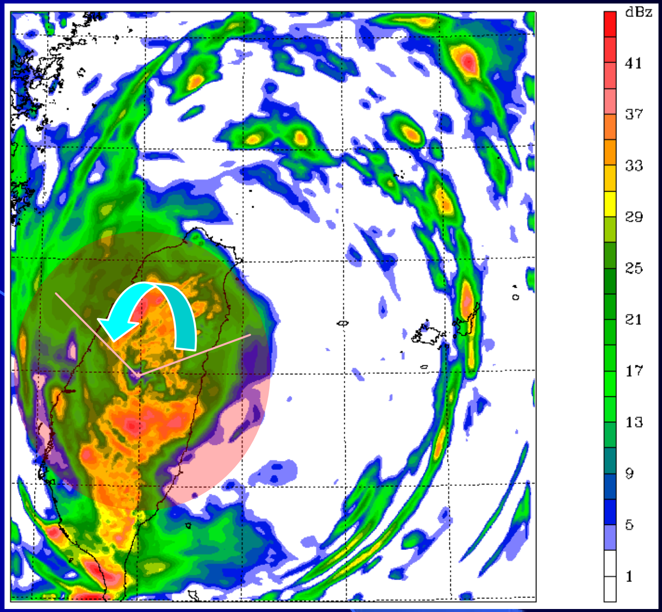


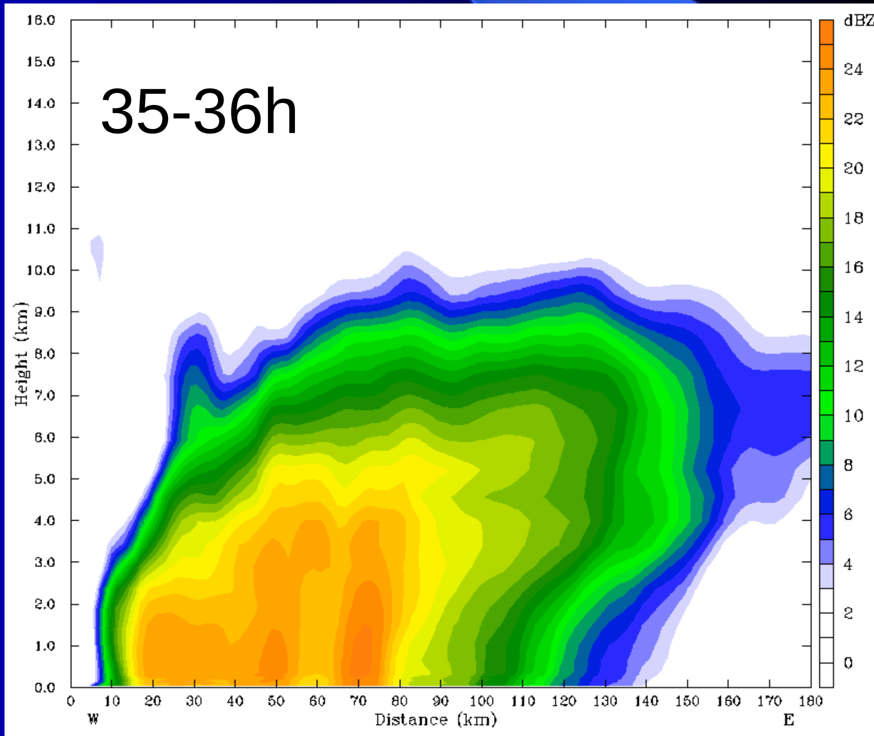

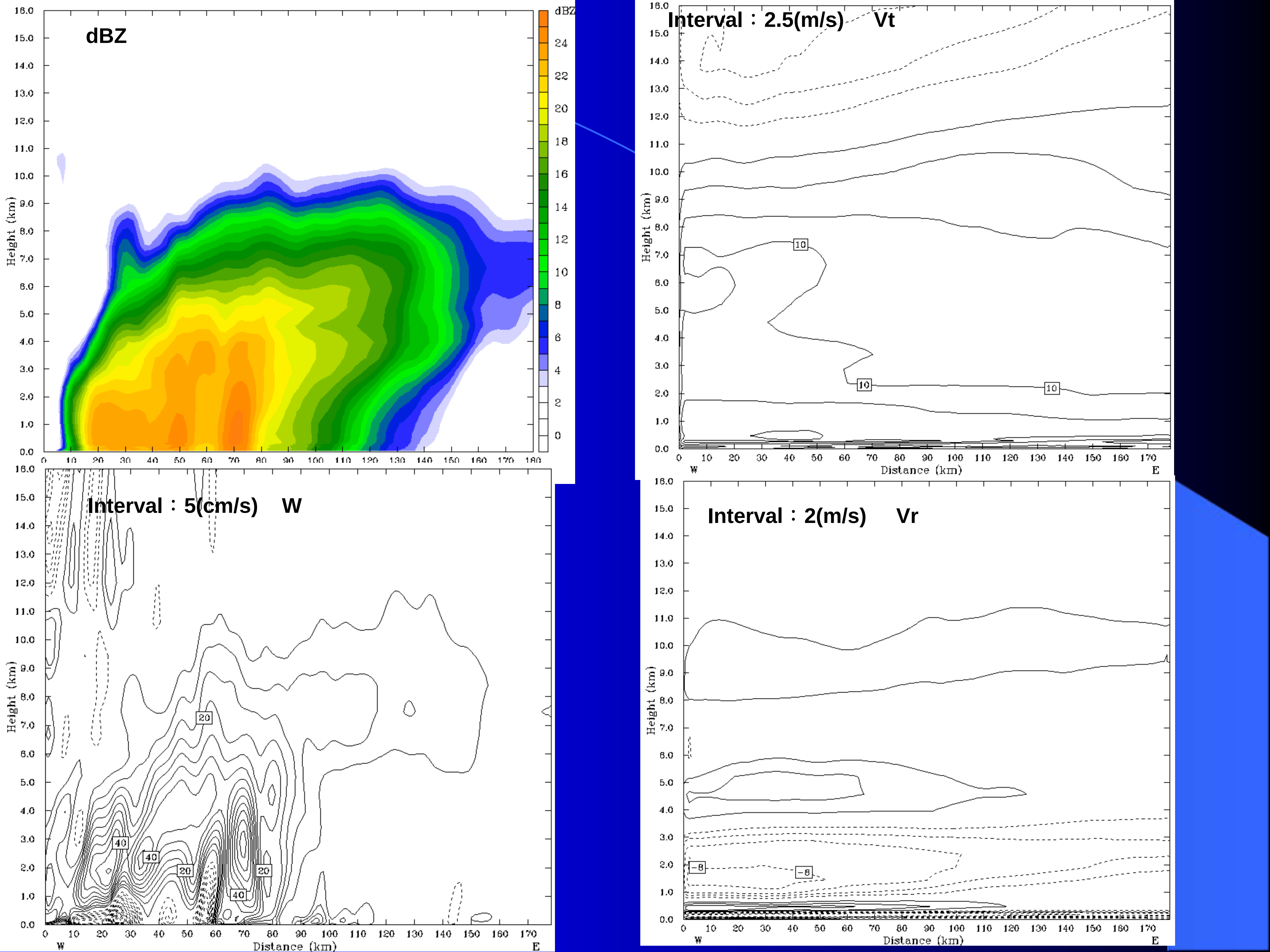

dBZ
Height (km)
Interval：2.5(m/s)　Vt
Distance (km)
W
E
10
Interval：5(cm/s)　W
20
40
Interval：2(m/s)　Vr
-8

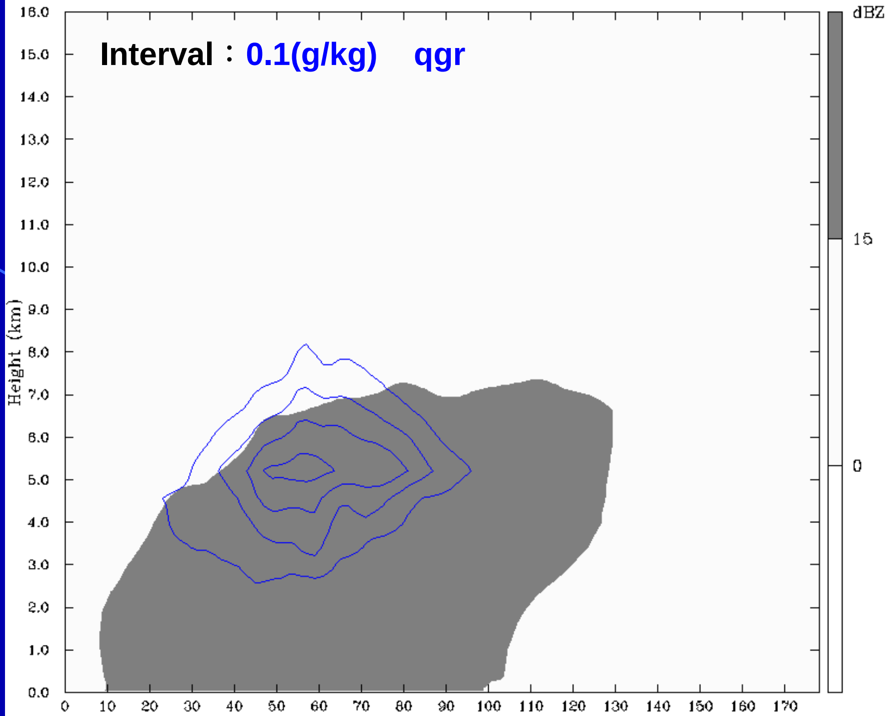
Interval：0.1(g/kg) qgr
Height (km)
dBZ
15
0
0 10 20 30 40 50 60 70 80 90 100 110 120 130 140 150 160 170

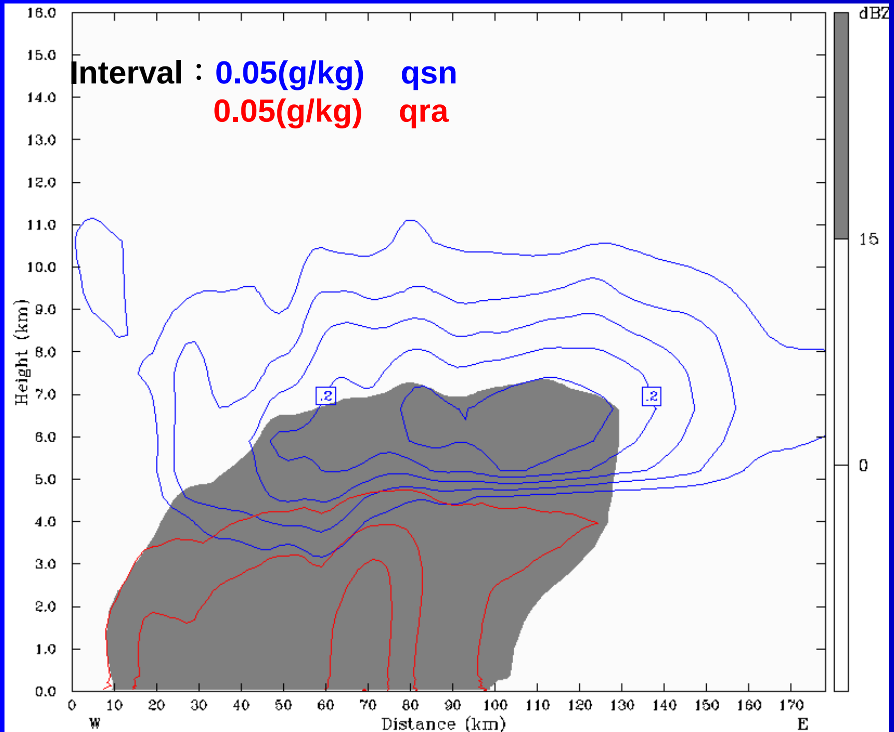
Interval：0.05(g/kg) qsn
0.05(g/kg) qra
.2
.2
Height (km)
Distance (km)
W
E
dBZ
15
0

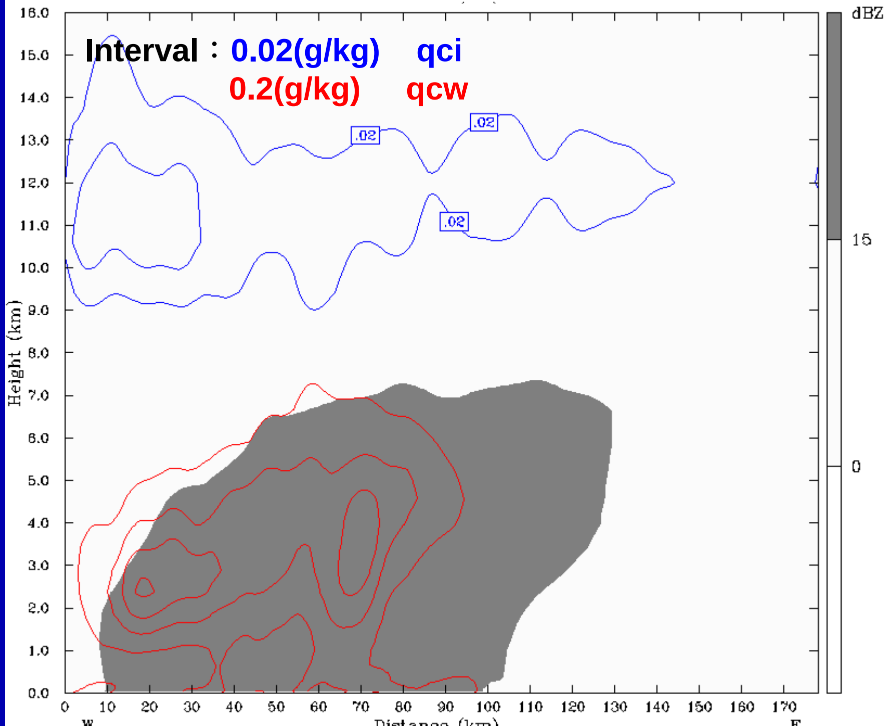
Interval：0.02(g/kg) qci
0.2(g/kg) qcw
.02
.02
.02
Height (km)
Distance (km)
W
E
dBZ
15
0

# The Center of Nari Typhoon on Land (dBZ & wind vector)

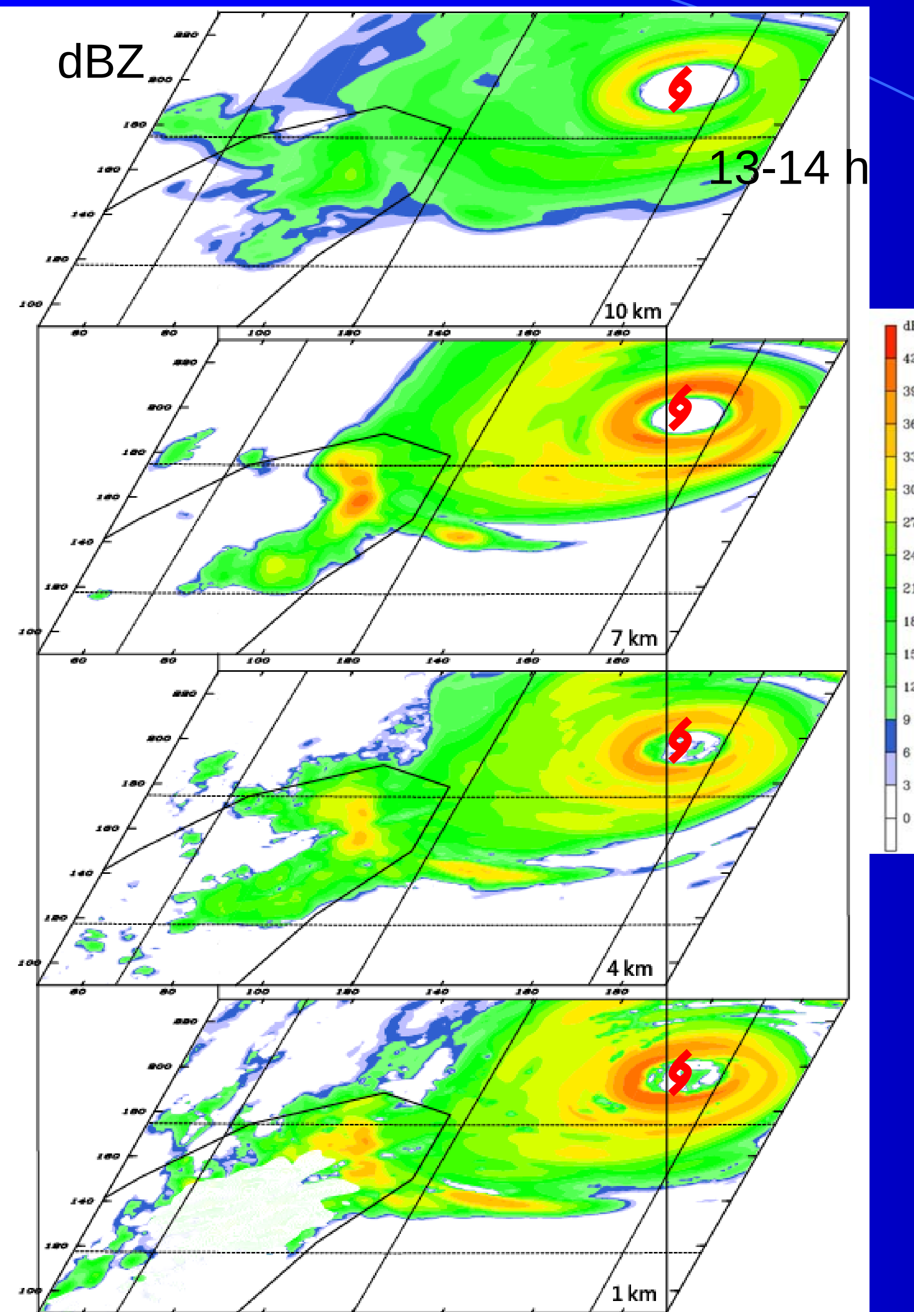
dBZ
13-14 h
10 km
7 km
4 km
1 km
42
39
36
33
30
27
24
21
18
15
12
9
6
3
0

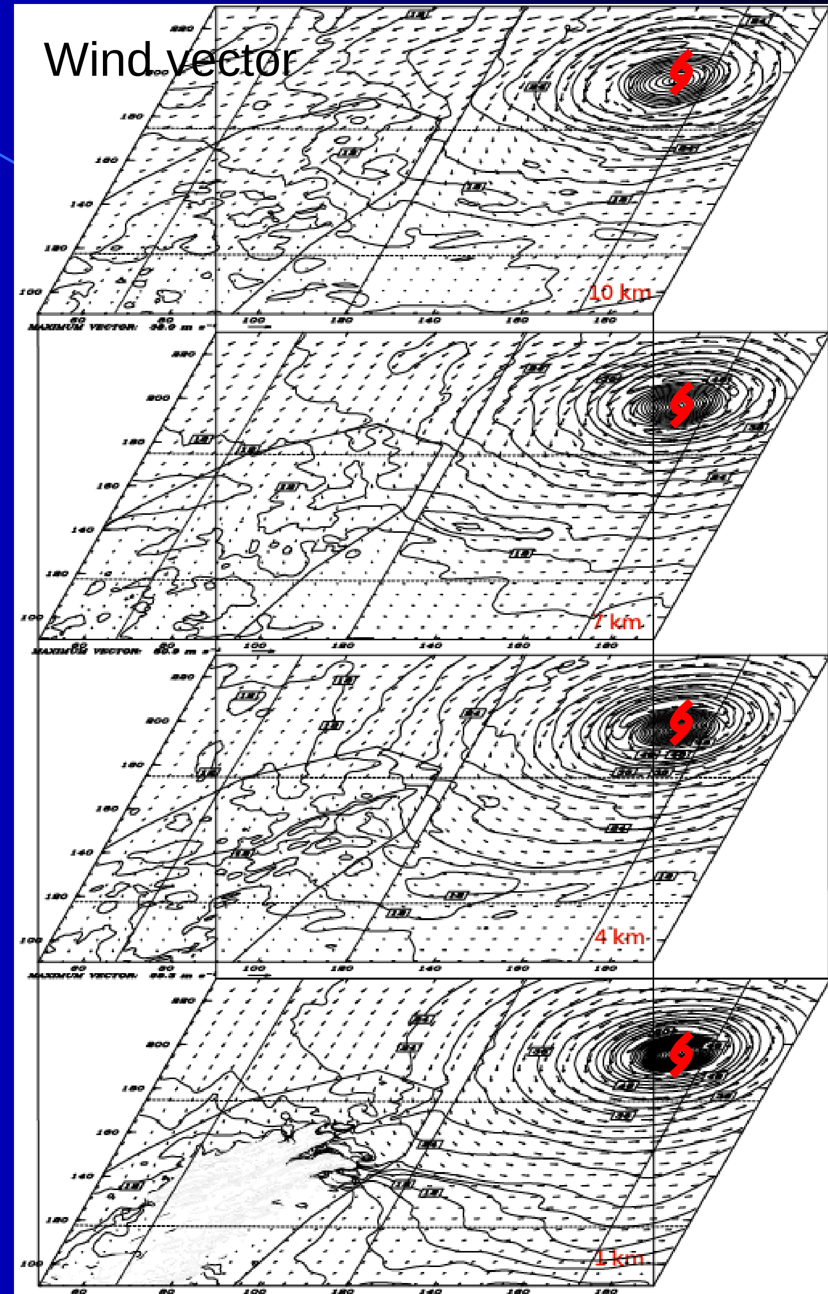
Wind vector
10 km
7 km
4 km
1 km

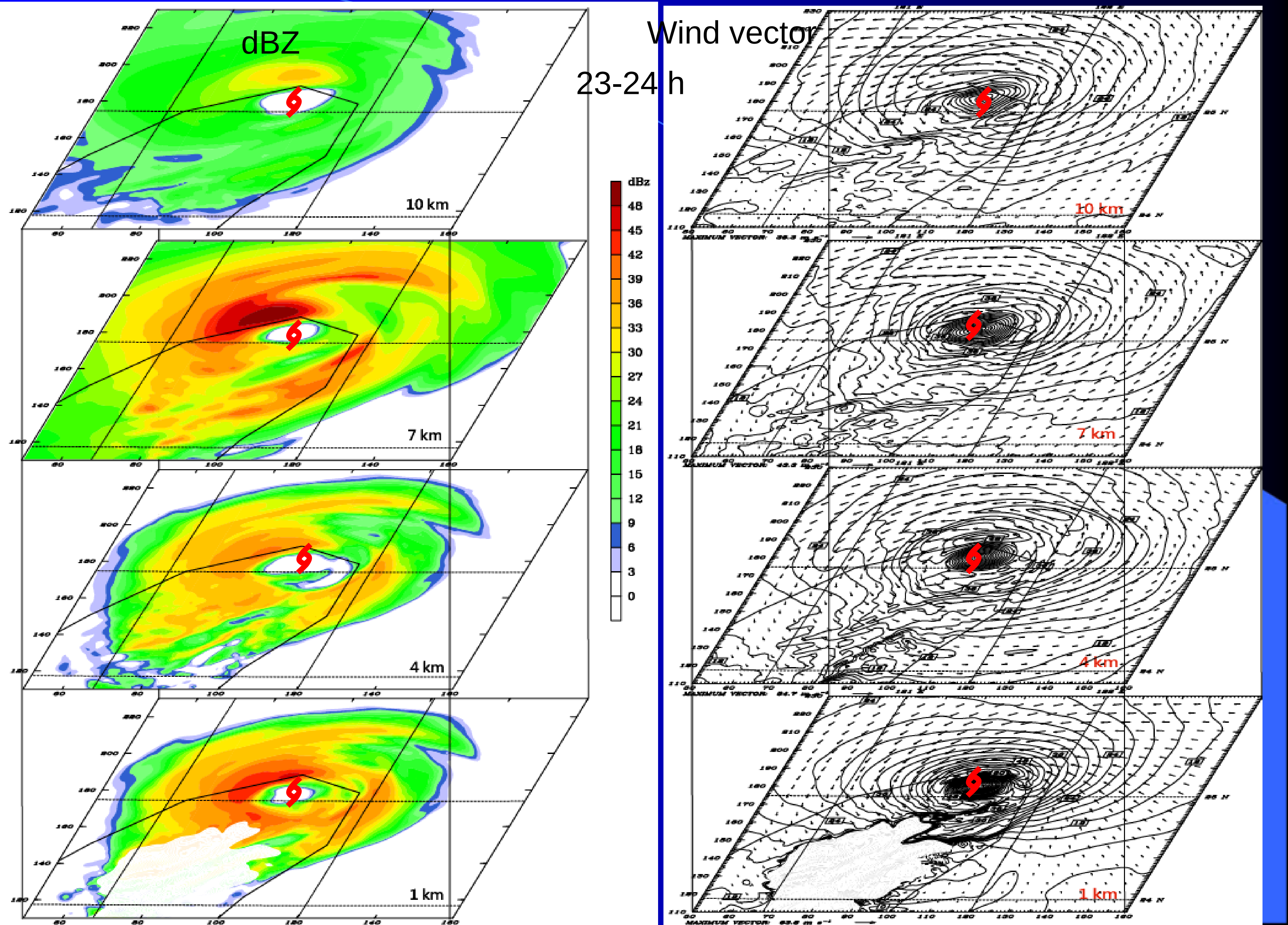
dBZ
Wind vector
23-24 h
10 km
7 km
4 km
1 km
dBz
48
45
42
39
36
33
30
27
24
21
18
15
12
9
6
3
0

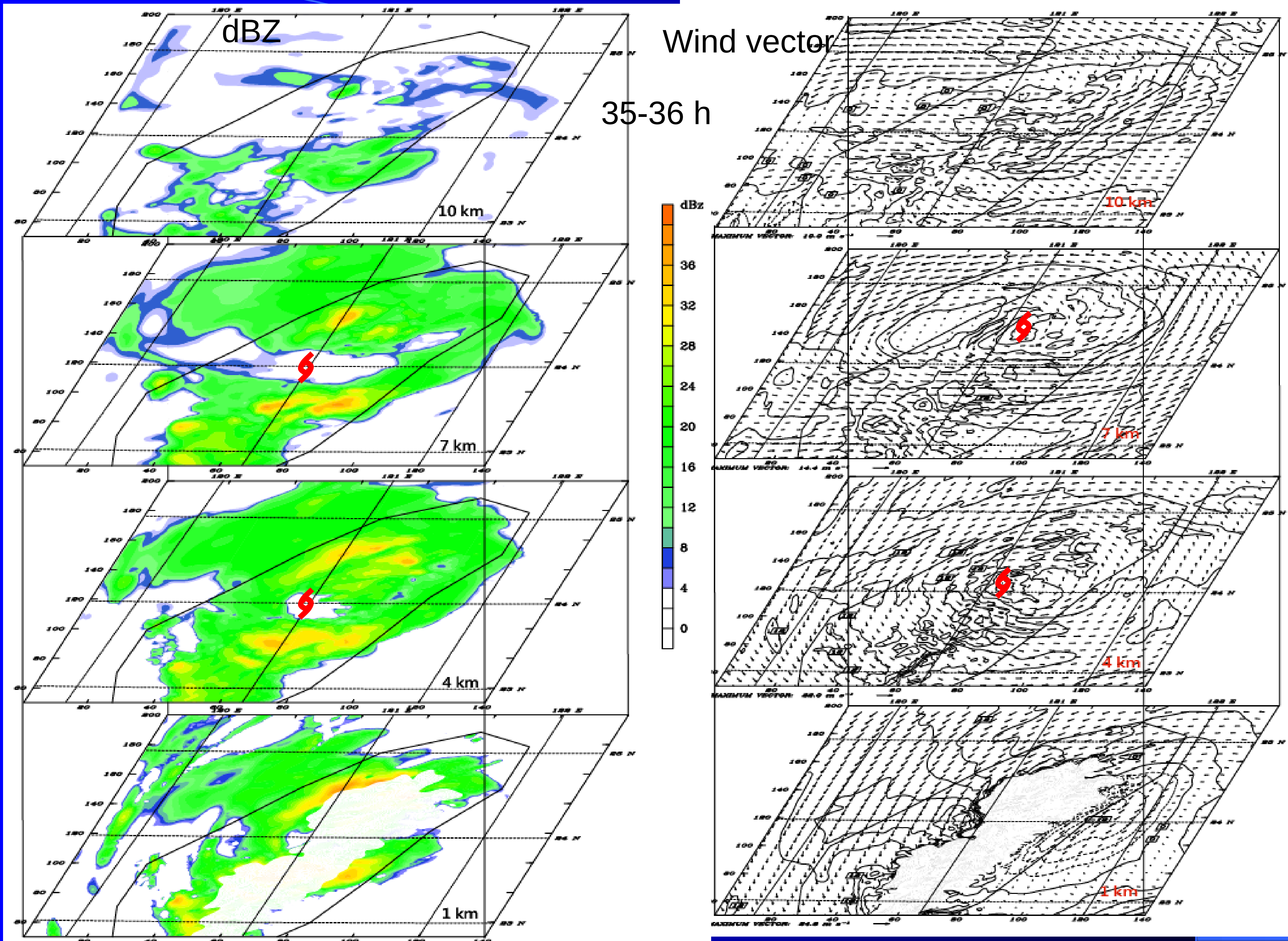

dBZ
Wind vector
35-36 h
10 km
7 km
4 km
1 km
dBz
36
32
28
24
20
16
12
8
4
0

# Conclusions (I)

- Precipitation structure changes:

→Precipitation is widely spread over a larger area.

→Cloud water amount averaged within the inner core is nearly doubled and maximized at lower level.

→Rain water amount averaged within the inner core is increased by 50-70%, mainly produced by melting by graupel particles.

→Ice-phase hydrometeors remain similar vertical profiles after landfall.

- The dominant latent heating (cooling) process within eyewall is condensational heating (evaporative cooling); ice-phase processes are more important in outer rainbands.

# Conclusions (II)

- Latent-heating/cooling structure changes:

→Condensational heating avg. within inner core is almost doubled, and maximized at lower height

→Evaporative cooling avg. within inner core is increased by 50-70%

→Total latent heating within inner core is stronger (almost doubled for peak intensity) and located at a lower height (5 km to 3.5 km) after landfall

- The vortex circulation center is not collocated with the precipitation minimum after Nari's landfall over the Central Mountain Range